NASA Contractor Report 159118

STUDY OF DESIGN CONSTRAINTS ON HELICOPTER NOISE

Harry Sternfeld, Jr., and Carl W. Wiedersum

BOEING VERTOL COMPANY
Philadelphia, Pennsylvania 19142

Contract NAS1-15226
July 1979

National Aeronautics and
Space Administration

Langley Research Center
Hampton, Virginia 23665

CONTENTS

ILLUSTRATIONS

TABLES

List of Symbols

A_b	Blade Area - Ft^2
C	Blade Chord - Ft
$\overline{C_L}$	Average Lift Coefficient
C_λ	Amplitude of the λth Sound Harmonic
C_o	Stationary Airload of the Rotating System
D,DL, or D/L	Disk Loading - Lb/ft^2
dBA	A Weighted Sound Pressure Level - dBA
dBC	C Weighted Sound Pressure Level - dBC
EPNL	Effective Perceived Noise Level - EPNdB
f_p	Peal Frequency - Hz
HP_r	Takeoff Horsepower - HP
K	Droop Constant
K_D	Weight Estimating Coefficient - No units
K_R	Weight Estimating Coefficient - No units
K_t	Configuration Factor
M_{DD}	Drag Divergence Mach Number
M_F or M_{TIP}	Advancing Tip Mach Number
N	Number of Blades
n	Harmonic Number
N_R	Rotational Speed at Takeoff - RPM
PNL	Perceived Noise Level - PNdB
PNLT	Tone Corrected Perceived Noise Level - PNdB
r	Distance to Observer - Ft
R	Blade Radius - Ft
r_1	Distance from C Rotation to Blade Attachment-Ft
SPL	Sound Pressure Level - dB re $2x10^{-5}$ N/m^2
$\overline{SPL}$	SPL of a Hovering Rotor at a Distance of 150m and an Altitude of 150m
t	Blade Thickness - Ft
T	Total Rotor Thrust - Lb
V_T or V_t	Rotor Tip Speed - Ft/sec
Z	Number of Stages of Gearing in Main Rotor Drive
λ	Air Loading Harmonic Number
θ	Angle Between Disk Plane and Field Point-Degrees
θ_1	Angle Between Rotor Shaft and Line to Observer Measured Down - Degrees
σ	Rotor Solidity
ρ	Mass Density of Air - $lb\text{-}sec^2/ft^4$

SUMMARY

This report provides a means of estimating the noise generated by a helicopter main rotor using information which is generally available during the preliminary design phase of aircraft development. The method utilizes design charts and tables which do not require an understanding of acoustical theory or computational procedures in order to predict the Perceived Noise Level, A Weighted Sound Pressure Level, or C Weighted Sound Pressure Level of a single hovering rotor. A method for estimating the Effective Perceived Noise Level in forward flight is also included.

In order to give the designer an assessment of the relative rotor performance, which may be traded off against noise, an additional chart for estimating the percent of available rotor thrust which must be expended in lifting the rotor and drive system, is included. The report also includes an approach for comparing the subjective acceptability of various rotors once the absolute sound pressure levels have been predicted.

INTRODUCTION

Recent years have been ones of marked change for the helicopter industry. Much of this change has been due to a transition from a military dominated market to one in which the civil customer is playing an ever increasing role. Along with the growing civil market there has developed an increasing concern for exterior noise. This concern is perhaps most strongly evidenced by regulatory agencies such as the FAA and other members of the International Congress of Aeronautical Organizations (ICAO) who are currently drafting noise regulations for helicopter certification. Even noise certification itself provides no guarantee to the operator that his activities will be permitted by the many local and state bodies who can still limit operation through curfews, heliport licensing, and other measures open to them as protection of the 'peace and well being' of their citizens. This growth of regulation and obvious concern has elevated the priority of rotor noise to the point where attainment of a target noise level, for a new rotor design, ranks with attainment of specific performance and stability criteria.

The external acoustical signature of a helicopter is derived from a combination of separate noise generating sources, as illustrated in Figure 1. In the preliminary design stages of a new helicopter, the main rotor and engines are usually the first elements to be defined. Since the main

rotor is usually the most predominant noise source, it is important that an estimate of its noise, or comparative estimates of the noise of contending rotors, be available early in the design cycle.

Noise control of a rotor is inherent in its initial design parameters such as tip speed, disc loading, and solidity. Once these parameters are finalized, there is little that can be done (with the possible exception of tip shape) that will exert any major influence on the noise of a rotor. Since the sizing of the rotor often dictates other major considerations of design such as fuselage, tail rotor and drive system, it is important that the designer have available a method for designing main rotors to noise constraints, which is reasonably easy to use and does not require detailed rotor design parameters such as airfoil and stiffness distributions since they are generally not known in the early stages. It is axiomatic that the earlier in the preliminary design cycle that a quality can be evaluated, the more likely it is to be factored into the final design. The objective of this report is to provide such a means in the hope that it will encourage the design of quieter rotors.

This study was directed specifically at providing a rapid and convenient means of estimating main rotor noise as guidance during the rotor selection phases of design. As the design progresses and more detailed information becomes available, more precise methods of main rotor noise prediction may be employed and combined with tail rotor, engine, and transmission noise prediction, as applicable, to provide more detailed noise predictions of the final aircraft. If, however, the basic rotor design considerations, which are factors in this study, have been badly violated, there is little which can be done by detail design which will result in a helicopter with acceptable noise characteristics.

PREDICTION METHODOLOGY

The aerodynamic environment of the helicopter main rotor is an extremely complex one (Figure 2).

The complexity is inherent in the fundamental principles of the rotary wing which has a linearly varying velocity along the radius of the blade which is superimposed on the forward flight velocity of the aircraft, and produces a resultant velocity which varies with a once per rotor revolution time base. This situation is further complicated by the fact that control inputs cause the angle of attack of the blade to vary around the azimuth. Since the blade is also twisted along its length, the net result is a time varying velocity and airloading

which differs at each radial station. Another very important aerodynamic influence is caused by the trailed vortex from the blade tip which may come very close to, or even be intersected by a following blade, thereby resulting in sudden large changes of effective angle of attack. Figure 3 presents a convenient breakdown of the components of rotor noise and established terminology which is commonly used to describe the various elements of rotor noise.

The general approach which has been used in this report is to provide sets of design charts for estimating the noise of a single rotor in hover. The charts are based on analytical predictions which are verified by comparison with data from a 3-bladed, 30 ft diameter (CH-47) rotor operating on a rotor test tower. Because hover tip speeds are substantially below Mach 1, compressibility and thickness noise are not significant and were not considered since the accuracy of analytical prediction of rotor noise in forward flight is not as well understood as the hover case and comparison between predictions and measured data is generally considerably poorer. Rather than depend on analysis at this time, a data based means for extrapolating hover predictions to forward flight is provided.

The components (Ref. Figure 3) which are included in the hover prediction are rotational noise due to airloading and broadband noise since tip speeds in hover are always too low to make compressibility and thickness noise a factor.

Hover Noise

Rotational Noise.—Rotor rotational noise occurs at certain multiples of blade passage frequency dependent on the number of blades per rotor. The noise is basically an aerodynamic phenomenon whose fundamental mechanism arises out of the action and reaction of rotor blade forces interacting with its flow environment. Reference 1 report indicates in detail how the oscillatory differential blade pressure or forces can be resolved into thrust, drag and radial force components for purposes of calculating the resulting harmonic noise according to:

$$p(t) = \left[\frac{(x_i - y_i)}{4\pi\,(1-M_s)^2\,cs^2}\left\{\frac{\partial F_i}{\partial t} + \frac{F_i}{1-M_s}\cdot\frac{\partial M_s}{\partial t}\right\}\right] \qquad (1)$$

$p(t)$ instantaneous far-field acoustic pressure

x_i observer coordinates

y_i source coordinates

M_s source Mach number in direction of observer

s distance between source and observer

F_i aerodynamic force components

c speed of sound

Equation (1) can be solved numerically if blade properties and airloads are known and specified. A computer program called Heron I, for the particular case of a single helicopter rotor has been written and published as Reference 2.

By making several assumptions, valid for the far-field only, a closed form solution was developed:

$$C_n = \sum_{\lambda=0}^{\infty} K \cdot \frac{1}{r} \cdot \left\{ \frac{nM}{R} \sin\theta \, C_{\lambda T} J_1^1 \frac{-c_{\lambda D}}{R} J_2^1 + \frac{nM}{R} \cos\theta \, C_{\lambda c} J_3^1 \right\} \quad (2)$$

C_n amplitude of nth sound harmonic

λ air loading harmonic number

K constant

r distance between rotor center and field point

$n=mB$ harmonic number x number of blades

M rotational Mach number

R radius of action of blade forces

θ angle between disc plane and field point

J_i^1 complex collections of Bessel functions

$C_{\lambda T}$, $C_{\lambda D}$, $C_{\lambda C}$ thrust, drag, radial force harmonic coefficients

Lowson and Ollerhead assumed that the thrust, drag and radial force components are randomized with respect to phase, that the ratio of their magnitudes are 10:1:1, respectively, that the magnitude of the higher harmonics of airloads fall off in some proportion to the harmonic number, and several other assumptions, the expression for the sound intensity

can then be written:

$$C_n = \sum_{\lambda=0}^{\infty} K \cdot \frac{T}{R_r \lambda^k} \left\{ (10\ nM \sin\theta) J_1^1 - J_2^1 + (nM \cos\theta) J_3^1 \right\} \qquad (3)$$

where T is the steady rotor thrust.

In Equation (3), the term $1/\lambda^k$ reflects the air loading harmonic drop-off, including the term $\lambda^{.5}$ which is due to random phasing effects.

The exponent of the term λ^k is referred to as the loading power law constant which was experimentally determined as having the value 2.0 based on the data contained in Reference 3. That report is a summary of flight data on the H-34 single rotor helicopter. Application by others, led to a realization that the method was giving quite close correlation with measured data for the first harmonic but the correlation with higher harmonics became progressively poorer, and that the calculated values were lower than the measured values. Mathematically it was apparent that the correlation could be improved by decreasing the value of the exponent K. In order to provide a logical basis for selection of an alternate value, more recent data on harmonic airloading was reviewed, including one program (Ref. 4) which was conducted for this particular purpose. The results of Ref. 4, and other available measurements (e.g. Ref. 5) indicated a range of harmonic airload decay rates ranging from 7 - 10 dB/octave. A value of 8 dB/octave was selected as typical which corresponds to a K exponent-1.3. Applying a similar assumption as Lowson and to account for random phasing results in a final definition of harmonic decay as:

$$C_\lambda = C_o\ \lambda^{-1.8}$$

which provided an improved correlation with measured data.

Broadband Noise.—Prediction of rotor broadband noise has generally been based on the empirical fit of blade operating parameters and dimensions to measured data. These typically included empirically derived relationships for determining maximum levels which are then applied to a typical spectrum shape whose peak frequency is defined by a relationship including thrust and velocity. Initially, it was intended to use existing formulas but recent correlations indicated that the amplitude was a stronger function of average lift coefficient than previously realized, and several iterations between NASA and the contractor in efforts to improve on existing calculations resulted in the following approach.

The recommended rotor-generated broadband noise equation is based on the work of Lowson (Ref. 6), Hubbard (Ref. 7), Schlegel (Ref. 8), and Munch (Ref. 9). To calculate the sound radiated by the random pressure field, the spectrum peak frequency is first calculated from equation (4) as:

$$f_p = -240 \log T + .746\, V_T + 786 \qquad (4)$$

The third octave band sound pressure levels can then be determined from the following equation based on data from rotor blades having constant chord, thickness, and airfoil section along the radius:

$$SPL_{1/3} = 20 \log \frac{V_T^3}{r} + 10 \log A_b(\cos^2\theta_1 + .1) + S_{1/3} + f(\overline{C_L}) - 53.3 \qquad (5)$$

where:

SPL_j $\triangleq$ Sound Pressure Level in the jth 1/3 Octave Band

f_p $\triangleq$ Peak Frequency - Hz

T $\triangleq$ Total Rotor Thrust - Lb

V_t $\triangleq$ Tip Speed - fps

A_b $\triangleq$ Total Blade Area - Ft^2

θ_1 $\triangleq$ Angle Between $\mathcal{L}$ Rotor Shaft and Line to Observer

r $\triangleq$ Distance to Observer - Ft

$\overline{C_L}$ $\triangleq$ Average Lift Coefficient = $\dfrac{6T}{V_T^2 \rho \sigma (\pi R^2)}$

σ $\triangleq$ Rotor Solidity

ρ $\triangleq$ Mass Density of Air - $\dfrac{LB\text{-}SEC^2}{FT^4}$

R $\triangleq$ Blade Radius - Ft

$S_{1/3}$ $\triangleq$ 1/3 Octave Band Correction from Figure 4

For average lift coefficients greater than .6, the method overpredicts data at a rapidly diverging rate and should not be used. At the present time, this point is probably academic since a review of modern helicopter designs indicates a range of operating lift coefficients from .31 to .56. All design charts in this report are limited to rotors with average lift coefficients of .6 or less.

Combined Noise.—Since the objective of the rotor noise prediction will generally be to permit calculation of one or more of the single number noise measures such as Perceived Noise Level, A Weighted Sound Pressure Level, or C Weighted Sound Pressure Level, it is desirable to combine the rotational and broadband noise sources into one-third octave band levels. Since the broadband noise has been calculated directly in the one-third octave band format, it will be necessary to transpose the rotational noise harmonics. The frequency of each harmonic can be found as follows:

$$f_n = \frac{V_T \cdot n \cdot N}{2\pi R} \tag{6}$$

Each harmonic can then be assigned to the preferred one-third octave band in which it falls (Ref. 10). At the higher frequencies, more than one rotor harmonic may fall within the limits of a particular band. The one-third octave band level can be calculated from:

$$SPL_{1/3} = \log^{-1}\left[\log SPL_{B_{1/3}} + \sum_{n_L}^{n_H} \log SPL_n\right] \tag{7}$$

where $SPL_{1/3} \triangleq$ Sound Pressure Level in the desired one-third octave band

$SPL_{B_{1/3}} \triangleq$ Broadband Sound Pressure Level in the desired one-third octave band from equation (5)

$SPL_n \triangleq$ Sound Pressure Level of the nth harmonic of rotational noise

$n_L \triangleq$ Harmonic number of the lowest harmonic whose frequency is above the lower limiting frequency of the desired one-third octave band

$n_H \triangleq$ Harmonic number of the highest harmonic whose frequency is below the upper limiting frequency of thedesired one-third octave band

If a particular harmonic has a frequency which is very close to the crossover frequency of two one-third octave bands, it should be apportioned to both according to the filter roll-off. An acceptable estimate, within the accuracy of the entire prediction, is to subtract 2 dB or 3 dB from the calculated harmonic level and assign the diminished value to each of the adjacent one-third octave bands. The one-third octave band levels can then be used to calculate other desired noise measures as described in Ref. 11.

Forward Flight

The aerodynamic loading, which produces rotor noise, is altered considerably between the hover and forward flight conditions. Not only do the harmonic and broadband airloads change due to the cyclic changes in tip speed and advance ratio, but at the higher speed range the components of compressibility induced profile drag noise and thickness noise which are negligible in hover increase so that they become significant, and in some cases the dominant noise source. Furthermore, the relative motion between the aircraft and the observer results in frequency distortion resulting in Doppler shift and a time dependent variation in spectrum and level due to continuously changing distance and directivity.

The analytical prediction of profile drag noise and thickness noise, at present, is considerably less well understood and verified than is rotational noise, while the prediction of broadband noise in forward flight is virtually unverified due to difficulties in separating it from other broadband sources such as airframe noise and engine noise. For these reasons, most forward flight noise predictions which are performed by industry are based on empirical extrapolation of hover noise.

A good aircraft to use as a basis for extrapolating noise of main rotors in flight is the Boeing Vertol Model 347 Technology Demonstrator. This aircraft, which is described in Ref. 12 is a tandem rotor helicopter whose airframe and rotor system were modified to minimize interactions between rotor blades and the tip vortices from other blades in the main rotor system. Since it is a tandem, there is, of course, no tail rotor noise and no noise due to interactions between the tail rotor and main rotor vortices. The acoustical signature of the 50,000 pound helicopter is probably the closest thing to pure rotor noise in forward flight which is available.

Figures 6 and 7 show the Perceived Noise Level and Effective Perceived Noise Level of the Model 347 helicopter as a function of advancing tip Mach number. The data was obtained from flight tests encompassing a forward speed range from 60 knots to 170 knots and rotational tip speeds from 653 to 738 ft per second. In hover, the Effective Perceived Noise Level becomes indeterminate due to the unlimited duration time, while at high forward speeds the increase in EPNL is due to the fact that the increase in sound pressure level more than offsets the decrease in exposure time due to speed. Also shown is the Perceived Noise Level in hover both measured and as predicted by the design charts. It is interesting to

note that while at the high advancing tip speeds maximum Perceived Noise Level does not increase as rapidly as does Effective Perceived Noise Level. This appears to be due to the fact that the high speed noise is primarily due to thickness and compressibility whose directivity maximizes in the plane of the rotor, thereby greatly increasing the time duration effect.

Work done by Boeing Vertol in 1970 related the high speed rise in noise level to the drag divergence Mach number of the blade. At, or near the tip, all subjective tests indicated that persons identified the noise as impulsive at an advancing tip speed of M_{DD} + .045. Figure 8, which is taken from the Boeing Vertol Technology Instruction Manual, shows the variation in M_{DD} with Mach number and lift coefficient for the cambered airfoil from which the data of Figures were derived. Figure 8b shows that near the tip the lift coefficient is approximately 0 so that M_{DD} is about .79. This value is indicated on Figure 6 and agrees very closely with the onset of noise increase.

For this level of prediction effort, it is suggested that the above data be considered as a basis for estimating the Effective Perceived Noise Level in forward flight through the relationship.

$$PNL_F = (PNL_H - 3.5) + f\ (M_{DD1,90} - M_{F1,90})$$

$$EPNL_F = (PNL_H - 10) + f\ (M_{DD1,90} - M_{F1,90})$$

where $PNL_F \triangleq$ Maximum Perceived Noise Level at forward speed (F)

$EPNL_F \triangleq$ Effective Perceived Noise Level at forward speed (F)

$PNL_H \triangleq$ Perceived Noise Level in hover

$M_{DD1,90} \triangleq$ Drag Divergence Mach Number at Blade Tip

$M_{F,1,90} \triangleq$ Advancing Tip Mach Number at Blade Tip

$f\ (M_{DD1,90} - M_{F1,90})$ is determined from Figure 9

It is best if M_{DD} is determined for each airfoil by wind tunnel testing. However since this may not always be the case, Figure 10 provides an estimate of M_{DD} at the tip as a function of blade thickness assuming a conventionally twisted blade with a cambered airfoil similar to a NASA-23010.

Performance Penalties

In order to assess the penalty which may be imposed by designing a rotor to a noise constraint, or in order to select the optimum rotor from several candidates which may produce the same noise levels, it is desirable to provide a means for measuring performance which can also be estimated using the same parameters which were required for the noise prediction. One such measure is the ratio of rotor and drive system weight to the thrust of the rotor. An example of the relationship between noise and this parameter can be seen by examining the impact of reducing noise by reducing tip speed. First of all, maintaining C_L will require increasing solidity such that the product $(V_t)^2$ (A_b) remains constant and hence an increase in blade radius chord, or number of blades is required, each with an attendant rotor weight increase. Secondly, decreasing rotor speed, while maintaining power, increases the torque in the drive system thereby requiring larger shafts, gears, transmission cases, bearings, etc. and causing the weight of the drive system to grow.

In order to develop an estimating procedure, two weight trends which had been developed by the Boeing Vertol Weights Engineering Staff for use in making preliminary design weight estimates were used. These curves which were slightly simplified for the current purpose are illustrated in Figure 11 in order to show goodness of fit to a wide variety of helicopters from which they were derived. Combining the two trend curves and converting horsepower to thrust, based on a rotor hover Figure of Merit of .55 resulted in Figure 12, which can be used to estimate the combined weight of the rotor and drive system. When divided by the rotor thrust, this becomes an index of relative lift efficiency. An example of the use of this procedure is given in Case 3 of Appendix B.

Design Parameters

The equations for Rotational and Broadband Sound Pressure Level predictions each include their own directivity functions and free field spherical spreading attenuation due to distance. No additional atmospheric or terrain effects on the propagated noise are included.

Examination of all the input parameters for rotational and broadband calculations indicates that they can be divided into three categories. The first group describes the constants associated with a given problem such as the distances and angles which define the geometrical location of the source and receiver, and the properties of the air such as density and speed of sound (for determining Mach number). A second

set of parameters are those which describe the airloading on the blade. The third set are those which describe the rotor design parameters, specifically they are:

$T \triangleq$ Total Rotor Thrust

$R \triangleq$ Blade Radius

$V_T \triangleq$ Blade Tip Speed

$A_b \triangleq$ Total Blade Area

$\sigma \triangleq$ Rotor Solidity

$N \triangleq$ Number of Blades

$C_L \triangleq$ Average Lift Coefficient

However,

$$\sigma = \frac{\pi R^2}{A_b}$$

$$C_L = \frac{6T}{V_t^2 \ \rho\sigma(\pi R^2)}$$

Since DL $\triangleq$ Disk Load $= \frac{T}{\pi R^2}$

$$C_L = \frac{6 \ DL}{V_t^2 \rho\sigma}$$

Thus, the rotor parameters which control noise can be collapsed to: T, V_t, σ, DL, N.

Since the formulation of the rotational noise involves complex Bessel functions, solution of that part of the noise spectrum is not very amenable to a hand calculation. In Ref. 1, Lowson and Ollerhead provide a set of design charts based on all their simplifying assumptions. Since it appears that, as a minimum, a different exponent for the harmonic decay term is advisable, these charts cannot be used directly. Rather than simply rederive the rotational noise charts as an independent effort by the Boeing Vertol Company, a computer program was written calculated the rotational noise and broadband noise independently, combined the rotational harmonics into the appropriate one-third octave bands, and then summed rotational and broadband noise in each third octave band. Calculations were then performed to obtain A and C weighted Sound Pressure Levels, Perceived Noise Level, and Tone Corrected Perceived Noise Level for the individual components

and combined signature. A sample output sheet is shown in Figures 5a, 5b, and 5c. This program leaves as input such variables as harmonic decay exponent, and thrust, drag, radial force ratios. The combined design charts resulting from this program are presented in a later section of this report.

DATA BASE

Comparison of Predicted and Measured Data

Figures 13 and 14 present comparisons between predicted levels using the methods described in the preceding section and measured sound pressure level spectra for a three-bladed, 60 ft diameter CH-47 rotor operating on a test tower (Figure 15 and Ref. 11). Since the tower was electrically powered, noise due to the drive system was well below that of the rotor. The comparisons which include the complete range of tip speeds and lift coefficients show very good agreement between predicted and measured spectra at high lift coefficient and adequate agreement at low lift coefficient. In general, it would be expected that the measured data might exceed the predicted values because the analytical procedures for harmonic noise prediction do not account for the low velocity winds and small scale turbulence which is invariably present. In all cases, it is noted that some of the low frequency predictions are very low with respect to the measurement. These are the one-third octave bands whose frequency limits do not encompass any rotor harmonic frequencies. In practice, actual data never seems to display these sharp dips, believed to be due to pseudo-noise due to rotor induced wind which is very high even at several diameters distance and can only be partially attenuated by microphone windscreens. Although this problem requires further investigation, it should be noted that these discrepancies always appear at frequencies of 40 Hz and below and, therefore, have no influence on Perceived Noise Level, which does not consider frequencies below the 50 Hz one-third octave band and on A Weighted Sound Pressure Level which is deemphasized about 30 dB at 50 Hz, but might make the data measured with a C weighted filter about 2 dB high.

A comparison of measured and predicted levels for 22 cases of the CH-47 rotor, covering the entire tip speed and thrust range indicates the following mean differences between measured and calculated values; +2.04 PNdB, +3.08 dBA, +2.52 dBC. In each case, the mean of the data exceeded the mean of the predictions. Although it is difficult to quantify a required prediction accurately, the above indicated correlations are completely adequate for comparing different rotor designs. Research to further improve absolute prediction accuracy is encouraged due to the performance penalties which

can be incurred by limiting rotor speeds in order to ensure meeting noise requirements.

Limits of Applicability

It should be recognized that both the harmonic and broadband prediction methods are based on data from an existing rotor and that application to rotors which are drastically dissimilar may lead to substantial error.

Rotational noise is sensitive to airload harmonic decay rate which was adjusted from the original assumptions as described in the preceding section. The relationships between rotor design and amplitude of higher harmonic airloads are not fundamentally understood but intuitively it is not unreasonable to associate them with airfoil shape and blade dynamic motion. A more specific example of the effect of blade stiffness on harmonic noise prediction is illustrated in Figure 16 which shows the measured harmonic noise levels from a helicopter with an all fiberglass blade which is torsionally rather soft. Also shown are analytical predictions based on the following airloads:

(1) Airloads measured on a steel spar blade. These are the airloads which are assumed in the Ref. 1 prediction method.

(2) Airloads which were analytically predicted assuming that the blade is infinitely rigid.

(3) Airloads which were analytically predicted using the best available torsional stiffness and inertia data for the actual blade.

From Figure 16, it is evident that although the first noise harmonic is relatively insensitive to blade stiffness, the same is not true of the higher harmonics. Unfortunately, the type of analysis which permits variation of blade stiffness is a rather complex computer program which is not amenable to reduction to chart format. It is believed that the adjustment to the loading law has essentially updated the analysis but care must be taken if rotors with radical changes in stiffness are contemplated.

Since the design charts in this section are for the prediction of hover noise only, even the maximum tip speed of 800 ft/sec results in a tip Mach number of only about .7 and considerations of thickness noise and/or drag divergence may be considered of secondary importance in the analysis. The same is not necessarily true in forward flight where advancing

tip Mach numbers are not inconsequential, and thickness is considered in that section of the report.

Broadband noise prediction, at the current stage of development, is even more empirical than harmonic noise. Although the change in the lift coefficient term at a value of .48 appears to fit data for current rotors up to values of .6, the reasons for this apparent discontinuity are not readily evident. It is possible that a transition from a trailing edge to tip vortex mechanism is taking place. On the other hand, there is also evidence (Ref. 13) to suggest that, under certain conditions, interaction between rotor blades and tip vortices shed by preceding blades results in harmonic noise generation in the frequency range normally attributed to broadband noise. Within the limits previously stated, the broadband prediction method used appears to give reasonable results but caution should be used in application to rotors with greatly different solidity, blade chord, or airfoil shape.

All predictions are for free field propagation only and do not consider either ground reflections or excess atmospheric attenuation.

NOISE PREDICTION CHARTS

Chart Design

The objective of this project was to reduce the noise prediction procedures to a simple task in a format readily available to the rotor designer. However, in order to perform such procedures, the noise must be calculated for a particular location from the rotor which can be considered as a reference location for comparing different rotors. The reference location selected was an altitude of 150 meters and a sideline distance of 150 meters. This location was selected because it appears fairly certain that it will correspond to one of the measurement locations being considered by the FAA and ICAO for noise certification. Furthermore, a 45° angle from the rotor plane is one at which prediction is most reliable due to avoidance of extremely rapid change of directivity such as occurs in the rotor plane, and directly below the rotor.

More than 1,000 different rotor configurations were predicted to form a basis for the design charts which are contained in Appendix A. They are divided into three main groups for prediction of Perceived Noise Level, A Weighted Sound Pressure Level, or C Weighted Sound Pressure Level. Within each group there is a separate chart for each tip speed. These charts permit prediction of the selected noise for a

six-bladed rotor. A table, associated with each chart, is provided for correction for other numbers of blades. After looking at the charts, some questions may arise about the shape of some of the curves. For example, on the PNL and dBA charts, at a tip speed of 500 fps, the noise at higher thrusts is predicted to be less than at lower thrusts. This is because at low tip speeds and high thrusts the peak broadband frequency is driven down into the insensitive range for PNL and dBA weighting. On the charts for tip speeds of 600 and 700 fps, notice that the highest disk load shown results in a large increase in noise level compared with the lower ones. This is caused by the use of two discontinuous functions for broadband noise prediction which separate at $C_L = .48$. For the C Weighted Sound Pressure Level, tip speed of 700 fps, and a disk load of 8 lb/ft^2, the curve has a much different shape than the others. These apparent inconsistencies in families of curves all arise from the complex interrelationships between the design parameters, rotor noise levels, spectrum shapes, and the weighting of the noise measuring units.

Use of the Noise Prediction Charts

The general format of the prediction charts provides a very simple method for estimating the noise of a hovering rotor at the reference sideline distance and altitude of 150 meters. The required charts and tables are contained in Appendix A and numerical examples are presented in Appendix B.

Cases Not Requiring Interpolation.—The most direct use of the charts is possible when all rotor design parameters can be found directly on the noise prediction charts. In these cases, proceed as described below and illustrated in Figure 17:

Step 1. Select chart corresponding to the desired tip speed.

Step 2. Enter upper chart at value of rotor thrust.

Step 3. Locate intersection ofthrust value with appropriate disk load curve.

Step 4. Select appropriate line in lower chart based on disk load and solidity using table on chart.

Step 5. Drop down vertically from point determined in Step 3 to line selected in Step 4.

Step 6. Read horizontally from point located in Step 5 and read value of partial SPL from lower vertical scale.

Step 7. Determine adjustment for number of rotor blades from appropriate table.

Step 8. Add adjustment from Step 7 to partial SPL found in Step 6 to obtain SP.

A numerical example of this type of calculation is presented in Appendix B, Case 1.

Cases Requiring Interpolation.—The most common use of the design charts is when some or all of the rotor parameters cannot be found directly and must be interpolated. In this case, it will be necessary to bracket the desired design with combinations of tip speeds, disk loads, and solidities which can be found directly from the charts, determine the corresponding Sound Pressure Levels for these points and using average lift coefficient as the unifying parameter perform interpolations using the procedure outlined below and Figures 18 and 19. It is assumed that the type of example given in Case 1 is fully understood.

Step 1. Calculate the C_L of the desired rotor at its design tip speed using the formula on page 11. If the C_L is greater than 0.6, these charts cannot be used. Also, calculate the C at 500, 600, 700, 800 ft/sec. If any C_L is above 0.6, do not use the chart for that tip speed.

Step 2. Select combinations of solidity and disk load values which appear on the design charts and bracket the design point.

A - Disk load less than design point
Solidity " " " "
B - Disk load " " " "
Solidity greater " " "
C - Disk load " " " "
Solidity " " " "
D - Disk load " " " "
Solidity less " " "

Step 3. For each point (A,B,C,D) use the procedure described in Case 1 to predict the noise levels at each tip speed.

Step 4. For each point (A,B,C,D) calculate the average lift coefficient using the formula on page 11 at each tip speed.

Step 5. Plot the points A,B,C, and D as shown in Figure 18 for each tip speed.

Step 6. Connect the points as illustrated in Figure 18 to form a grid with constant disk load and constant solidity lines.

Step 7. Linearly interpolate design disk load and design solidity lines. The intersection of these lines defines the desired design point at each tip speed.

Step 8. As a check, the C indicated for the design point at the considered tip speed should equal the calculated C for design input values and the tip speed being considered.

Step 9. Read the Design Reference SPL's from the plots.

Step 10. Having obtained the results from Steps 1 through 9 plot the Design Reference SPL's against tip speed as shown in Figure 19.

Step 11. Using the points plotted in Step 10, construct an SPL-tip speed trend curve.

Step 12. Locate the design tip speed on the horizontal axis and proceed vertically to the SPL-V_T curve.

Step 13. Read horizontally to the left and round off to the nearest 0.5 dB to obtain the Design SPL.

A numerical example of this type of calculation is presented in Appendix B, Case 2.

Design of a Rotor to Meet a Noise Limit.—As the commercial market for helicopters increases, it will be necessary in the preliminary design stages to choose a rotor to meet a noise limit. The thrust of the aircraft is known and the number of blades is usually confined to two or three possibilities. For each number of blades possibility, it is necessary to find the solidity-disk load-tip speed combination that comes closest to the noise limit. Then, using the Rotor and Drive System Weight Trend Curve, Figure 12, the most efficient rotor possibility can be found. A good understanding of Cases 1 and 2 is recommended for this example.

Step 1. Start at a tip speed of 500 ft/sec.

Step 2. Enter the chart at the design thrust and cross all the disk load curves as shown in Figure 20.

Step 3. Drop lines vertically from the intersections of the design thrust and the disk loads to the appropriate solidity-disk load curves obtained from the table at the bottom of the page.

Step 4. Move to the left from each solidity-disk load line to obtain the noise levels for each combination.

Step 5. Identify the combination that falls closest to the limit without exceeding it. Be certain the number of blades correction does not put the combination above the noise limit. If the rotor combination is less than the prescribed noise limit, the tip speed can be increased to raise the noise level up to the limit. This is done by plotting the noise level versus tip speed for the rotor combination and by noting the tip speed where the curve crosses the noise limit as illustrated in Figure 21.

Step 6. Repeat Steps 2 through 5 for tip speeds of 600, 700, and 800 ft/sec.

Step 7. Using the parameters found in Steps 1 through 6, for each rotor configuration calculate K_R and K_D as formulated in Figure 12.

Step 8. Entering Figure 12 at each value of $K_R + K_D$, find the rotor and drive system weight for each rotor configuration.

Step 9. The lowest rotor and drive system weight represents the most efficient rotor meeting the noise specification.

A numerical example of this type of calculation is presented in Appendix B, Case 3.

CONVERSION TO SUBJECTIVE NOISE SCALES

There are occasions when it is desirable to compare two rotors on the basis of subjective response, or potential annoyance to the public. Such situations may arise when one knows of an existing rotor which is throught to have an acceptable acoustical signature and wishes to use it as a standard for the design of new rotors. Another use of such information is if one is evaluating candidate rotors for a given helicopter and wishes to determine which ones will be judged preceptibly more or less annoying than others. Still a third use of subjective response evaluations are in comparing the noise of a helicopter rotor with other noises to which people may be exposed, such as automobile traffic, railroad trains, or construction noise.

An investigation into the annoyance due to helicopter rotor noise which is directly applicable to the results of the noise prediction procedures developed in this study is reported in Reference 14. Figure 22 presents the level of broadband noise, measured in PNdB, which is as annoying as a helicopter rotor also measured in PNdB. This chart might be used in equating that annoyance due to helicopter rotors with that of subsonic jet airplanes. Note, for example, that a 95 PNdB rotor and 95 PNdB broadband noise are subjectively equivalent but that an 85 PNdB rotor is judged no more annoying than a 75 PNdB broadband noise, while a 105 PNdB rotor is considered as annoying as a 108 PNdB broadband noise.

Figure 23 provides a method for determining the equivalent A Weighted Sound Pressure Level of a rotor in terms of its dBA and dBC levels. As described in Reference 14, this is based on the fact that as a rotor becomes more impulsive due to rapid increase in the higher harmonics as compared with the first few rotor harmonics. Referring to Figure 23, it can be seen that a combination of 75 dBA and 110 dBC or 80 dBA and 93 dBC are both judged equally annoying as a broadband noise whose level is 80 dBA.

Another useful way of using this format is in comparing the potential annoyance of different candidate rotor designs as illustrated in Figure 24 and the following table:

POINT (Ref. Fig. 24)	dBA	dBC	EQUIVALENT BROADBAND dBA
1	85	95	85
2	80	100	82.5
3	90	90	88

APPENDIX A

This appendix contains the Noise Prediction Charts

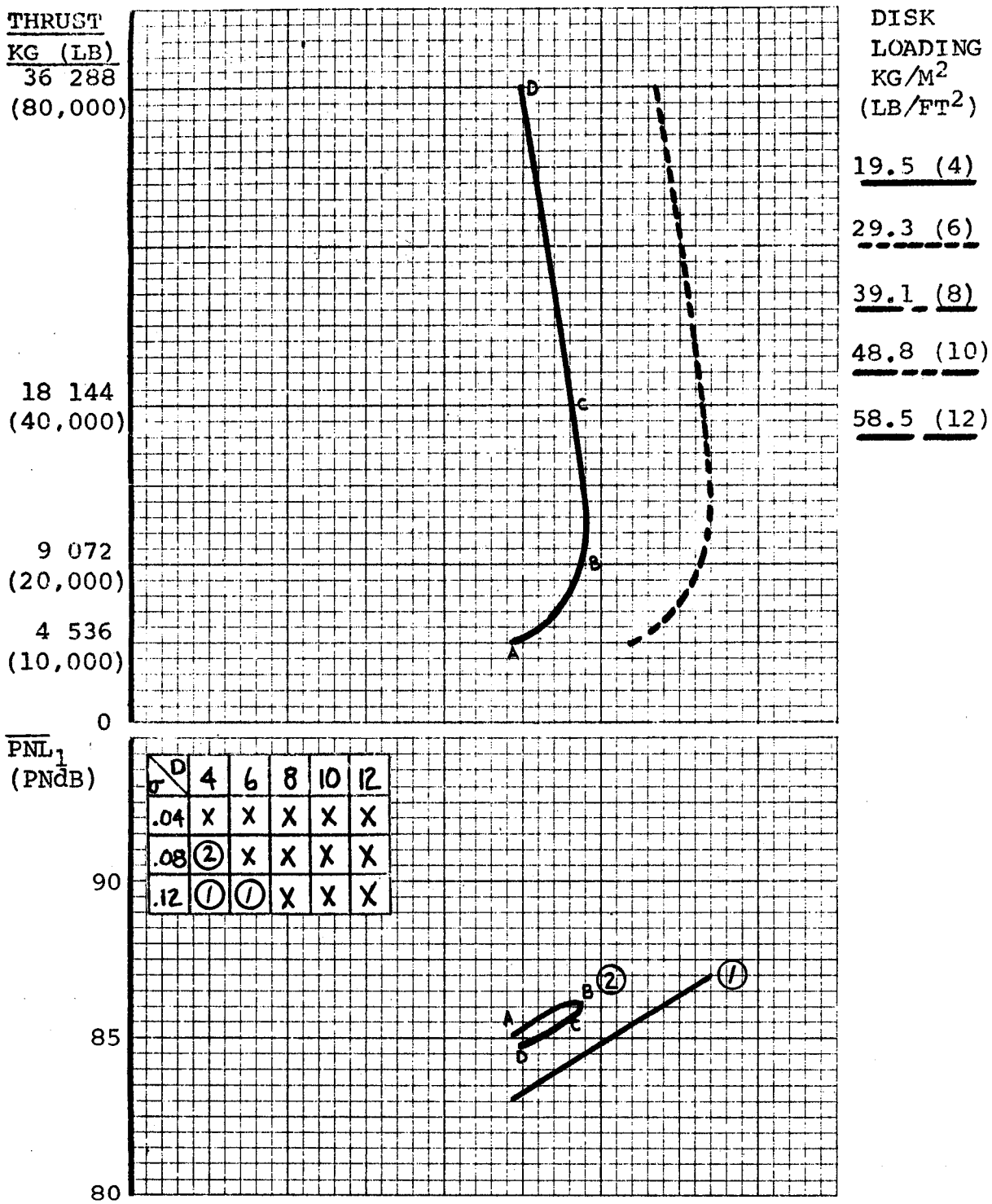

FIGURE A-1 PERCEIVED NOISE LEVEL PREDICTION CHART - V_T=153 M/S (500 FT/S); N=6

TABLE A-1 ADJUSTMENT FOR NUMBER OF BLADES

PERCEIVED NOISE LEVEL - V_T = 153 M/S (500 FT/S)

		σ = .04				σ = .08				σ = .12			
D	N	THRUST, KG/LB				THRUST, KG/LB				THRUST, KG/LB			
KG/M^2		4536	9072	18144	36287	4536	9072	18144	36287	4536	9072	18144	36287
LB/FT^2		10000	20000	40000	80000	10000	20000	40000	80000	10000	20000	40000	80000
19.5	2					0	0	-0.5	-0.5	+0.5	0	+0.5	-2.0
4	3					0	0	-0.5	-0.5	0	0	+0.5	-1.0
	4					0	0	0	-1.0	0	0	0	-1.0
	5					0	0	0	-0.5	0	0	-0.5	-1.0
29.3	2									+0.5	+0.5	-0.5	-1.0
6	3									+0.5	0	0	-0.5
	4									0	0	0	-0.5
	5									0	0	-0.5	-0.5
39.1	2												
8	3												
	4												
	5												
48.8	2												
10	3												
	4												
	5												
58.5	2												
12	3												
	4												
	5												

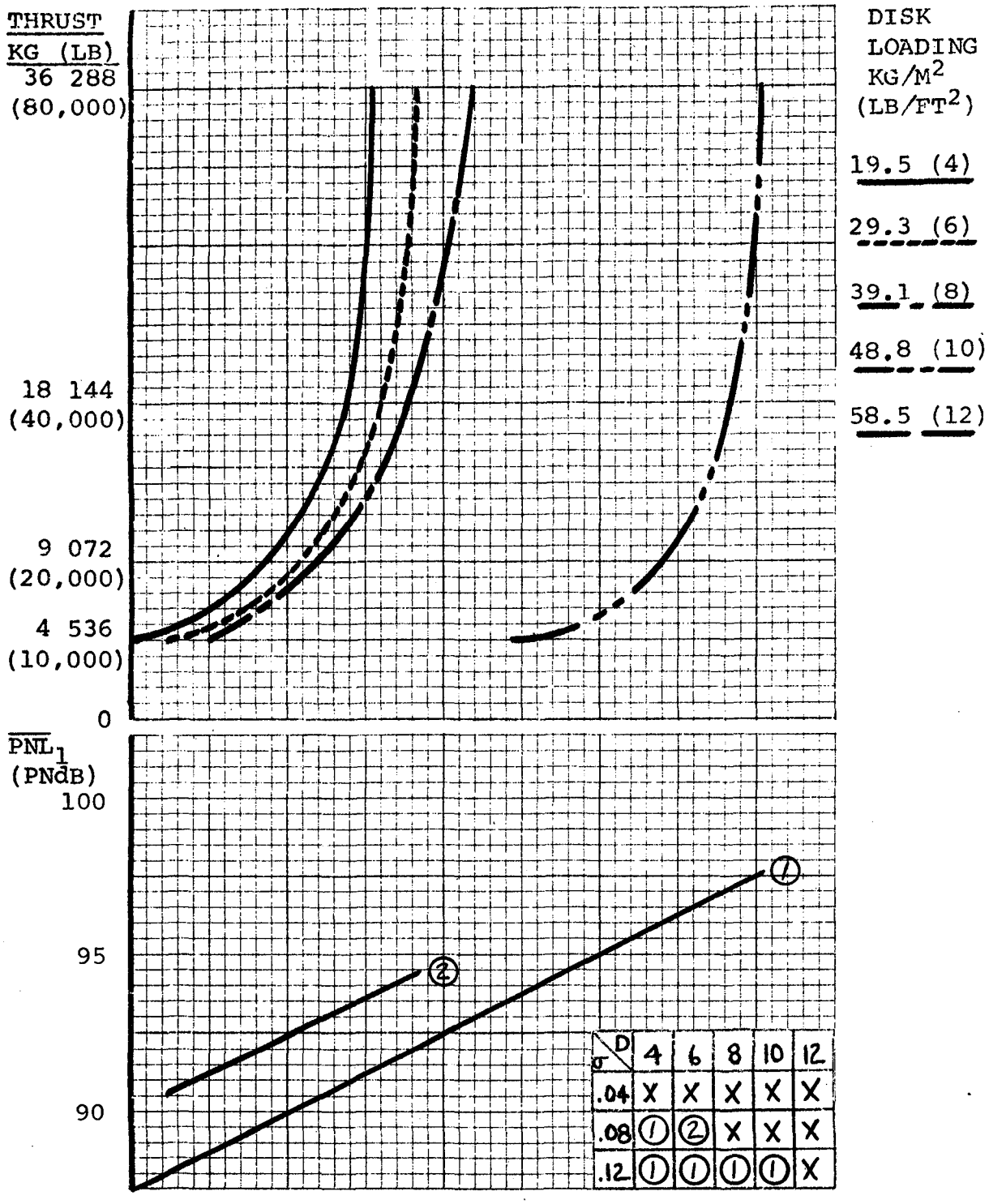

FIGURE A-2 PERCEIVED NOISE LEVEL PREDICTION CHART - V_T=183 M/S (600 FT/S); N=6

TABLE A-2 ADJUSTMENT FOR NUMBER OF BLADES PERCEIVED NOISE LEVEL - V_T = 183 M/S (600 FT/S)

		σ = .04				σ = .08				σ = .12			
D	N	THRUST, KG/LB				THRUST, KG/LB				THRUST, KG/LB			
KG/M^2		4536	9072	18144	36287	4536	9072	18144	36287	4536	9072	18144	36287
LB/FT^2		10000	20000	40000	80000	10000	20000	40000	80000	10000	20000	40000	80000
19.5	2					+0.5	+0.5	0	-0.5	+0.5	+0.5	0	-0.5
4	3					+0.5	0	0	-0.5	+0.5	0	0	-0.5
	4					0	0	0	-0.5	0	0	0	-0.5
	5					0	0	0	0	0	0	0	0
29.3	2					+0.5	+0.5	0	-0.5	+0.5	+0.5	0	-0.5
6	3					+0.5	0	0	-0.5	+0.5	0	0	-0.5
	4					0	0	0	0	0	0	0	0
	5					0	0	0	0	0	0	0	0
39.1	2									+1.5	+1.0	+0.5	-0.5
8	3									+0.5	+0.5	+0.5	-0.5
	4									+0.5	+0.5	+0.5	-0.5
	5									0	0	0	-0.5
48.8	2									+0.5	+0.5	+0.5	0
10	3									+0.5	+0.5	0	0
	4									0	0	0	0
	5									0	0	0	0
58.5	2												
12	3												
	4												
	5												

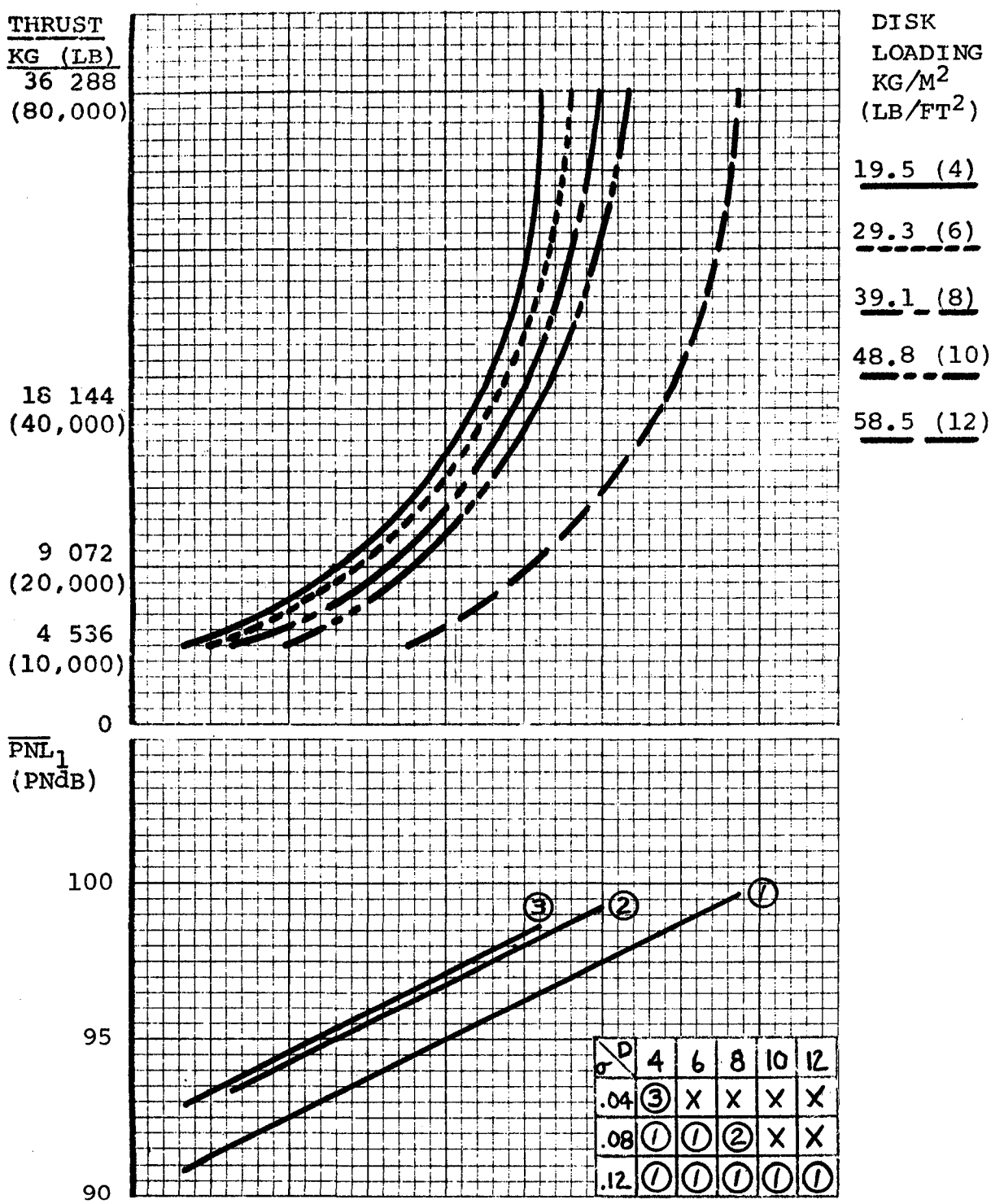

FIGURE A-3 PERCEIVED NOISE LEVEL PREDICTION CHART - V_T=214 M/S (700 FT/S); N=6

TABLE A-3 ADJUSTMENT FOR NUMBER OF BLADES
PERCEIVED NOISE LEVEL - V_T = 214 M/S (700 FT/S)

		σ = .04				σ = .08				σ = .12			
D	N	THRUST, KG/LB				THRUST, KG/LB				THRUST, KG/LB			
KG/M^2		4536	9072	18144	36287	4536	9072	18144	36287	4536	9072	18144	36287
LB/FT^2		10000	20000	40000	80000	10000	20000	40000	80000	10000	20000	40000	80000
19.5	2	+0.5	0	0	0	+0.5	+0.5	0	0	+0.5	+0.5	0	0
4	3	+0.5	0	0	0	+0.5	0	0	0	+0.5	0	0	0
	4	0	0	0	0	0	0	0	0	0	0	0	0
	5	0	0	0	0	0	0	0	0	0	0	0	0
29.3	2					+1.0	+0.5	+0.5	0	+1.0	+0.5	+0.5	0
6	3					+0.5	+0.5	+0.5	0	+0.5	+0.5	+0.5	0
	4					+0.5	0	0	0	+0.5	0	0	0
	5					0	0	0	0	0	0	0	0
39.1	2					+1.0	+0.5	+0.5	0	+1.5	+1.0	+0.5	0
8	3					+0.5	+0.5	0	0	+1.0	+0.5	+0.5	0
	4					0	0	0	0	+0.5	0	0	0
	5					0	0	0	0	0	0	0	0
48.8	2									+1.5	+1.0	+1.0	0
10	3									+1.0	+1.0	+0.5	0
	4									+0.5	+0.5	+0.5	0
	5									0	0	0	0
58.5	2									+1.5	+1.0	+1.0	+0.5
12	3									+0.5	+0.5	+0.5	+0.5
	4									0	+0.5	0	0
	5									-0.5	0	0	0

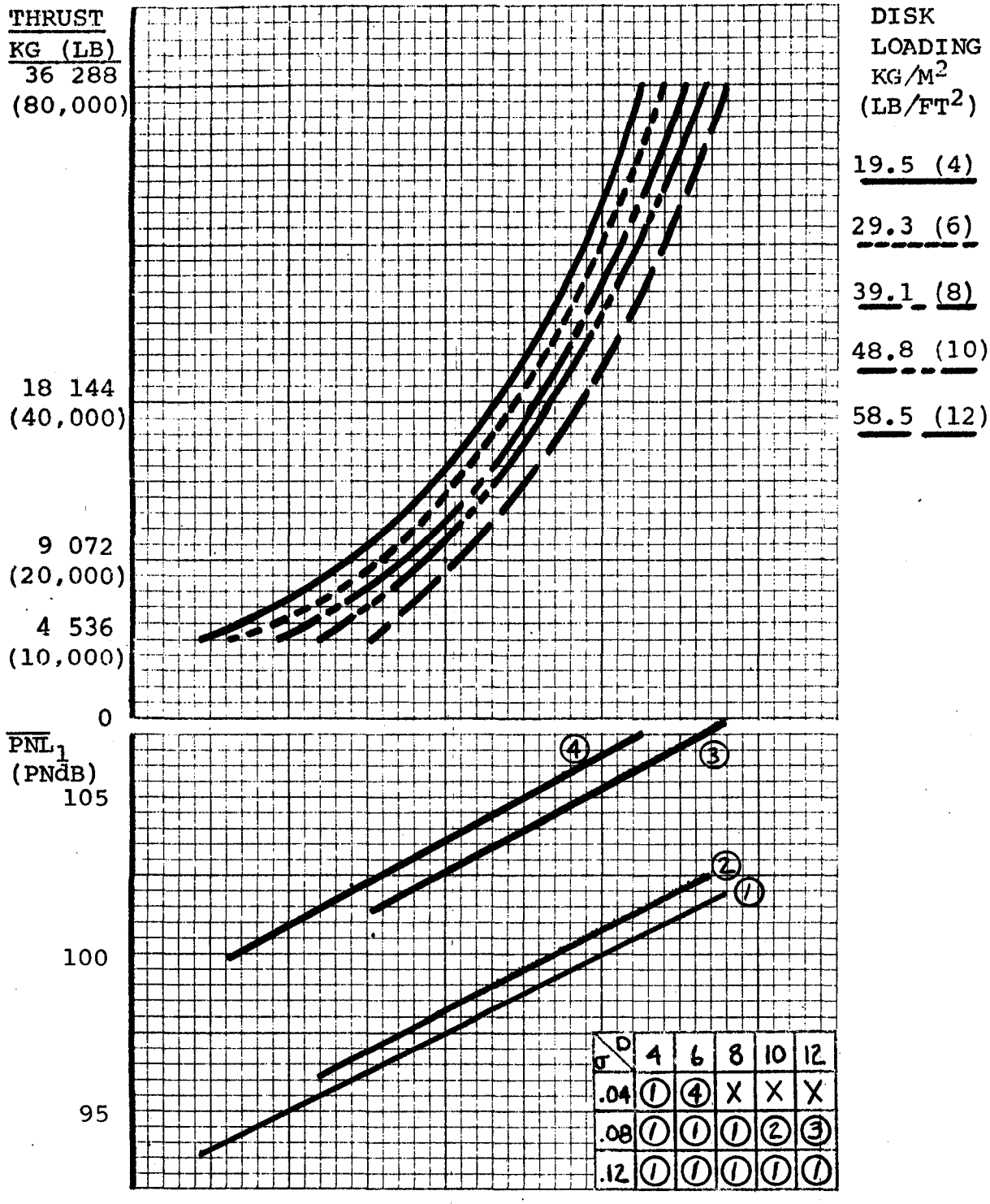

FIGURE A-4 PERCEIVED NOISE LEVEL PREDICTION CHART - V_T=244 M/S (800 FT/S); N=6

TABLE A-4 ADJUSTMENT FOR NUMBER OF BLADES PERCEIVED NOISE LEVEL - V_T = 244 M/S (800 FT/S)

		σ = .04				σ = .08				σ = .12			
D	N	THRUST, KG/LB				THRUST, KG/LB				THRUST, KG/LB			
KG/M^2		4536	9072	18144	36287	4536	9072	18144	36287	4536	9072	18144	36287
LB/FT^2		10000	20000	40000	80000	10000	20000	40000	80000	10000	20000	40000	80000
19.5	2	+1.0	+0.5	+0.5	0	+1.0	+0.5	+0.5	0	+1.0	+0.5	+0.5	0
4	3	+0.5	+0.5	0	0	+0.5	+0.5	0	0	+0.5	+0.5	0	0
	4	0	0	0	0	0	0	0	0	0	0	0	0
	5	0	0	0	0	0	0	0	0	0	0	0	0
29.3	2	+0.5	+0.5	0	0	+1.0	+0.5	+0.5	+0.5	+1.0	+0.5	+0.5	+0.5
6	3	+0.5	0	0	0	+0.5	+0.5	0	0	+0.5	+0.5	0	0
	4	0	0	0	0	+0.5	+0.5	0	0	+0.5	+0.5	0	0
	5	0	0	0	0	0	0	0	0	0	0	0	0
39.1	2					+1.5	+1.0	+0.5	+0.5	+1.5	+1.0	+0.5	+0.5
8	3					+0.5	+0.5	+0.5	0	+0.5	+0.5	+0.5	0
	4					+0.5	+0.5	+0.5	0	+0.5	+0.5	+0.5	0
	5					0	+0.5	0	0	0	+0.5	0	0
48.8	2					+1.5	+1.5	+1.0	+0.5	+1.5	+1.5	+1.0	+0.5
10	3					+0.5	+1.0	+0.5	0	+0.5	+1.0	+0.5	0
	4					0	+0.5	0	0	0	+0.5	0	0
	5					-0.5	0	0	0	-0.5	0	0	0
58.5	2					+0.5	+0.5	+0.5	0	+1.5	+1.5	+1.0	+0.5
12	3					+0.5	+0.5	+0.5	0	+0.5	+1.0	+0.5	+0.5
	4					0	0	0	0	0	+0.5	+0.5	0
	5					-0.5	0	0	0	-1.0	+0.5	0	0

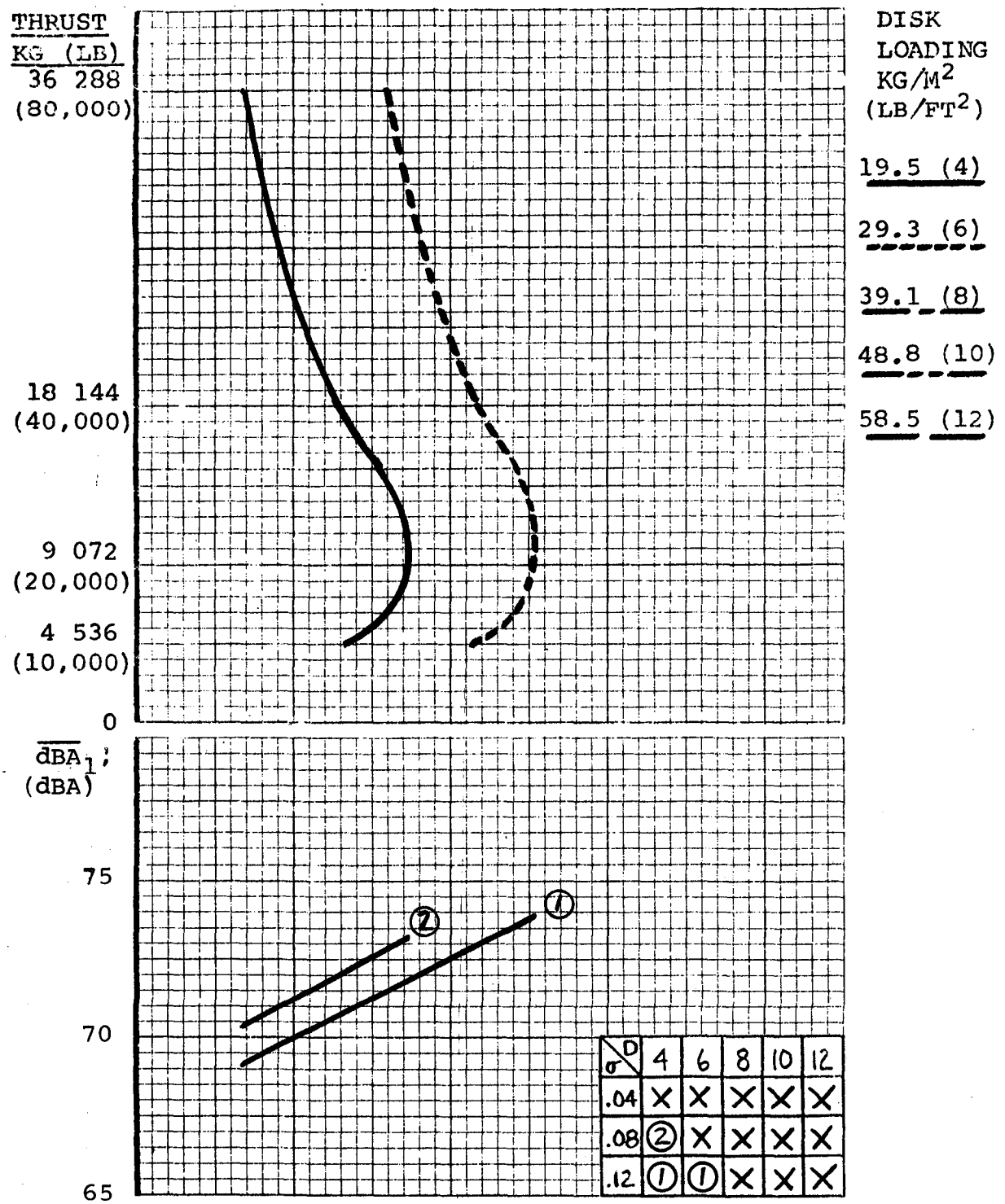

FIGURE A-5 A WEIGHTED SOUND PRESSURE LEVEL PREDICTION CHART - V_T=153 M/S (500 FT/S); N=6

TABLE A-5 ADJUSTMENT FOR NUMBER OF BLADES

A WEIGHTED SOUND PRESSURE LEVEL - V_T = 153 M/S (500 FT/S)

		σ = .04				σ = .08				σ = .12			
D	N	THRUST, KG/LB				THRUST, KG/LB				THRUST, KG/LB			
KG/M^2		4536	9072	18144	36287	4536	9072	18144	36287	4536	9072	18144	36287
LB/FT^2		10000	20000	40000	80000	10000	20000	40000	80000	10000	20000	40000	80000
19.5	2					-0.5	-0.5	-0.5	-1.0	-0.5	-0.5	-0.5	-1.0
4	3					0	-0.5	-0.5	-0.5	-0.5	-0.5	-0.5	-1.0
	4					0	0	-0.5	-0.5	0	-0.5	-0.5	-1.0
	5					0	0	0	-0.5	0	0	-0.5	-0.5
29.3	2									-0.5	-0.5	-1.0	-1.5
6	3									-0.5	-0.5	-1.0	-1.5
	4									-0.5	-0.5	-0.5	-1.0
	5									0	-0.5	-0.5	-0.5
39.1	2												
8	3												
	4												
	5												
48.8	2												
10	3												
	4												
	5												
58.5	2												
12	3												
	4												
	5												

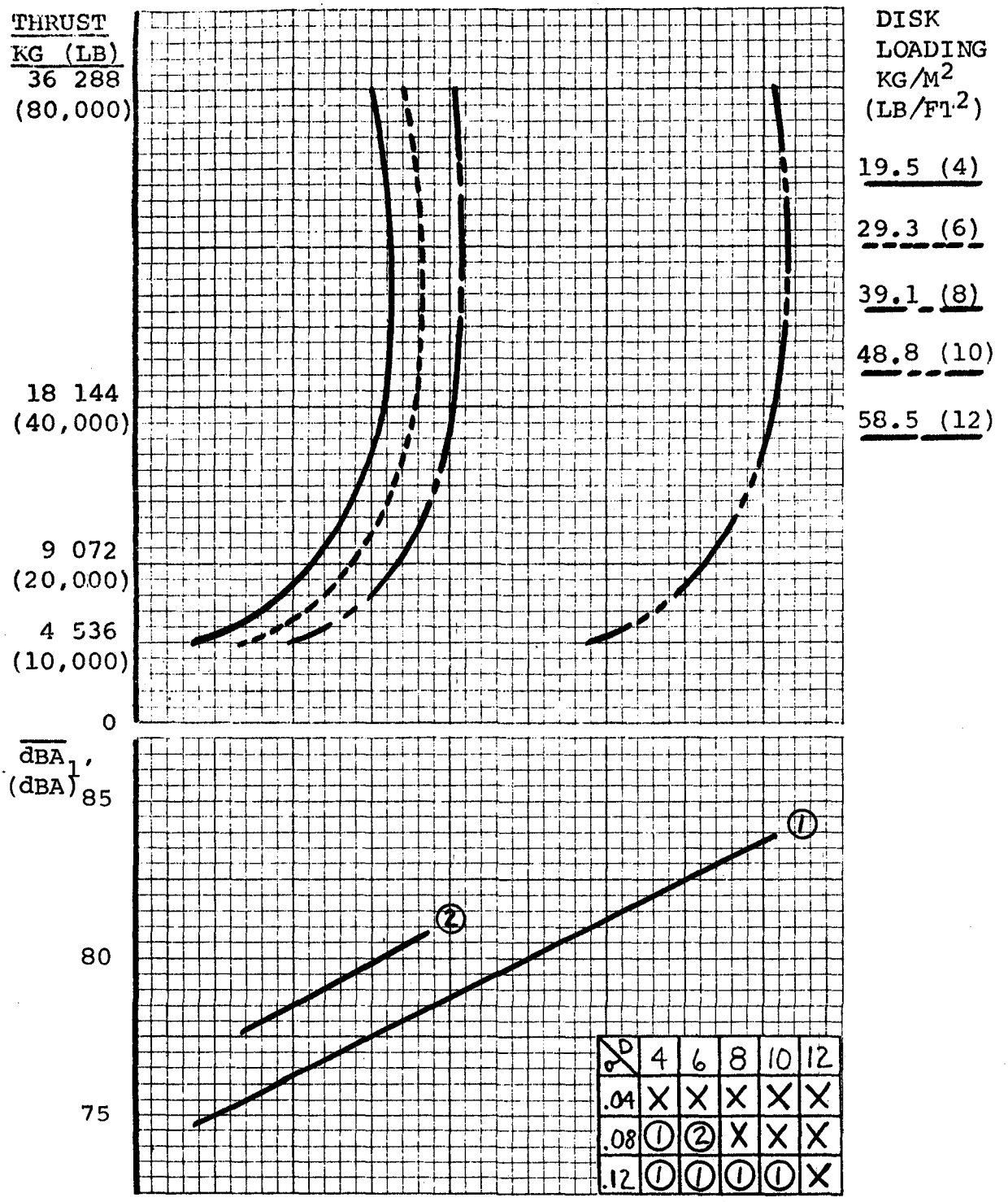

FIGURE A-6 A WEIGHTED SOUND PRESSURE LEVEL PREDICTION CHART - V_T=183 M/S (600 FT/S); N=6

TABLE A-6 ADJUSTMENT FOR NUMBER OF BLADES

A WEIGHTED SOUND PRESSURE LEVEL - V_T = 183 M/S (600 FT/S)

		σ = .04				σ = .08				σ = .12			
D	N	THRUST, KG/LB				THRUST, KG/LB				THRUST, KG/LB			
KG/M^2		4536	9072	18144	36287	4536	9072	18144	36287	4536	9072	18144	36287
LB/FT^2		10000	20000	40000	80000	10000	20000	40000	80000	10000	20000	40000	80000
19.5	2					-0.5	-0.5	-0.5	-0.5	-0.5	-0.5	-0.5	-0.5
4	3					-0.5	-0.5	-0.5	-0.5	-0.5	-0.5	-0.5	-0.5
	4					0	0	0	0	0	0	0	0
	5					0	0	0	0	0	0	0	0
29.3	2					-0.5	-0.5	-0.5	-0.5	-0.5	-0.5	-0.5	-0.5
6	3					0	0	-0.5	-0.5	-0.5	-0.5	-0.5	-0.5
	4					0	0	0	-0.5	0	-0.5	-0.5	-0.5
	5					0	0	0	0	0	0	-0.5	0
39.1	2									-0.5	-1.0	-1.0	-1.0
8	3									-0.5	-0.5	-0.5	-1.0
	4									0	-0.5	-0.5	-0.5
	5									0	-0.5	-0.5	-0.5
48.8	2									0	-0.5	-0.5	-0.5
10	3									0	0	0	-0.5
	4									0	0	0	-0.5
	5									0	0	0	0
58.5	2												
12	3												
	4												
	5												

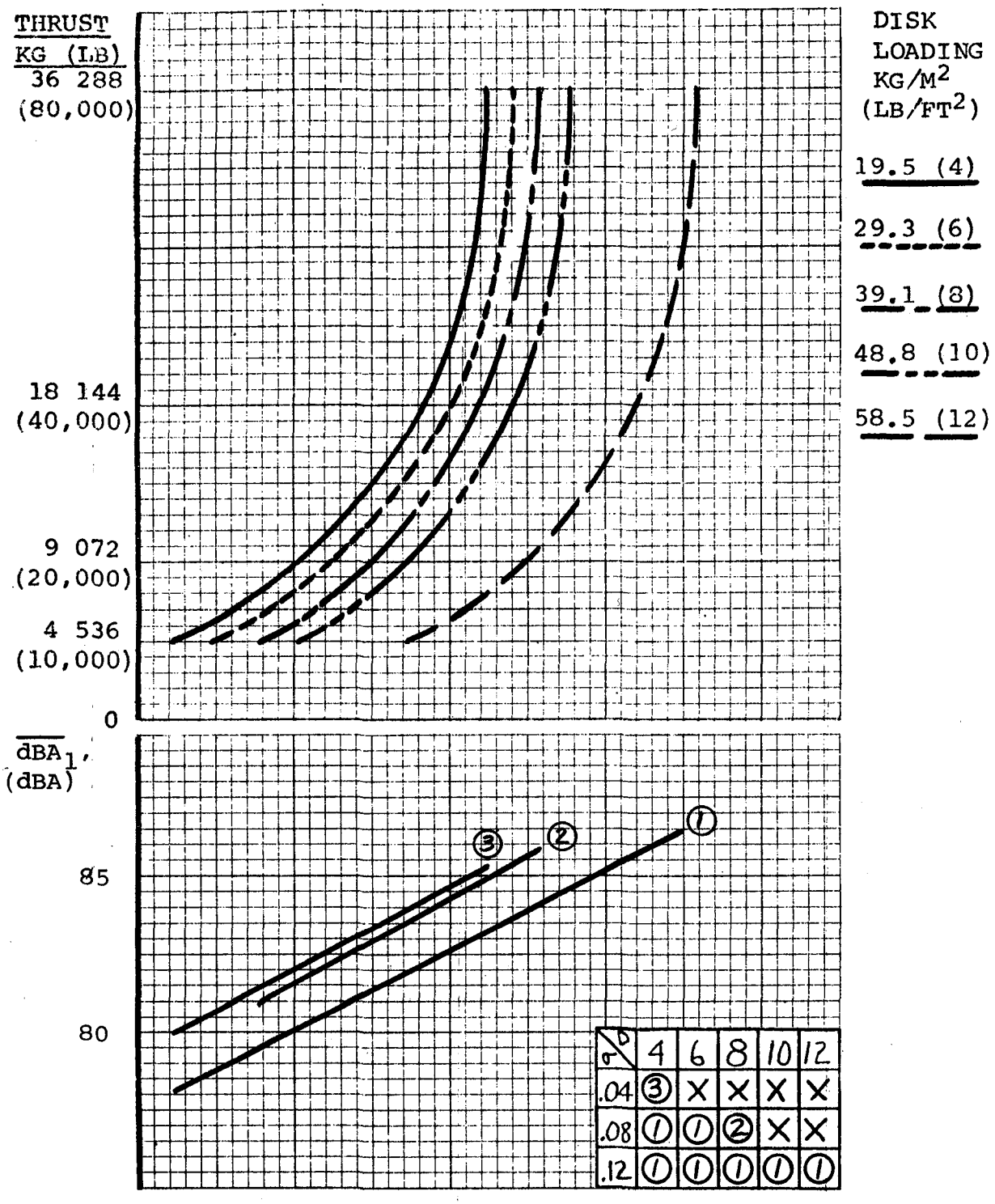

FIGURE A-7 A WEIGHTED SOUND PRESSURE LEVEL PREDICTION CHART - V_T=214 M/S (700 FT/S); N=6

TABLE A-7 ADJUSTMENT FOR NUMBER OF BLADES

A WEIGHTED SOUND PRESSURE LEVEL - V_T = 214 M/S (700 FT/S)

		σ = .04				σ = .08				σ = .12			
D	N	THRUST, KG/LB				THRUST, KG/LB				THRUST, KG/LB			
KG/M^2		4536	9072	18144	36287	4536	9072	18144	36287	4536	9072	18144	36287
LB/FT^2		10000	20000	40000	80000	10000	20000	40000	80000	10000	20000	40000	80000
19.5	2	0	0	0	0	-0.5	-0.5	-0.5	0	-0.5	-0.5	-0.5	0
4	3	0	0	0	0	0	0	0	0	0	0	0	0
	4	0	0	0	0	0	0	0	0	0	0	0	0
	5	0	0	0	0	0	0	0	0	0	0	0	0
29.3	2					-0.5	-0.5	-0.5	-0.5	-0.5	-0.5	-0.5	-0.5
6	3					0	-0.5	-0.5	-0.5	0	-0.5	-0.5	-0.5
	4					0	0	-0.5	-0.5	0	0	-0.5	-0.5
	5					0	0	0	0	0	0	0	0
39.1	2					0	-0.5	-0.5	-0.5	-0.5	-0.5	-0.5	-0.5
8	3					0	-0.5	-0.5	-0.5	0	-0.5	-0.5	-0.5
	4					0	0	0	-0.5	0	0	-0.5	-0.5
	5					0	0	0	0	0	0	0	-0.5
48.8	2									0	-0.5	-0.5	-1.0
10	3									0	-0.5	-0.5	-0.5
	4									0	-0.5	-0.5	-0.5
	5									0	-0.5	-0.5	-0.5
58.5	2									0	-0.5	-0.5	-0.5
12	3									0	0	-0.5	-0.5
	4									0	0	-0.5	-0.5
	5									0	0	-0.5	0

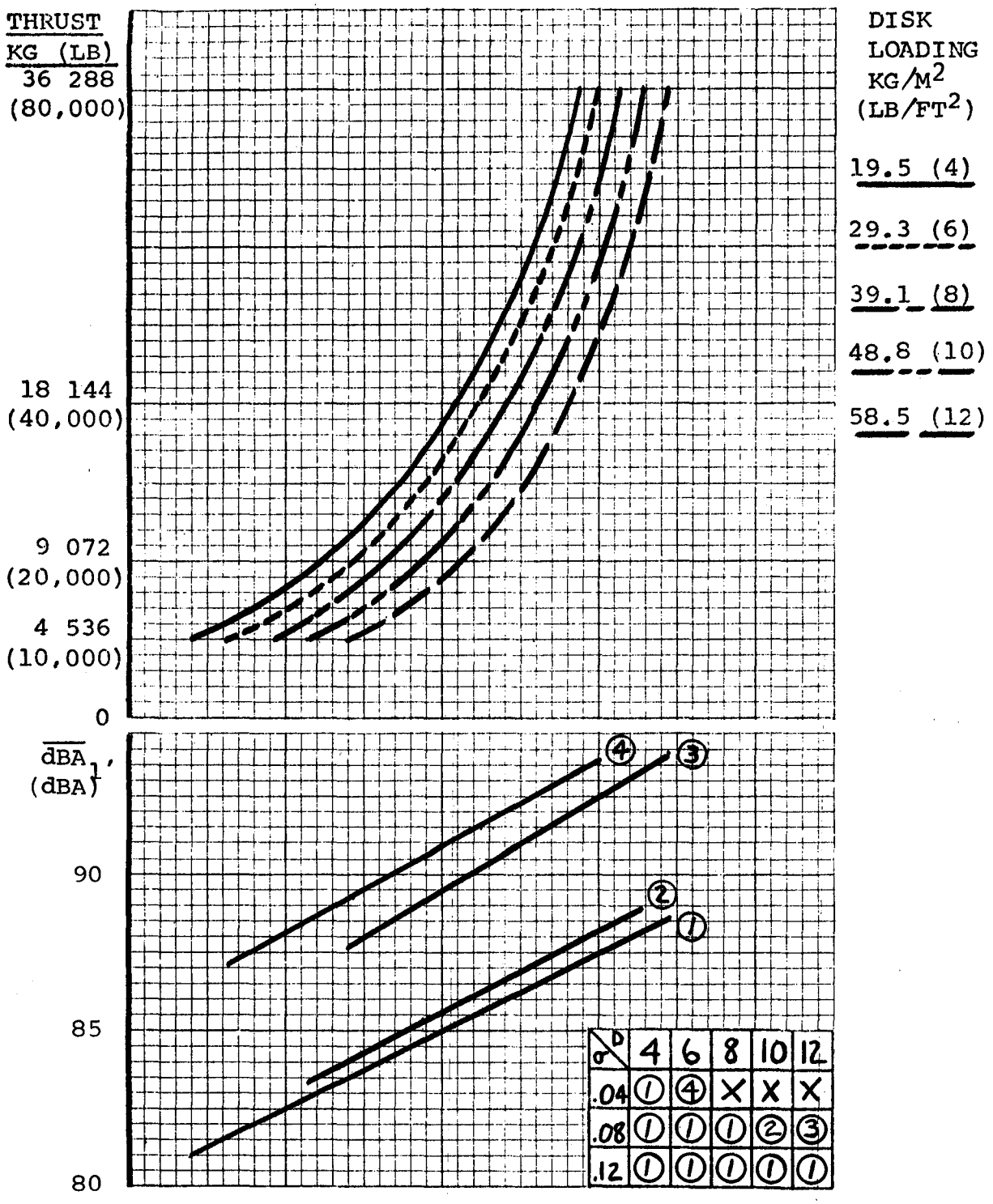

FIGURE A-8 A WEIGHTED SOUND PRESSURE LEVEL PREDICTION CHART - V_T=244 M/S (800 FT/S); N=6

TABLE A-8. ADJUSTMENT FOR NUMBER OF BLADES
A WEIGHTED SOUND PRESSURE LEVEL - V_T = 244 M/S
(800 FT/S)

D	N	σ = .04				σ = .08				σ = .12			
		THRUST, KG/LB				THRUST, KG/LB				THRUST, KG/LB			
KG/M^2		4536	9072	18144	36287	4536	9072	18144	36287	4536	9072	18144	36287
LB/FT^2		10000	20000	40000	80000	10000	20000	40000	80000	10000	20000	40000	80000
19.5	2	0	0	0	0	0	0	0	0	0	0	0	0
4	3	0	0	0	0	0	0	0	0	0	0	0	0
	4	0	0	0	0	0	0	0	0	0	0	0	0
	5	0	0	0	0	0	0	0	0	0	0	0	0
29.3	2	0	0	0	0	0	-0.5	-0.5	-0.5	0	-0.5	-0.5	-0.5
6	3	0	0	0	0	0	0	-0.5	0	0	0	-0.5	0
	4	0	0	0	0	0	0	0	0	0	0	0	0
	5	0	0	0	0	0	0	0	0	0	0	0	0
39.1	2					0	-0.5	-0.5	-0.5	0	-0.5	-0.5	-0.5
8	3					0	0	-0.5	-0.5	0	0	-0.5	-0.5
	4					0	0	0	0	0	0	0	0
	5					0	0	0	0	0	0	0	0
48.8	2					0	-0.5	-0.5	-0.5	0	-0.5	-0.5	-0.5
10	3					0	0	-0.5	-0.5	0	0	-0.5	-0.5
	4					0	0	0	-0.5	0	0	0	-0.5
	5					0	0	0	0	0	0	0	0
58.5	2					0	0	0	-0.5	0	-0.5	-0.5	-1.0
12	3					0	0	0	0	-0.5	0	-0.5	-0.5
	4					0	0	0	0	0	0	-0.5	-0.5
	5					0	0	0	0	0	0	-0.5	-0.5

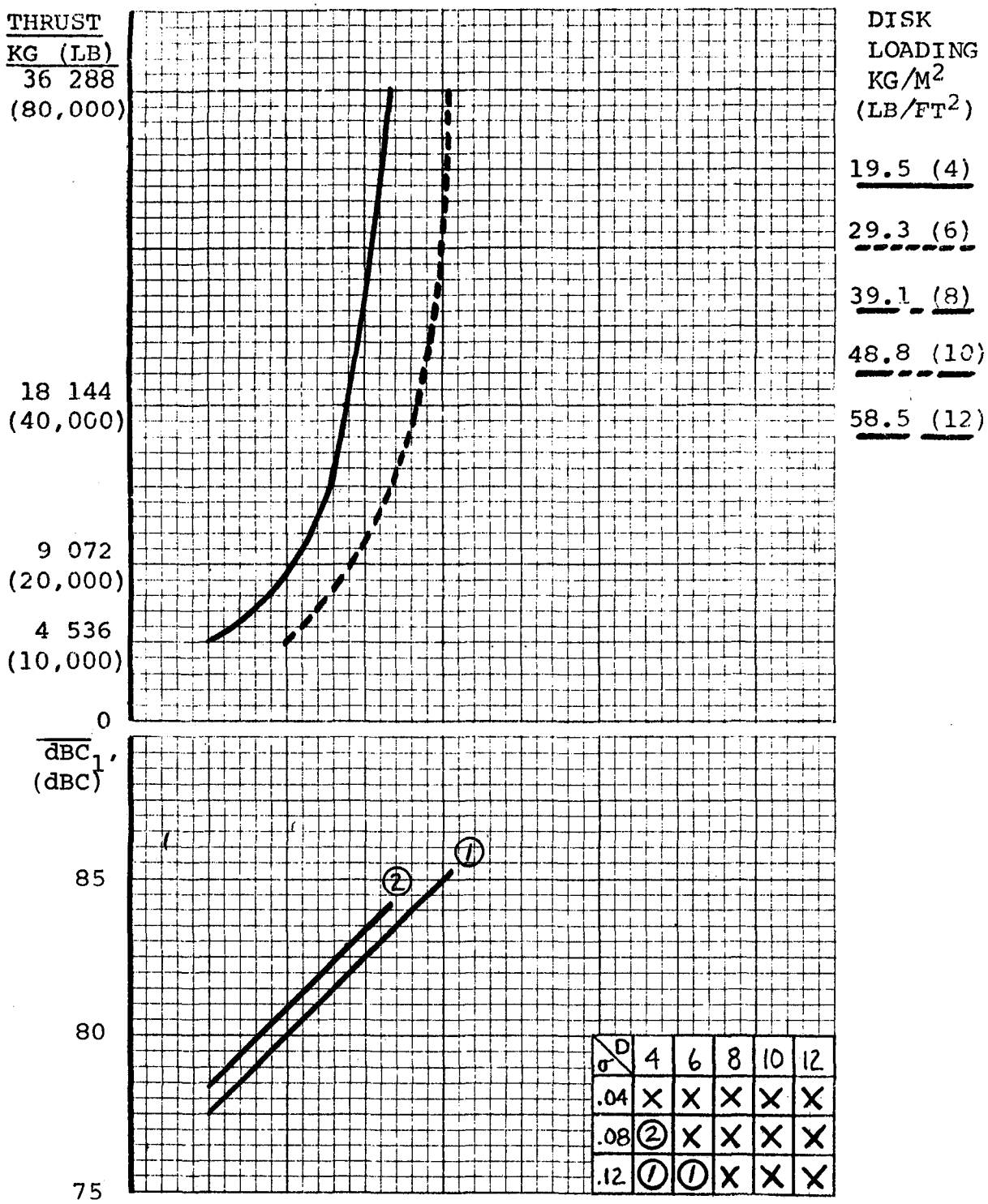

FIGURE A-9 C WEIGHTED SOUND PRESSURE LEVEL PREDICTION CHART - V_T=153 M/S (500 FT/S); N=6

TABLE A-9. ADJUSTMENT FOR NUMBER OF BLADES C WEIGHTED SOUND PRESSURE LEVEL-V_T = 153 M/S (500 FT/S)

D	N	σ = .04 THRUST, KG/LB				σ = .08 THRUST, KG/LB				σ = .12 THRUST, KG/LB			
KG/M^2		4536	9072	18144	36287	4536	9072	18144	36287	4536	9072	18144	36287
LB/FT^2		10000	20000	40000	80000	10000	20000	40000	80000	10000	20000	40000	80000
19.5	2					+2.5	+1.5	+1.5	+1.5	+3.0	+2.0	+2.0	+1.5
4	3					+1.5	+1.0	+1.0	+1.0	+1.5	+1.5	+1.0	+1.0
	4					+1.0	+0.5	+0.5	+0.5	+1.0	+0.5	+0.5	+0.5
	5					+0.5	0	0	0	+0.5	+0.5	+0.5	0
29.3	2									+2.5	+2.5	+2.0	+2.0
6	3									+1.5	+1.5	+1.0	+1.5
	4									+0.5	+1.0	+0.5	+1.0
	5									0	+0.5	0	+0.5
39.1	2												
8	3												
	4												
	5												
48.8	2												
10	3												
	4												
	5												
58.5	2												
12	3												
	4												
	5												

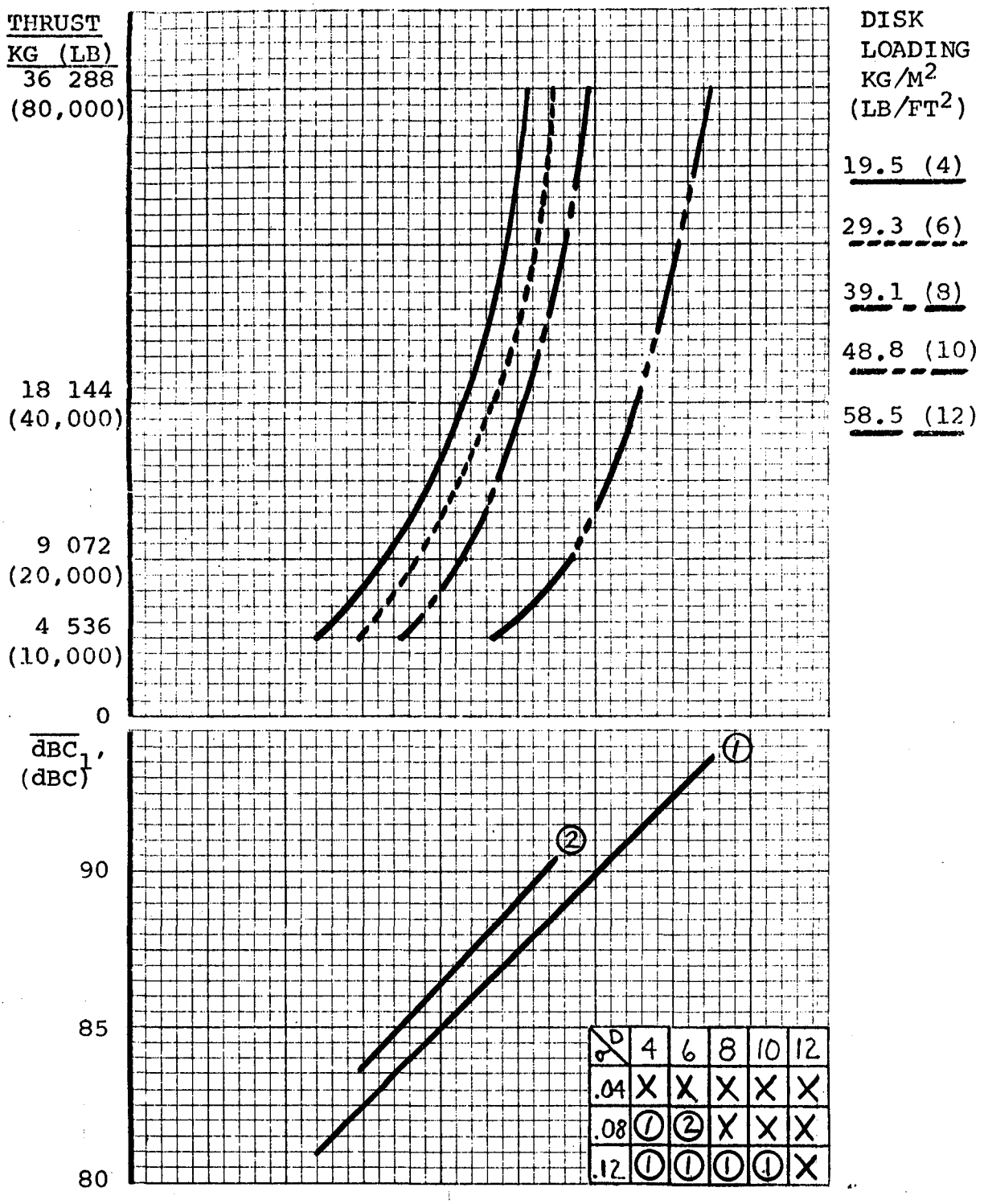

FIGURE A-10 C WEIGHTED SOUND PRESSURE LEVEL PREDICTION CHART - V_T=183 M/S (600 FT/S); N=6

TABLE A-10. ADJUSTMENT FOR NUMBER OF BLADES C WEIGHTED SOUND PRESSURE LEVEL-V_T = 183 M/S (600 FT/S)

D	N	σ = .04 THRUST, KG/LB				σ = .08 THRUST, KG/LB				σ = .12 THRUST, KG/LB			
KG/M^2		4536	9072	18144	36287	4536	9072	18144	36287	4536	9072	18144	36287
LB/FT^2		10000	20000	40000	80000	10000	20000	40000	80000	10000	20000	40000	80000
19.5	2					+2.0	+2.0	+1.5	+1.5	+2.0	+2.0	+1.5	+1.5
4	3					+1.5	+1.5	+1.0	+1.0	+1.5	+1.5	+1.0	+1.0
	4					+0.5	+1.0	+0.5	+0.5	+0.5	+1.0	+0.5	+0.5
	5					0	+0.5	0	0	0	+0.5	0	0
29.3	2					+2.0	+2.5	+1.5	+1.5	+2.5	+3.0	+2.5	+2.0
6	3					+1.5	+1.5	+1.0	+1.0	+1.5	+1.5	+1.5	+1.5
	4					+0.5	+1.0	+0.5	+0.5	+0.5	+1.5	+0.5	+1.0
	5					+0.5	+0.5	+0.5	0	+0.5	+0.5	+0.5	+0.5
39.1	2									+3.5	+3.0	+3.0	+2.5
8	3									+1.5	+2.0	+1.5	+1.5
	4									+1.5	+0.5	+1.0	+1.0
	5									+0.5	0	+0.5	0
48.8	2									+2.5	+2.0	+2.0	+1.5
10	3									+1.0	+1.0	+1.0	+1.0
	4									+1.0	+0.5	+0.5	+0.5
	5									+0.5	+0.5	0	+0.5
58.5	2												
12	3												
	4												
	5												

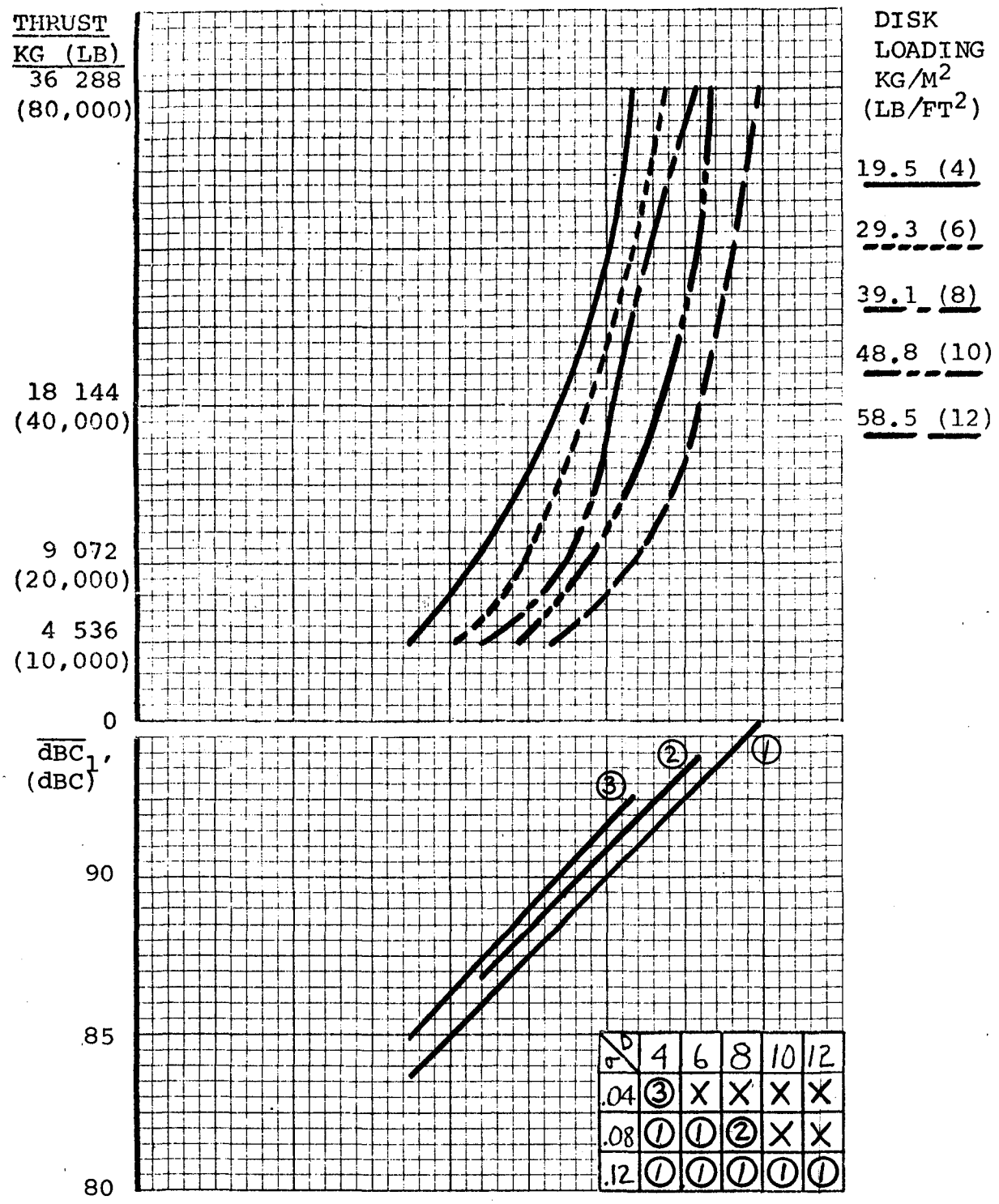

FIGURE A-11 C WEIGHTED SOUND PRESSURE LEVEL PREDICTION CHART - V_T=214 M/S (700 FT/S); N=6

TABLE A-11. ADJUSTMENT FOR NUMBER OF BLADES C WEIGHTED SOUND PRESSURE LEVEL-V_T = 214 M/S (700 FT/S)

		σ = .04				σ = .08				σ = .12			
D	N	THRUST, KG/LB				THRUST, KG/LB				THRUST, KG/LB			
KG/M^2		4536	9072	18144	36287	4536	9072	18144	36287	4536	9072	18144	36287
LB/FT^2		10000	20000	40000	80000	10000	20000	40000	80000	10000	20000	40000	80000
19.5	2	+2.0	+1.5	+1.0	+1.0	+2.0	+2.0	+1.5	+1.5	+2.0	+2.0	+1.5	+1.5
4	3	+1.0	+1.0	+0.5	+0.5	+1.5	+1.5	+1.0	+1.0	+1.5	+1.5	+1.0	+1.0
	4	+0.5	+0.5	+0.5	0	+0.5	+1.0	+0.5	+0.5	+0.5	+1.0	+0.5	+0.5
	5	+0.5	+0.5	0	0	+0.5	+0.5	0	0	+0.5	+0.5	0	0
29.3	2					+3.0	+2.5	+2.5	+2.0	+3.0	+2.5	+2.5	+2.0
6	3					+1.5	+1.5	+1.5	+1.0	+1.5	+1.5	+1.5	+1.0
	4					+1.5	+0.5	+1.0	+0.5	+1.5	+0.5	+1.0	+0.5
	5					+0.5	0	+0.5	0	+0.5	0	+0.5	0
39.1	2					+3.0	+2.5	+2.5	+2.0	+3.5	+2.5	+3.0	+2.5
8	3					+1.5	+1.5	+1.5	+1.0	+1.5	+1.5	+2.0	+2.0
	4					+1.0	+0.5	+1.0	+0.5	+1.5	+0.5	+1.0	+1.0
	5					+0.5	+0.5	+0.5	+0.5	+0.5	+0.5	+0.5	+0.5
48.8	2									+4.0	+3.0	+3.0	+2.5
10	3									+3.0	+2.0	+1.5	+2.0
	4									+1.5	+0.5	+0.5	+1.0
	5									+1.0	+0.5	0	+0.5
58.5	2									+3.5	+3.5	+2.5	+2.5
12	3									+3.0	+1.5	+1.5	+1.5
	4									+1.5	+1.5	+0.5	+1.0
	5									+1.0	+0.5	0	+0.5

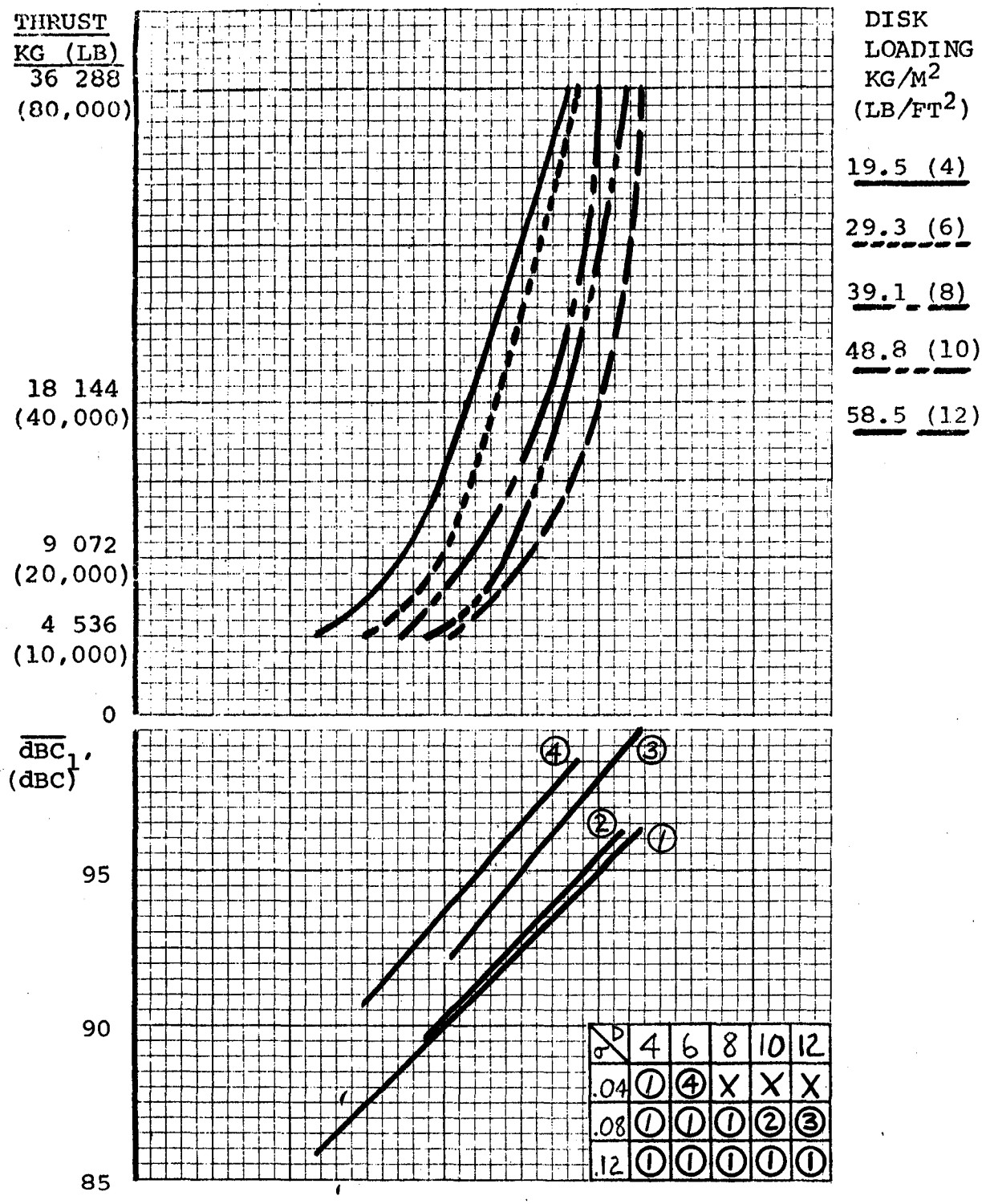

FIGURE A-12 C WEIGHTED SOUND PRESSURE LEVEL PREDICTION CHART - V_T=244 M/S (800 FT/S); N=6

TABLE A-12. ADJUSTMENT FOR NUMBER OF BLADES C WEIGHTED SOUND PRESSURE LEVEL-V_T = 244 M/S (800 FT/S)

D	N	σ = .04 THRUST, KG/LB				σ = .08 THRUST, KG/LB				σ = .12 THRUST, KG/LB			
KG/M^2		4536	9072	18144	36287	4536	9072	18144	36287	4536	9072	18144	36287
LB/FT^2		10000	20000	40000	80000	10000	20000	40000	80000	10000	20000	40000	80000
19.5	2	+3.0	+2.0	+2.0	+1.0	+3.0	+2.0	+2.0	+1.0	+3.0	+2.0	+2.0	+1.0
4	3	+1.5	+1.5	+1.0	+1.0	+1.5	+1.5	+1.0	+1.0	+1.5	+1.5	+1.0	+1.0
	4	+1.5	+0.5	+1.0	+0.5	+1.5	+0.5	+1.0	+0.5	+1.5	+0.5	+1.0	+0.5
	5	+1.0	0	+0.5	0	+1.0	0	+0.5	0	+1.0	0	+0.5	0
29.3	2	+1.5	+1.0	+1.0	+1.0	+3.0	+2.5	+2.5	+2.0	+3.0	+2.5	+2.5	+2.0
6	3	+0.5	+0.5	+0.5	+0.5	+1.5	+1.5	+1.5	+1.0	+1.5	+1.5	+1.5	+1.0
	4	+0.5	0	+0.5	0	+1.5	+0.5	+1.0	+0.5	+1.5	+0.5	+1.0	+0.5
	5	0	0	0	0	+0.5	+0.5	+0.5	+0.5	+0.5	+0.5	+0.5	+0.5
39.1	2					+3.5	+3.5	+2.5	+3.0	+3.5	+3.5	+2.5	+3.0
8	3					+3.0	+1.5	+1.5	+1.5	+3.0	+1.5	+1.5	+1.5
	4					+1.5	+2.0	+0.5	+1.0	+1.5	+2.0	+0.5	+1.0
	5					+1.0	+1.0	−0.5	+0.5	+1.0	+1.0	−0.5	+0.5
48.8	2					+4.0	+3.5	+3.0	+2.5	+4.0	+3.5	+3.0	+3.0
10	3					+3.0	+1.5	+1.5	+2.0	+3.0	+1.5	+2.0	+2.0
	4					+2.5	+1.5	+1.5	+1.0	+2.5	+1.5	+1.0	+1.0
	5					+1.0	+0.5	+1.0	+0.5	+1.5	+0.5	+1.0	+0.5
58.5	2					+3.0	+2.5	+2.5	+1.5	+4.0	+3.5	+3.0	+3.0
12	3					+2.5	+1.0	+1.0	+1.0	+3.5	+1.5	+1.5	+2.0
	4					+1.5	+1.0	0	+0.5	+2.0	+1.5	+0.5	+1.5
	5					+0.5	+0.5	+0.5	+0.5	+1.0	+0.5	+0.5	+0.5

APPENDIX B

This appendix contains examples of the use of the Rotor Design Charts.

Case 1:

Find the Perceived Noise Level of a rotor where all values can be read directly from the charts.

$T = 20{,}000$ lb
$D/L = 8$ ft/ft^2
$\sigma = .08$
$V_T = 700$ ft/sec
$N = 3$ blades

Procedure

Step 1. Select PNL charts with a tip speed of 700 ft/sec (Figure B-1).

Step 2. Enter the chart at a thrust of 20,000 lb.

Step 3. Follow line (1) to a disk load of 8 lb/ft^2.

Step 4. Read the table in the lower chart to see if line ①, ②, or ③ is to be used. The solidity-disk load combination in this example indicates that line ② is to be used.

Step 5. Drop straight down on line (2) from the intersection of T = 20,000 lb and D/L = 8 lb/ft^2 to line ②.

Step 6. Follow line (3) to the left and read the partial PNL. This PNL is for a 6-bladed rotor. In this example, the partial PNL = 96 PNdB.

Step 7. Turn to Table B-1 and locate the correction for N=3, T=20,000 lb, σ=.08, and D/L=8 lb/ft^2. The correction in this example is + .5 PNdB.

Step 8. Add the result from Step 6 to the result of Step 7 to obtain the final answer.
PNL = 96 + .5 = 96.5 PNdB.

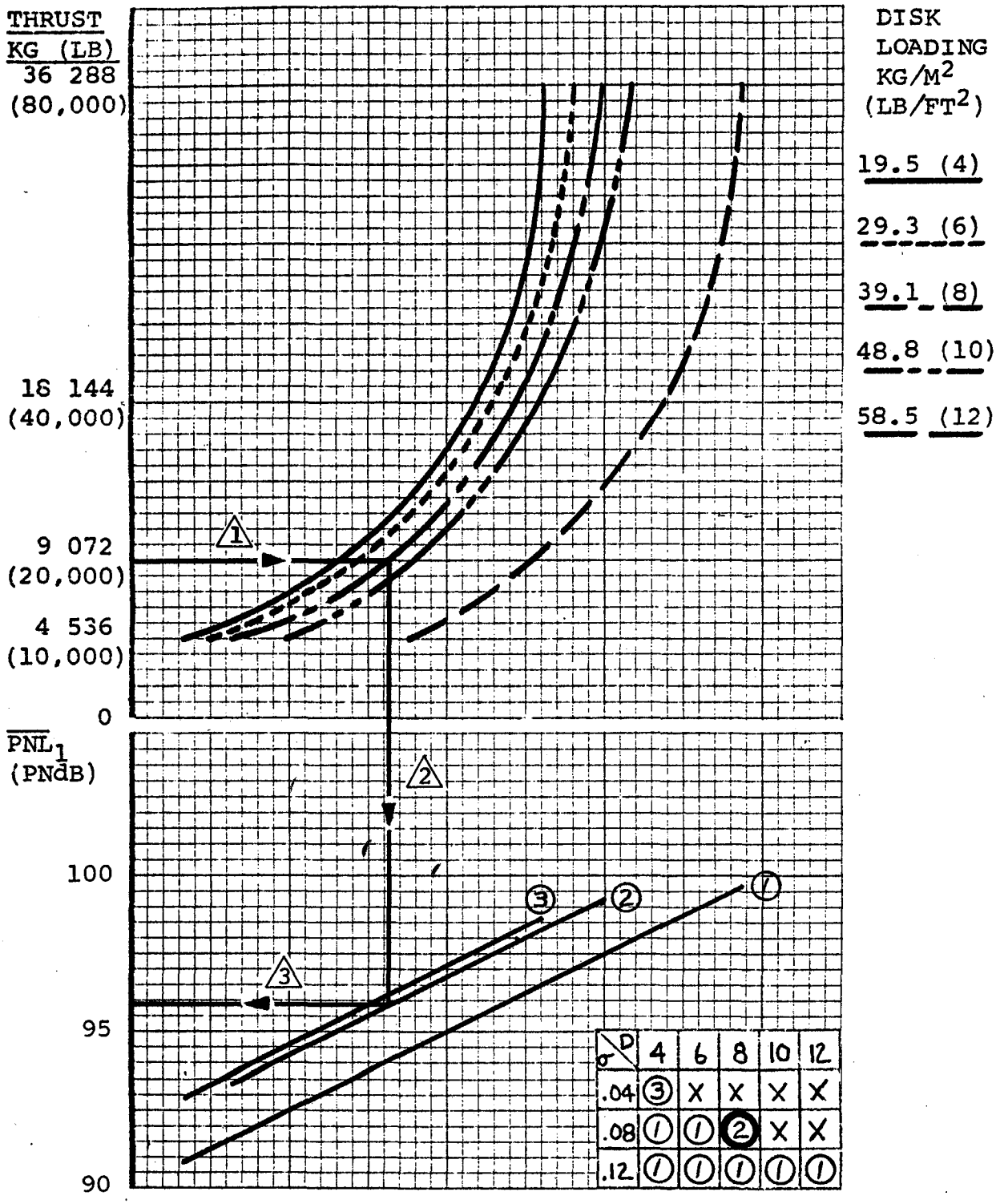

FIGURE B-1 PERCEIVED NOISE LEVEL PREDICTION CHART - V_T=214 M/S (700 FT/S); N=6

(SAME AS FIGURE A-3 OF APPENDIX A)

TABLE B-1 ADJUSTMENT FOR NUMBER OF BLADES
PERCEIVED NOISE LEVEL - V_T = 214 M/S (700 FT/S)
(SAME AS TABLE A-3 OF APPENDIX A)

		σ = .04				σ = .08				σ = .12			
D	N	THRUST, KG/LB				THRUST, KG/LB				THRUST, KG/LB			
KG/M^2		4536	9072	18144	36287	4536	9072	18144	36287	4536	9072	18144	36287
LB/FT^2		10000	20000	40000	80000	10000	20000	40000	80000	10000	20000	40000	80000
19.5	2	+0.5	0	0	0	+0.5	+0.5	0	0	+0.5	+0.5	0	0
4	3	+0.5	0	0	0	+0.5	0	0	0	+0.5	0	0	0
	4	0	0	0	0	0	0	0	0	0	0	0	0
	5	0	0	0	0	0	0	0	0	0	0	0	0
29.3	2					+1.0	+0.5	+0.5	0	+1.0	+0.5	+0.5	0
6	3					+0.5	+0.5	+0.5	0	+0.5	+0.5	+0.5	0
	4					+0.5	0	0	0	+0.5	0	0	0
	5					0	0	0	0	0	0	0	0
39.1	2					+1.0	+0.5	+0.5	0	+1.5	+1.0	+0.5	0
8	3					+0.5	+0.5	0	0	+1.0	+0.5	+0.5	0
	4					0	0	0	0	+0.5	0	0	0
	5					0	0	0	0	0	0	0	0
48.8	2									+1.5	+1.0	+1.0	0
10	3									+1.0	+1.0	+0.5	0
	4									+0.5	+0.5	+0.5	0
	5									0	0	0	0
58.5	2									+1.5	+1.0	+1.0	+0.5
12	3									+0.5	+0.5	+0.5	+0.5
	4									0	+0.5	0	0
	5									-0.5	0	0	0

Case 2:

This case uses rotor parameters which require interpolation.

Find the C Weighted Sound Pressure Level for the following rotor:

$T = 30{,}000$ lbs
$N = 4$ blades
$V_T = 725$ ft/sec
$D/L = 7$ lbs/ft^2
$\sigma = .09$

Procedure

Step 1. Determine that the design $\overline{C_L}$ is less than 0.6. If not, then the charts cannot be used.

$$\overline{C_L} = \frac{(6)\ (7)}{(.002378)(.09)(725)^2} = .373 \quad \text{(page 11)}$$

Step 2. Select the bracketing combinations of disk load and solidity for this case. $\sigma = .08$ and .12 and $D/L = 6$ and 8 lb/ft^2.

Step 3. Using the procedure outlined in Case 1, determine the dBC for each combination of disk load and solidity in Step 2 and for tip speeds of 600, 700, and 800 ft/sec. (500 ft/sec gives a $\overline{C_L}$ greater than .6 and cannot be used).

Step 4. Calculate the average lift coefficients for each combination of parameters for which the dBC's were determined. Tabulate the results of this step and Step 3 as shown in Table B-2.

Step 5. Plot the predicted dBC's vs average lift coefficient for each tip speed.

Step 6. Connect points of constant solidity and points of constant disk load.

Step 7. Linearly interpolate lines of $\sigma = .09$ and $D/L = 7$ lb/ft^2. Figure B-2 illustrates Steps 5, 6 and 7 for a tip speed of 700 ft/sec. Similar plots are used for $V_T = 600$ and 800 ft/sec.

Step 8. Check that the $\overline{C_L}$ indicated from each plot is close to the $\overline{C_L}$ calculated using the parameters on the plots. For 700 ft/sec:

$$\overline{C_L} = \frac{(6)\ (7)}{(.002378)\,(.09)\,(700)^2} = .40$$

$\overline{C_L}$ from plot $\approx$ .41

Step 9. Read the Design Reference dBC's from each plot.

Step 10. Plot the Design Reference dBC's against tip speed.

Step 11. Construct a dBC - tip speed trend curve.

Step 12. Locate the design tip speed of 725 ft/sec and proceed vertically to the dBC-V_T curve.

Step 13. Read horizontally to the left and round off to the nearest 0.5 dBC to obtain a Design dBC of 91 dBC. Steps 10 through 13 are illustrated in Figure B-3.

T	V_T	D/L	σ	dBC	$\overline{C_L}$
30,000 lb	600	6	.08	88.1	.526
	600	6	.12	86.6	.350
	600	8	.08	-	>.6
	600	8	.12	87.8	.467
	700	6	.08	89.4	.386
	700	6	.12	89.4	.257
	700	8	.08	91.6	.515
	700	8	.12	90.7	.343
	800	6	.08	91.8	.296
	800	6	.12	91.8	.197
	800	8	.08	93.3	.394
	800	8	.12	93.3	.263

Table B-2 - Example 2 - Tabulation of Results

V_T = 700 Ft/sec

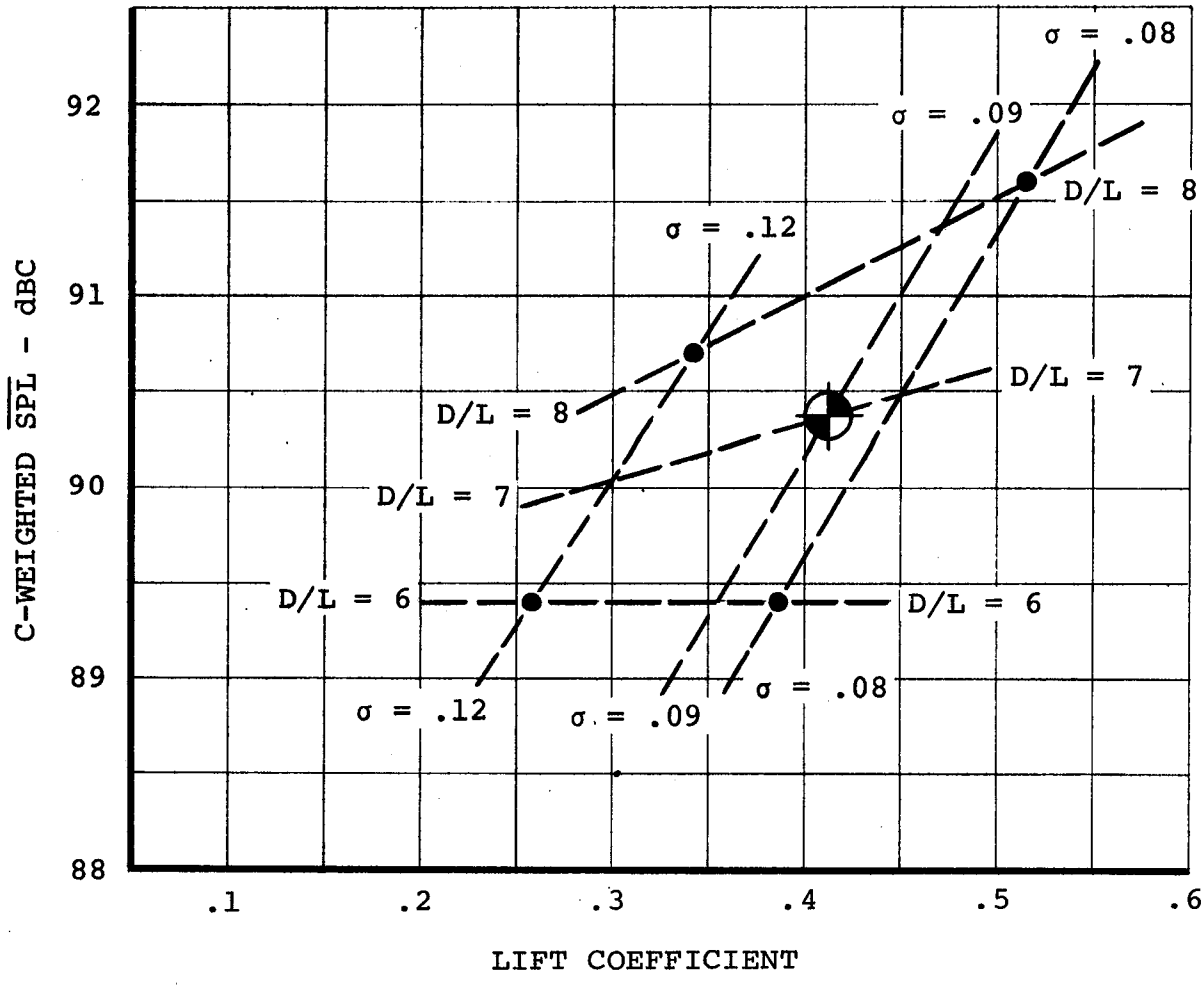

Figure B-2 - Example 2 - Interpolation of Disk Load and Solidity for V_T = 700 fps

(Perform Similar Operation for Other Tip Speeds)

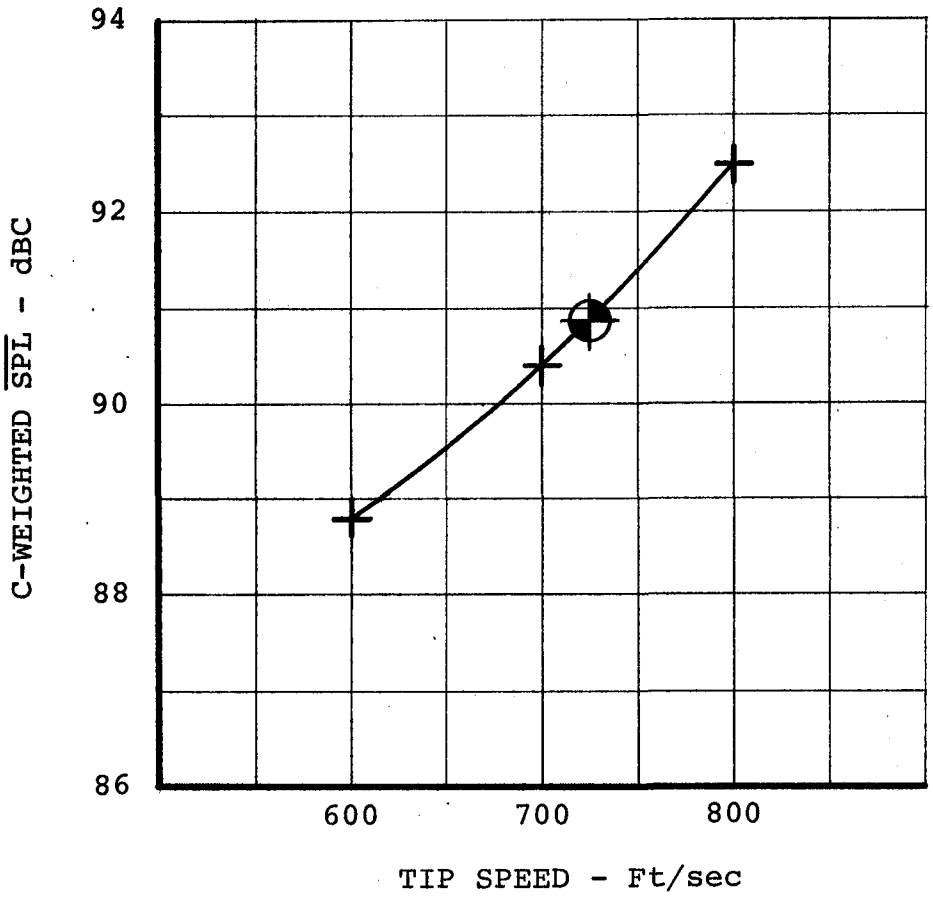

Figure B-3 - Example 2 - Interpolation of Tip Speed

Case 3:

It is desired to design a rotor whose thrust is 20,000 pounds and whose Perceived Noise Level does not exceed 95.0 PNdB. Potential candidates are a 3- or a 4-bladed rotor.

Procedure:

It is assumed that the reader has a clear understanding of Cases 1 and 2. Therefore, Steps 1 through 4 and 6 have been omitted. The candidates for a 3- and a 4-bladed rotor at each tip speed are listed below:

	V_T	σ	D/L	PNL
N = 3	500	.12	6	86.6 PNdB
	600	.08	6	92.6
	700	.12	8	94.5
	800	-	-	>95.0
N = 4	500	.12	6	86.6
	600	.08	6	92.6
	700	.12	10	94.9
	800	-	-	>95.0

Step 5. Using the above table and Figure B-4, the following two rotors best meet the noise requirement of less than 95.0 PNdB.

N	σ	D/L	V_T
3	.12	8	712
4	.12	10	700

Step 7. Based on the above rotors, calculate K_R and K_D as formulated on Figure 12:

3 Blades

$$K_R = (1.08 \times 10^{-5})(20{,}000)^{1.625}(8)^{-.875}(712)(.12)$$
$$= 1458$$

$$K_D = (3.53 \times 10^{-3})\frac{(20{,}000)^{1.5}}{712}$$
$$= 14$$

$$K_R + K_D = 1472$$

Repeating for the 4-bladed rotor gives:

$$K_R + K_D = 1190$$

Step 8. Entering Figure B-5 at the above values of $K_R + K_D$ gives the following weights of the rotor and drive systems:

3 Blades - $W_R + W_D$ = 3800 lbs.
4 Blades - $W_R + W_D$ = 3200 lbs.

Step 9. From Step 8, it can be concluded that the selection of the 4-bladed rotor will meet the required noise level for 600 pounds lower rotor/drive system weight or a 3% increase in useful load.

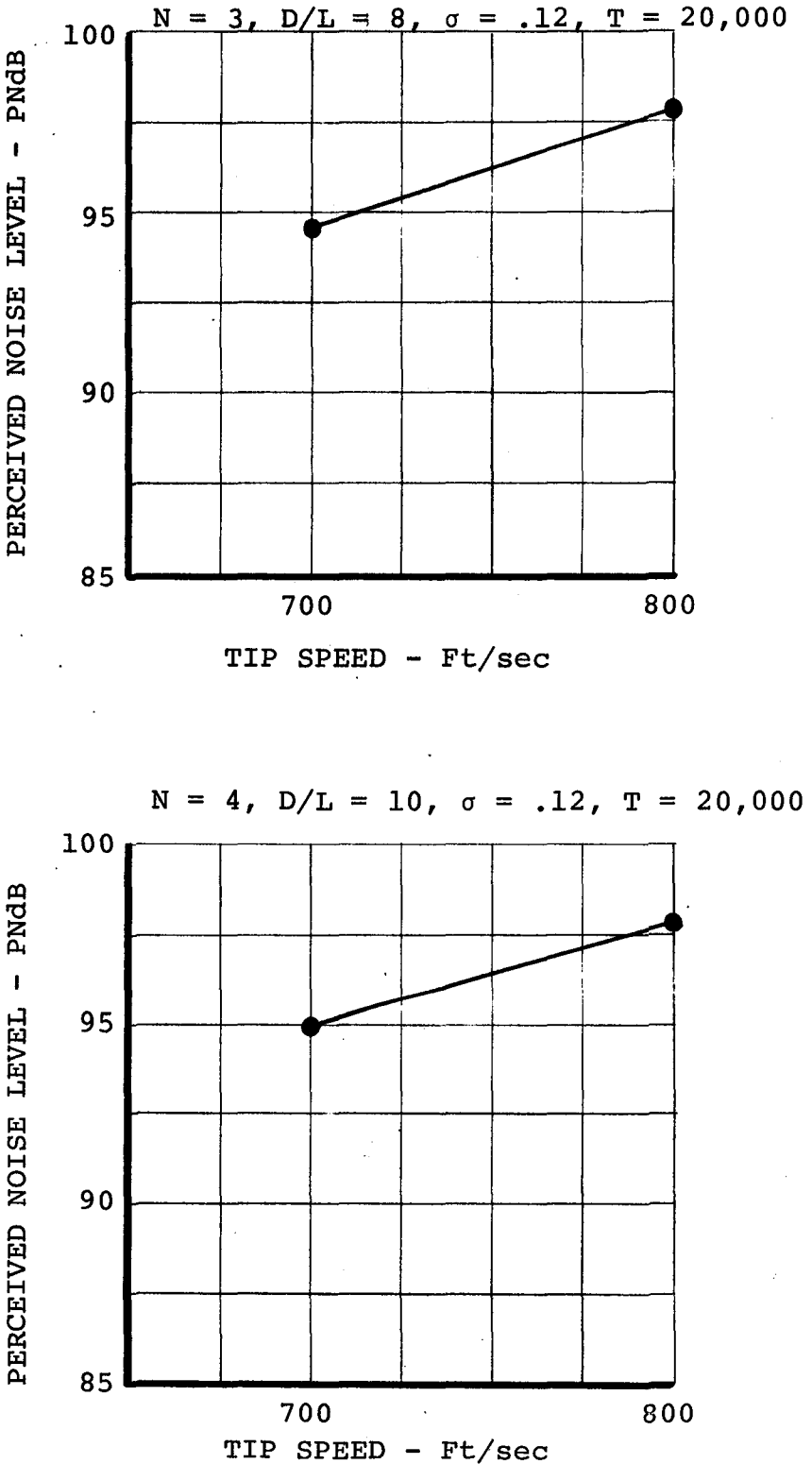

Figure B-4 - Example 3 - Effect of Tip Speed on Perceived Noise Level

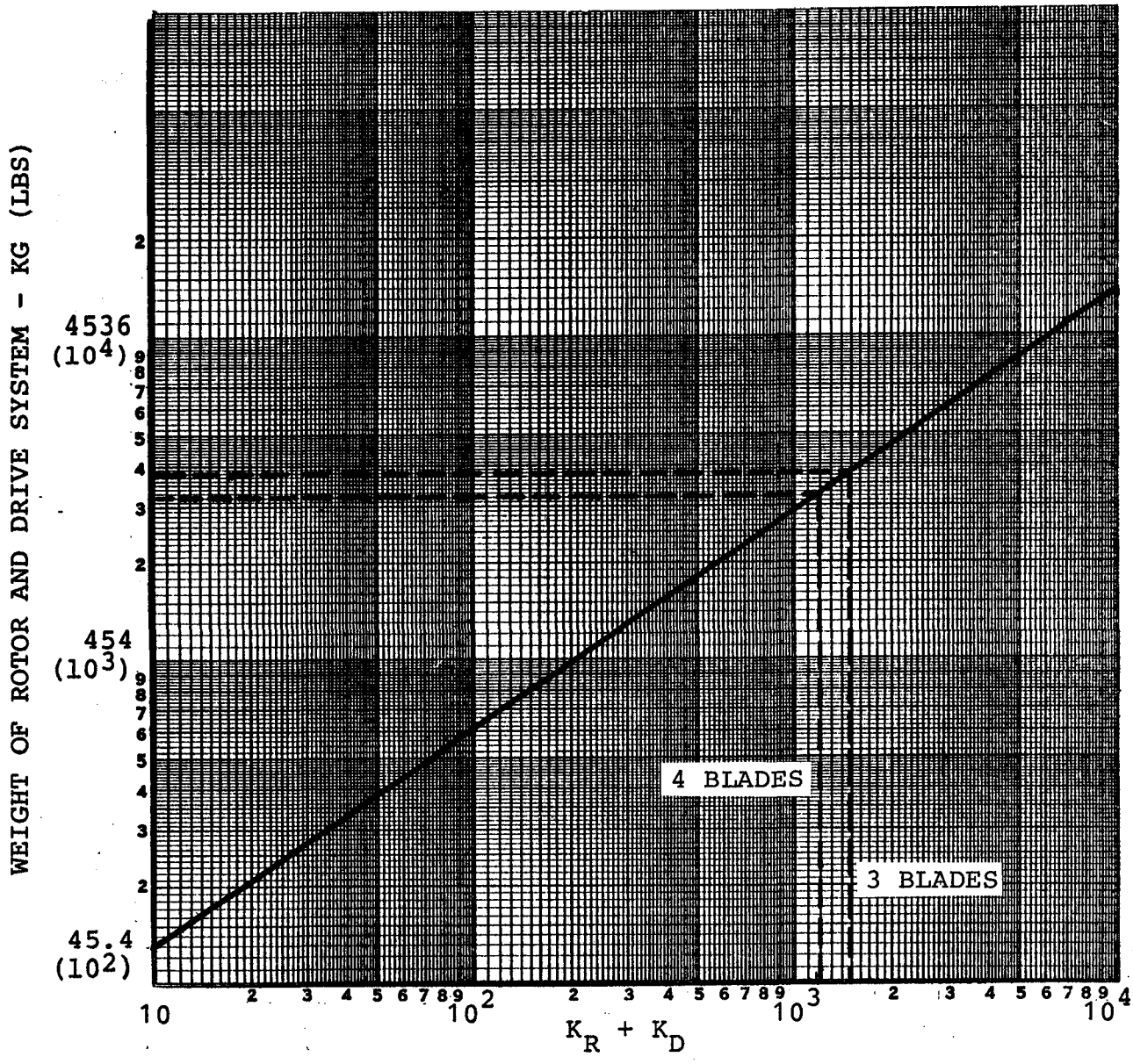

$$K_R = 1.08 \times 10^{-5} (T^{1.625}) (D/L^{-.875}) (V_T) (\sigma)$$

$$K_D = 3.53 \times 10^{-3} \frac{(T^{1.5})}{V_T}$$

Figure B-5 - Example 3 - Rotor and Drive System Weight Estimating Procedure

REFERENCES

1. Lowson, M.V. and Ollerhead, J.B., Studies of Helicopter Rotor Noise, USAAVLABS Technical Report 68-60, U.S. Army Aviation Materiel Laboratories, Fort Eustis, Virginia, January 1969.

2. Ollerhead, J.B. and Taylor, R.B., Description of a Helicopter Rotor Noise Computer Program, USAAVLABS Technical Report 68-61, U.S. Army Aviation Materiel Laboratories, Fort Eustis, Virginia, January 1969.

3. Scheiman, J., A Tabulation of Helicopter Rotor Blade Differential Pressures, Stresses, and Motions as Measured in Flight, NASA TM X-952, Langley Research Center, National Aeronautics and Space Administration, Washington, D.C., March 1964.

4. Hosier, R.N. and Ramakrishnan, R., Helicopter Rotor Rotational Noise Predictions Based on High Frequency Loads, NASA TN-7624, December 1974.

5. Kasper, P.K., Determination of Rotor Harmonic Blade Loads from Acoustical Measurements, NASA CR 2580, October 1975.

6. Lowson, M.V., Thoughts on Broad Band Noise Radiation by a Helicopter, Wyle Laboratories WR 68-20, 1968.

7. Hubbard, H.H., Propeller-Noise Charts for Transport Airplanes, NACA TN 2968.

8. Schlegel, R., King, R., and Mull, H., Helicopter Rotor Noise Generation and Propagation, USAAVLABS Technical Report No. 66-4, October 1966.

9. Munch, C.L., Prediction of V/STOL Noise for Applications to Community Noise Exposure, DOT-TSC-OST-73-19, May 1973.

10. ANSI 51.11-1966, Octave, Half-Octave and One-Third Octave Filter Sets, American National Standard Institute, 1966.

11. Sternfeld, H., Spencer, R., and Schairer, J., An Investigation of Noise Generation on a Hovering Rotor, Army Research Office Contract DAHC04-69-C-0087, January 1971.

12. Hinterkeuser, E., and Sternfeld, H., Civil Helicopter Noise Assessment Study, Boeing Vertol Model 347, NASA CR 132420, May 1974.

13. Sternfeld, H., Bobo, C., Carmichael, D., Fukushima, T., and Spencer, R., An Investigation of Noise Generation on a Hovering Rotor, Part II, Army Research Office Contract DAHC04-69-0087, November 1972.

14. Sternfeld, H., and Doyle, L.B., Evaluation of the Annoyance Due to Helicopter Rotor Noise, NASA CR-3001, June 1978.

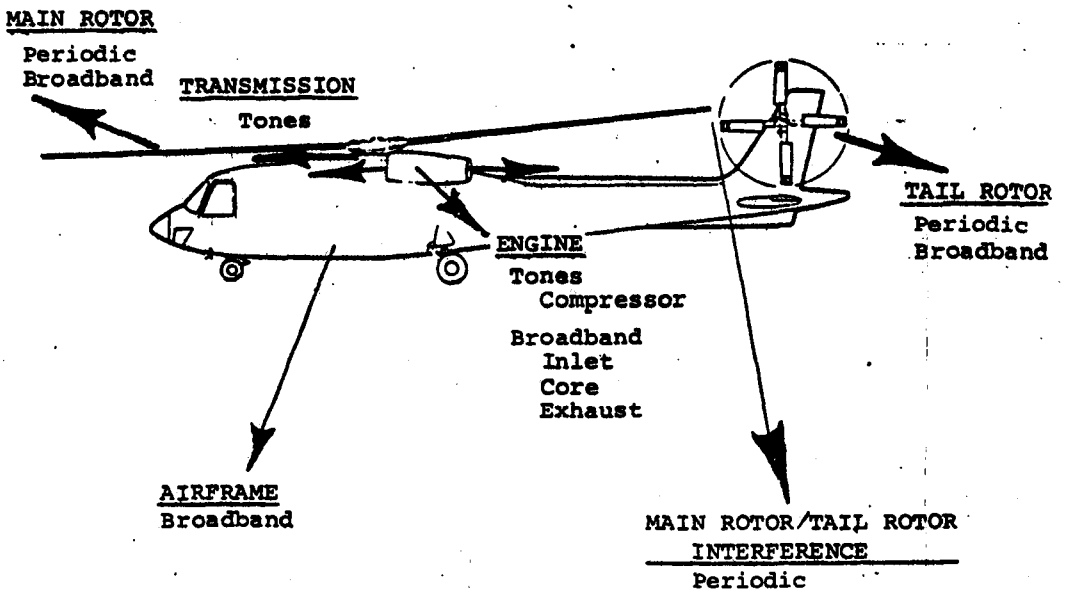

Single Rotor

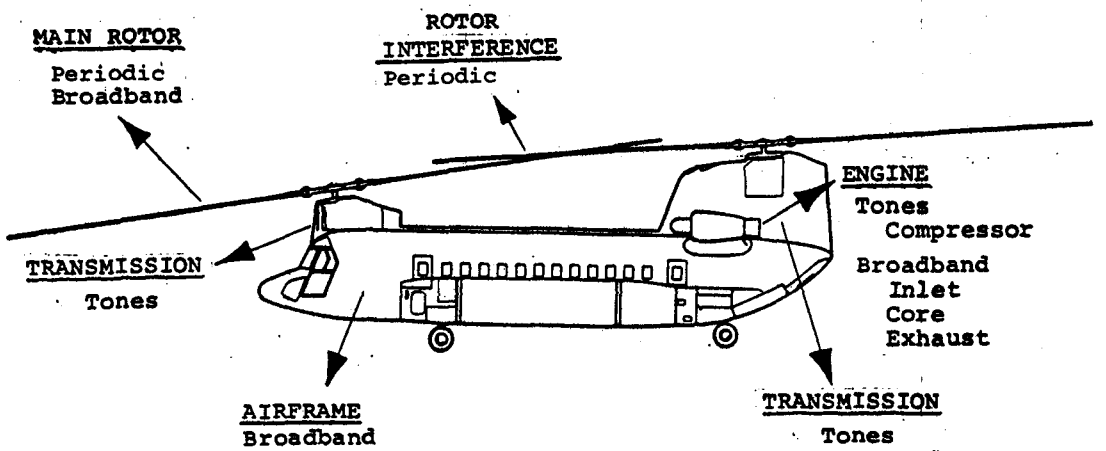

Tandem Rotor

Figure 1. Helicopter Noise Sources

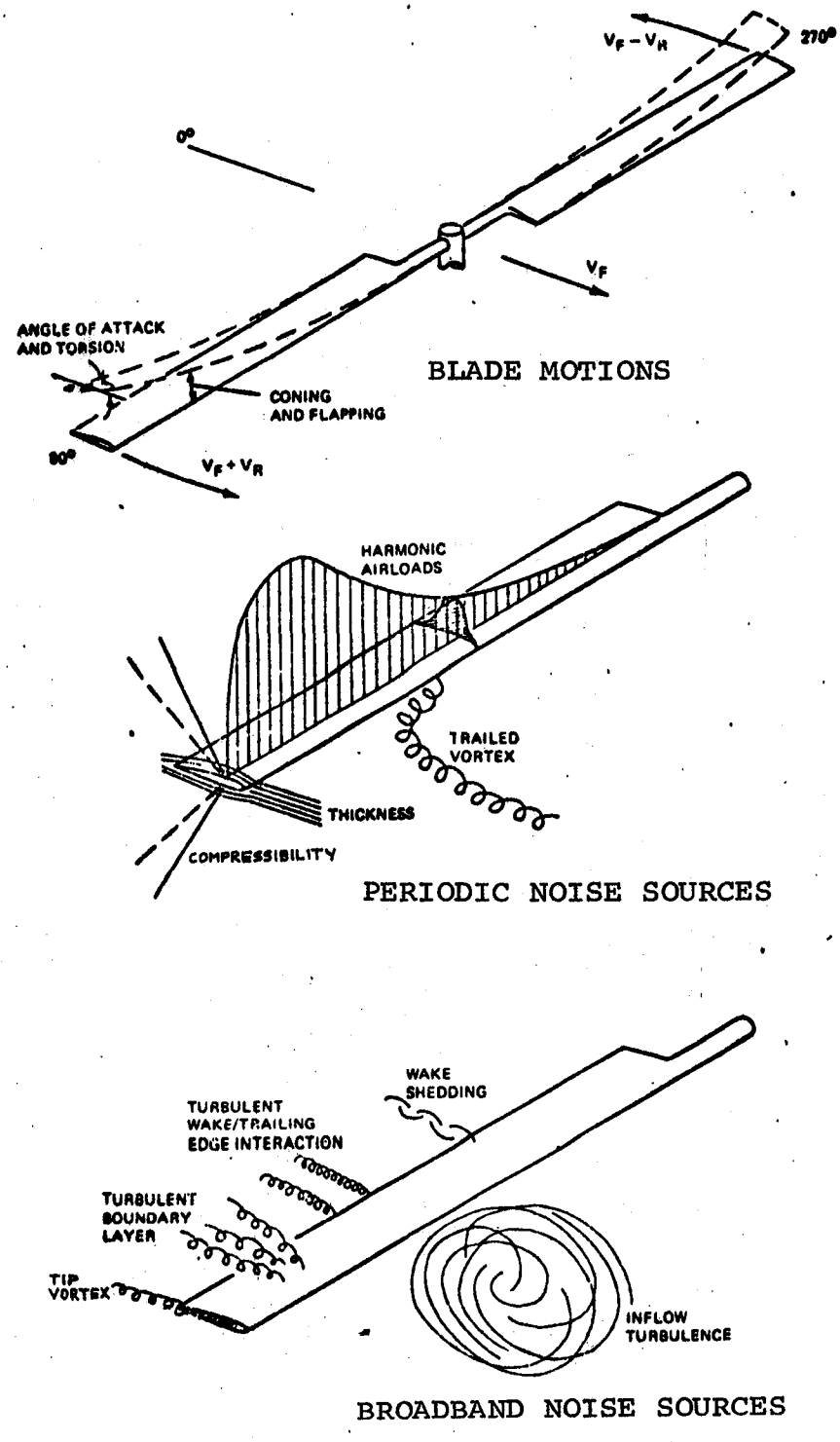

Figure 2. Aerodynamic Sources of Rotor Noise

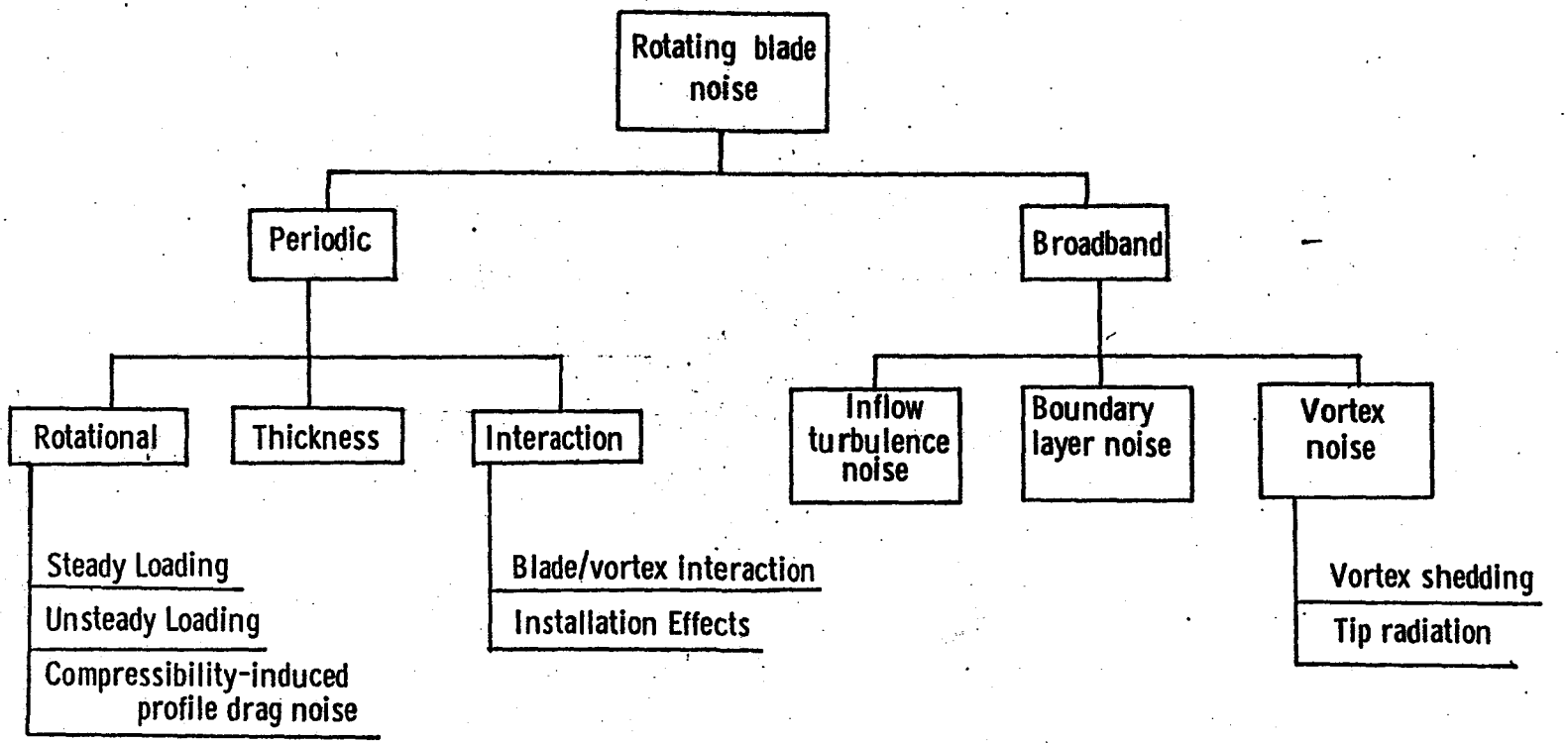

Figure 3. Outline of Rotating Blade Noise Components
(Ref: Unpublished NASA Source)

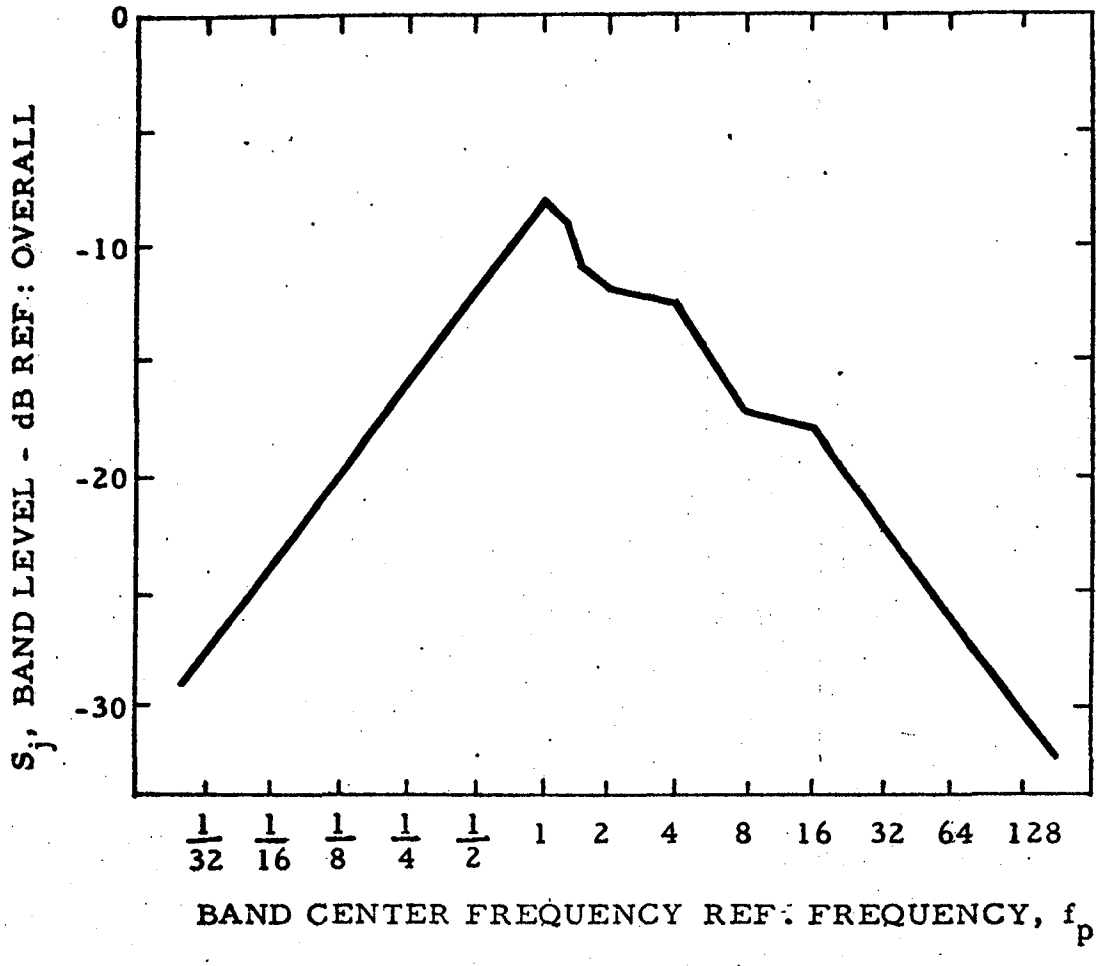

BAND CENTER FREQUENCY, BAND LEVEL

1/32 = -29.0	2 = -11.5
1/16 = -24.5	4 = - 12.1
1/8 = -19.5	8 = -16.5
1/4 = -15.3	16 = -17.0
1/2 = -11.7	32 = -21.8
1 = -7.5	64 = -26.4
	128 = -30.0

Figure 4. Rotor Broadband Noise Empirical Spectrum Shape (Ref: Unpublished NASA Source)

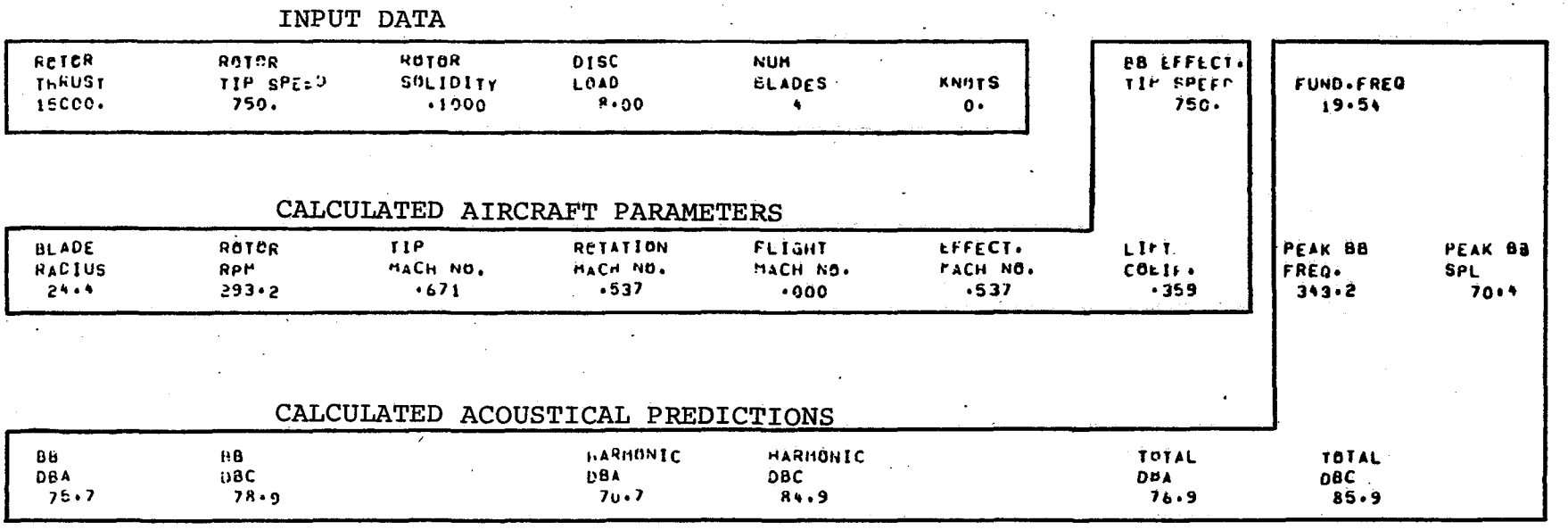

Figure 5a. Noise Prediction Program - Computer Output

****** BROADBAND NOISE ******

FREQ BAND	FREQ	SPL
****	********	*******
20	21.5	53.4
25	27.0	55.1
31	34.1	56.7
40	42.9	58.4
50	54.1	59.8
63	68.1	61.2
80	85.8	62.6
100	108.1	63.8
125	136.2	65.0
160	171.6	66.2
200	216.2	67.6
250	272.4	69.0
315	343.2	70.4
400	432.5	69.1
500	544.9	67.7
630	686.5	66.4
800	864.9	66.2
1000	1089.7	66.0
1250	1373.0	65.8
1600	1729.8	64.3
2000	2179.4	62.9
2500	2745.9	61.2
3150	3459.6	61.1
4000	4358.8	60.9
5000	5491.8	59.4
6300	6919.3	57.9
8000	8717.7	56.1
10000	10983.6	54.6

********** ROTATIONAL NOISE **********

HARMONIC	FREQ	SPL	FREQ BAND	SPL
********	******	*****	****	******
1	19.5	87.1	20	87.1
2	39.1	80.7	25	.0
3	58.6	75.6	31	.0
4	78.2	72.7	40	80.7
5	97.7	70.9	50	.0
6	117.3	69.4	63	75.8
7	136.8	68.3	80	72.7
8	156.4	67.3	100	70.9
9	175.9	66.4	125	71.0
10	195.4	65.6	160	69.9
11	215.0	64.9	200	68.3
12	234.5	64.3	250	68.5
13	254.1	63.7	315	68.0
14	273.6	63.2	400	66.9
15	293.2	62.6	500	66.6
16	312.7	62.2	630	66.1
17	332.2	61.7	800	61.9
18	351.8	61.3	1000	.0
19	371.3	60.9	1250	.0
20	390.9	60.6	1600	.0
21	410.4	60.2	2000	.0
22	430.0	59.9	2500	.0
23	449.5	59.5	3150	.0
24	469.1	59.2	4000	.0
25	488.6	58.9	5000	.0
26	508.1	58.7	6300	.0
27	527.7	58.4	8000	.0
28	547.2	58.1	10000	.0
29	566.8	57.9		
30	586.3	57.6		
31	605.9	57.4		
32	625.4	57.2		
33	645.0	56.9		
34	664.5	56.7		
35	684.0	56.5		
36	703.6	56.3		
37	723.1	56.1		
38	742.7	55.9		
39	762.2	55.7		
40	781.8	55.6		

* TOTAL NOISE *

FREQ BAND	SPL
****	*******
20	87.1
25	55.1
31	56.7
40	80.7
50	59.8
63	75.8
80	73.1
100	71.6
125	72.7
160	71.4
200	70.9
250	71.7
315	72.4
400	71.0
500	70.2
630	69.3
800	67.5
1000	66.0
1250	65.8
1600	64.3
2000	62.9
2500	61.2
3150	61.1
4000	60.9
5000	59.4
6300	57.9
8000	56.1
10000	54.6

Figure 5b. Noise Prediction Program - Computer Output

********** COMBINED BROADBAND AND HARMONIC PERCEIVED NOISE DATA **********

FREQUENCY - HZ	LEVEL - DB	NOYS	CORRECTION
50	59.8	.57	.00
63	75.8	4.36	1.55
80	73.1	4.27	.00
100	71.6	4.86	.00
125	72.7	5.85	.00
160	71.4	6.03	.00
200	70.9	6.79	.00
250	71.7	7.75	.00
315	72.4	8.79	.00
400	71.0	8.55	.00
500	70.2	8.10	.00
630	69.3	7.60	.00
800	67.5	6.74	.00
1000	66.0	6.05	.00
1250	65.8	6.85	.00
1600	64.3	8.06	.00
2000	62.9	8.41	.00
2500	61.2	8.58	.00
3150	61.1	9.13	.00
4000	60.9	9.01	.00
5000	59.4	7.58	.00
6300	57.9	6.38	.00
8000	56.1	4.58	.00
10000	54.6	3.36	.00

PNLT = 91.3
PNL = 89.8
*CORRECTION = 1.55

Figure 5c. Noise Prediction Program - Computer Output

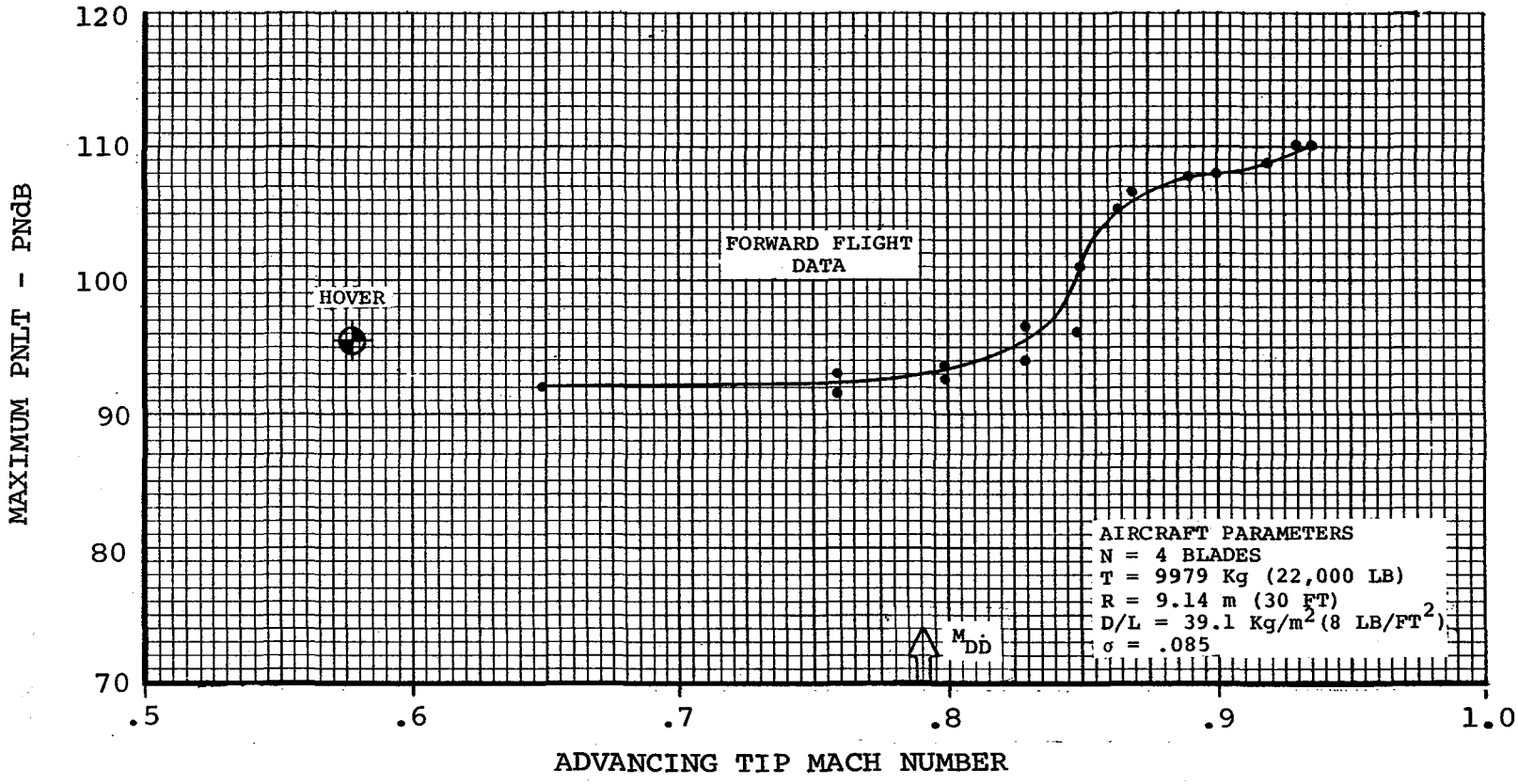

Figure 6. Tone Corrected Perceived Noise Level Trend with Forward Flight - Boeing Vertol Model 347

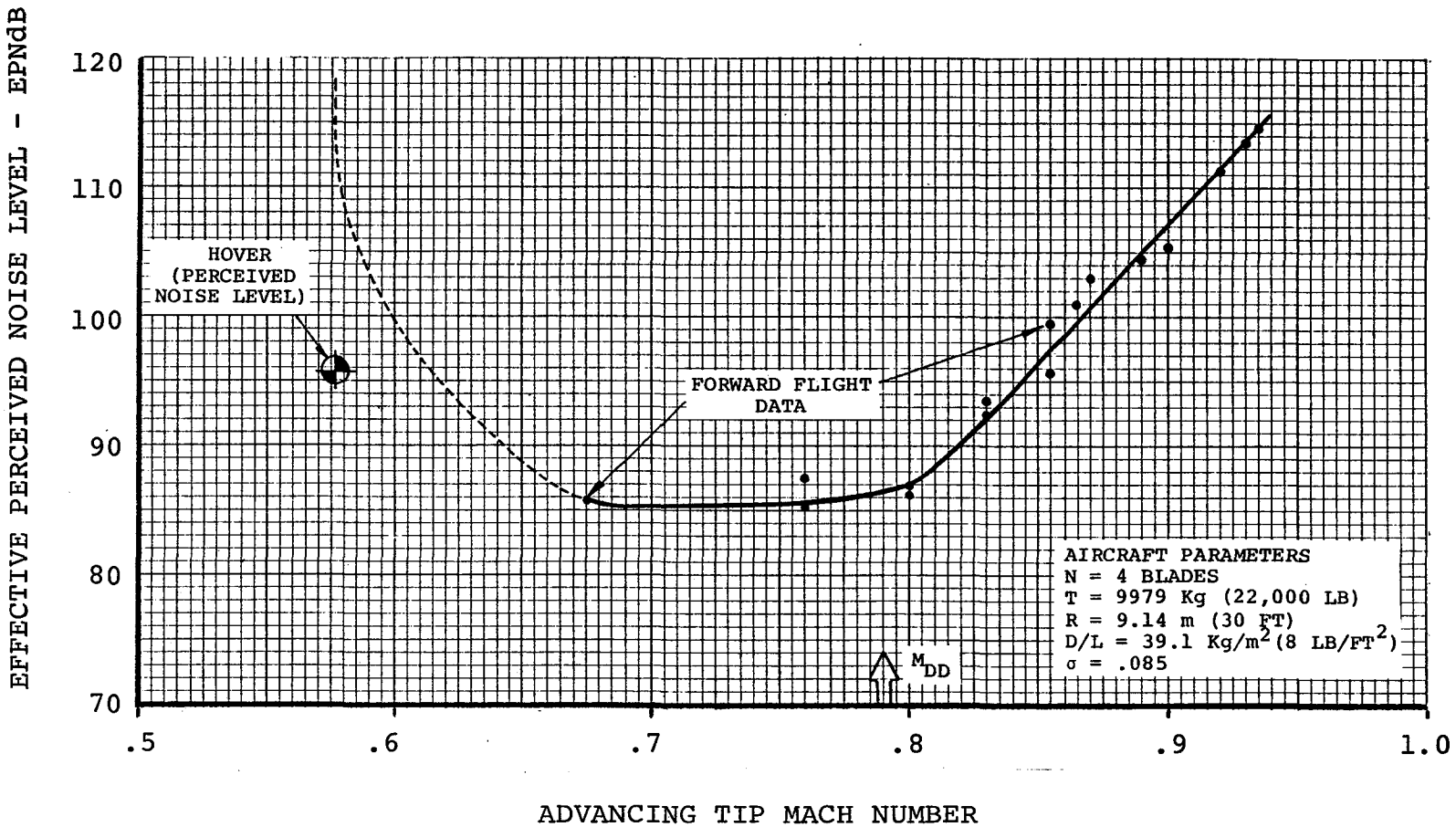

Figure 7. Effective Perceived Noise Level Trend With Forward Flight - Boeing Vertol Model 347

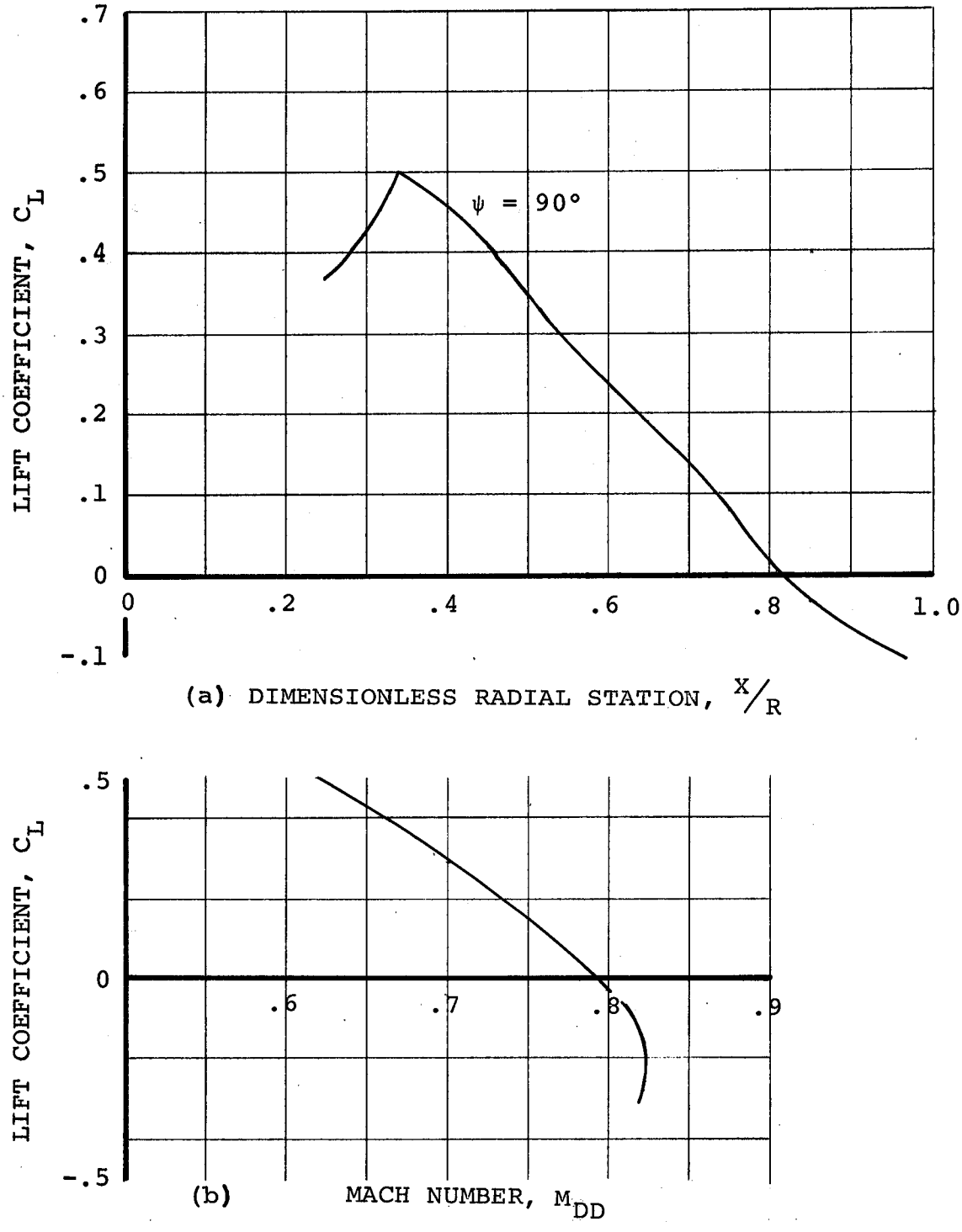

(NASA - 23010 Cambered Airfoil)

Figure 8. Drag Divergence as a Function of Lift Coefficient

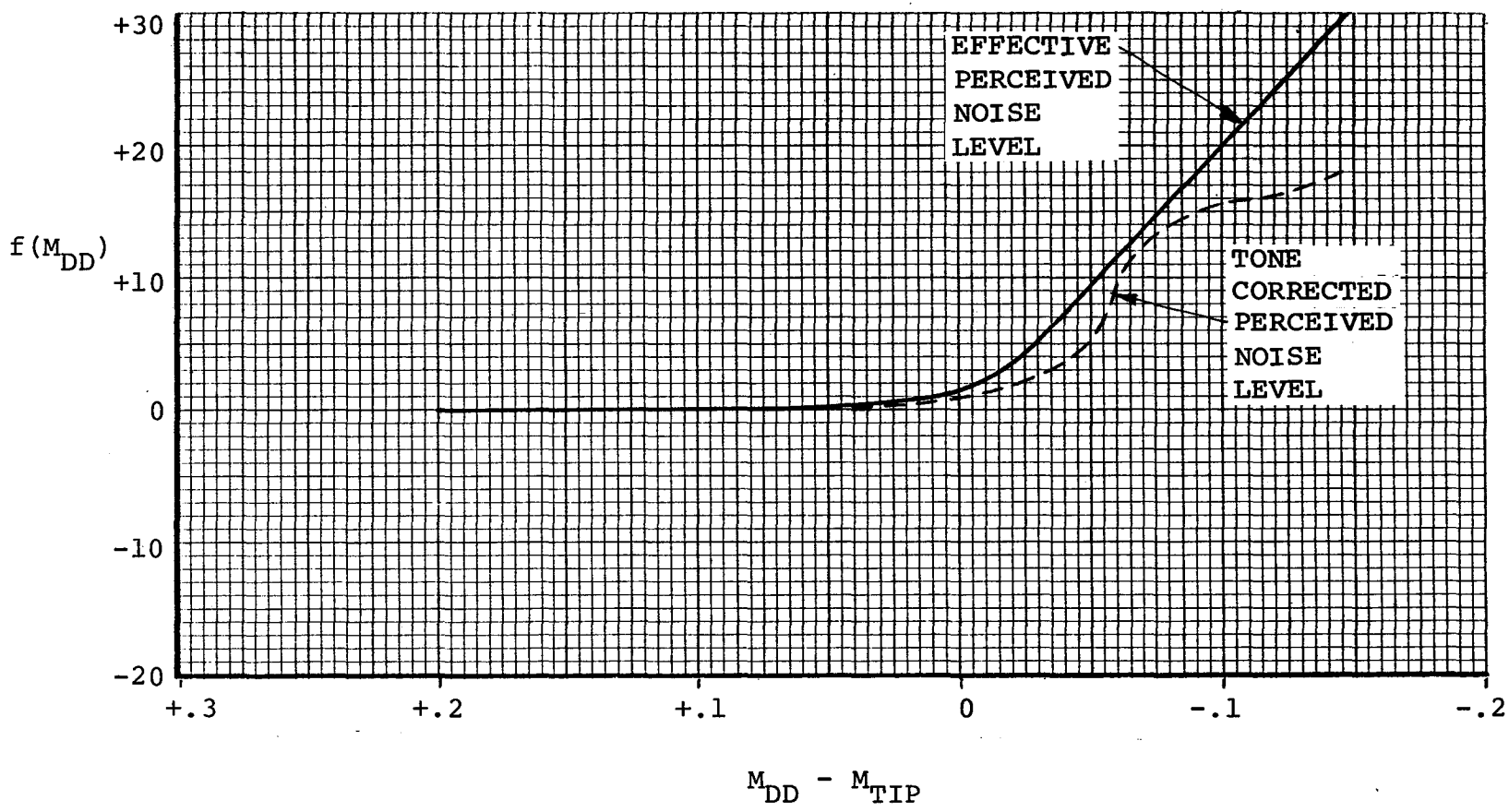

Figure 9. Forward Flight PNLT and EPNL Estimating Function

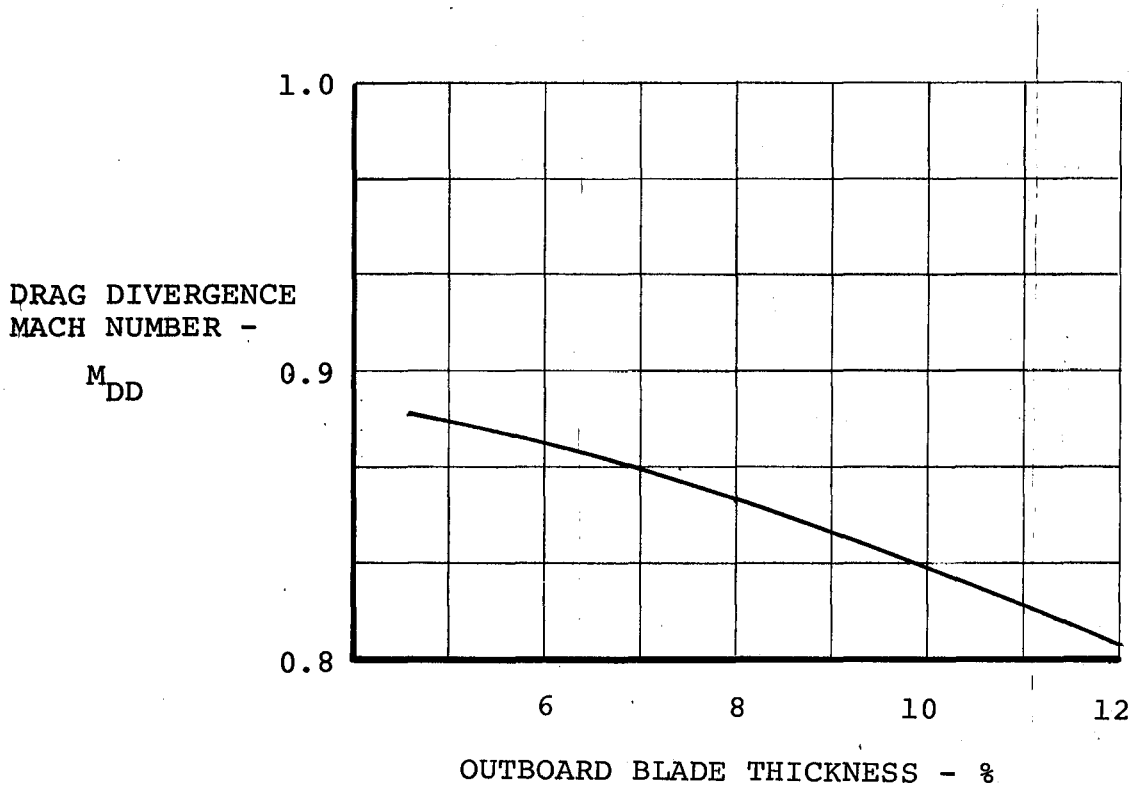

Figure 10. Drag Divergence Mach Number as a Function of Tip Thickness

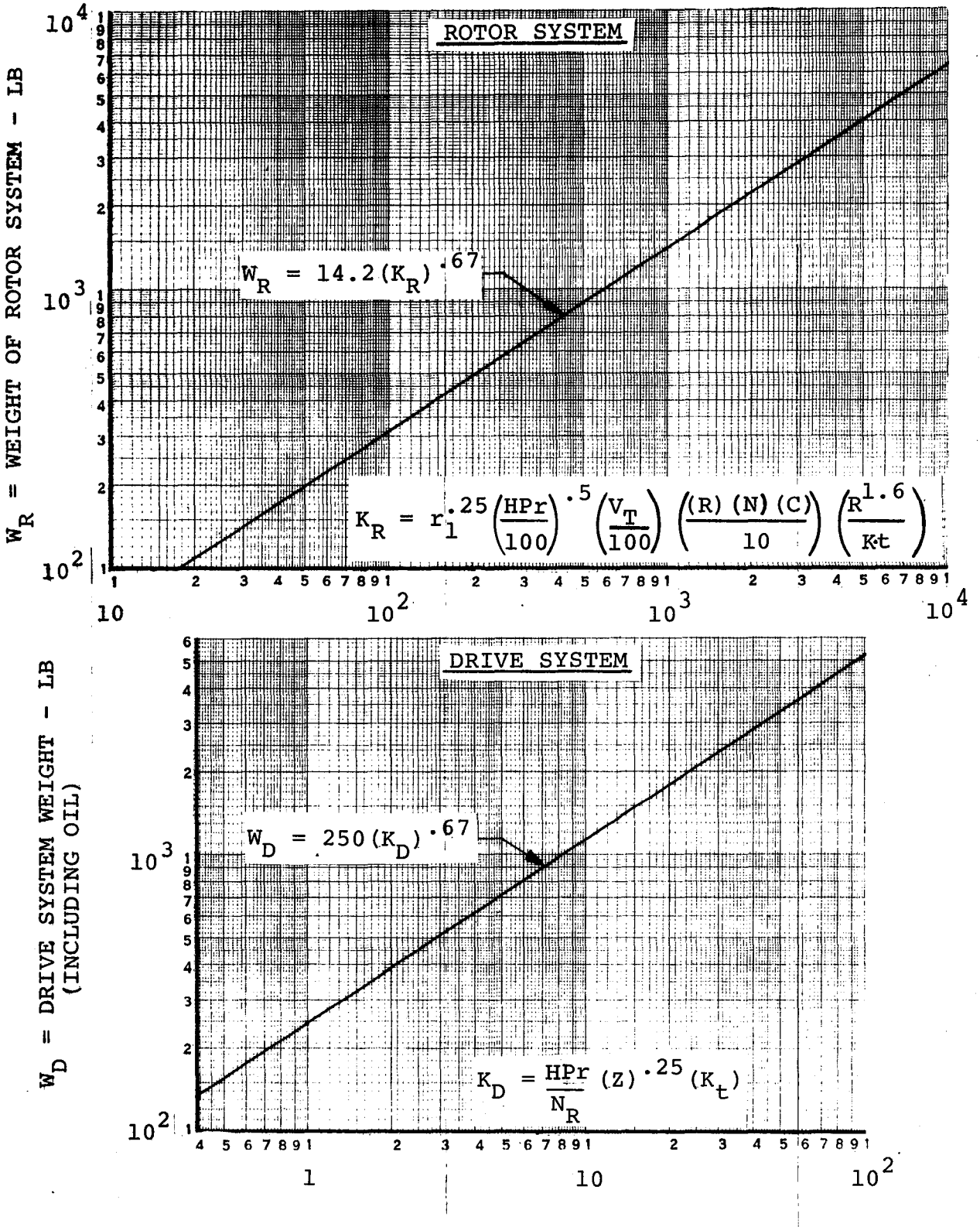

Figure 11. Weight Trend Curves

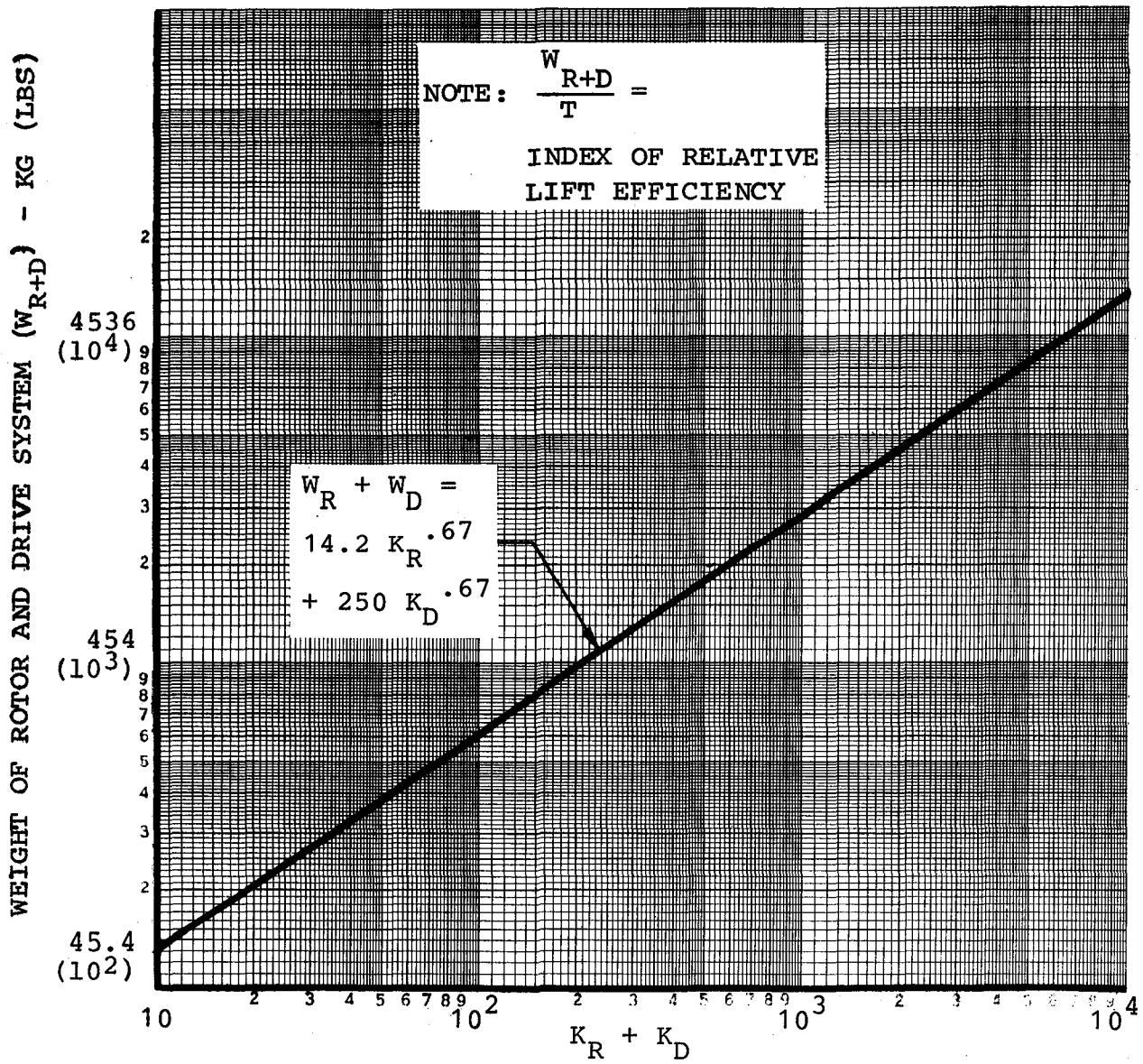

$$K_R = 1.08 \times 10^{-5} (T^{1.625}) (D/L^{-.875}) (V_T) (\sigma)$$

$$K_D = 3.53 \times 10^{-3} \frac{(T^{1.5})}{V_T}$$

Figure 12. Rotor and Drive System Weight Trend Curve

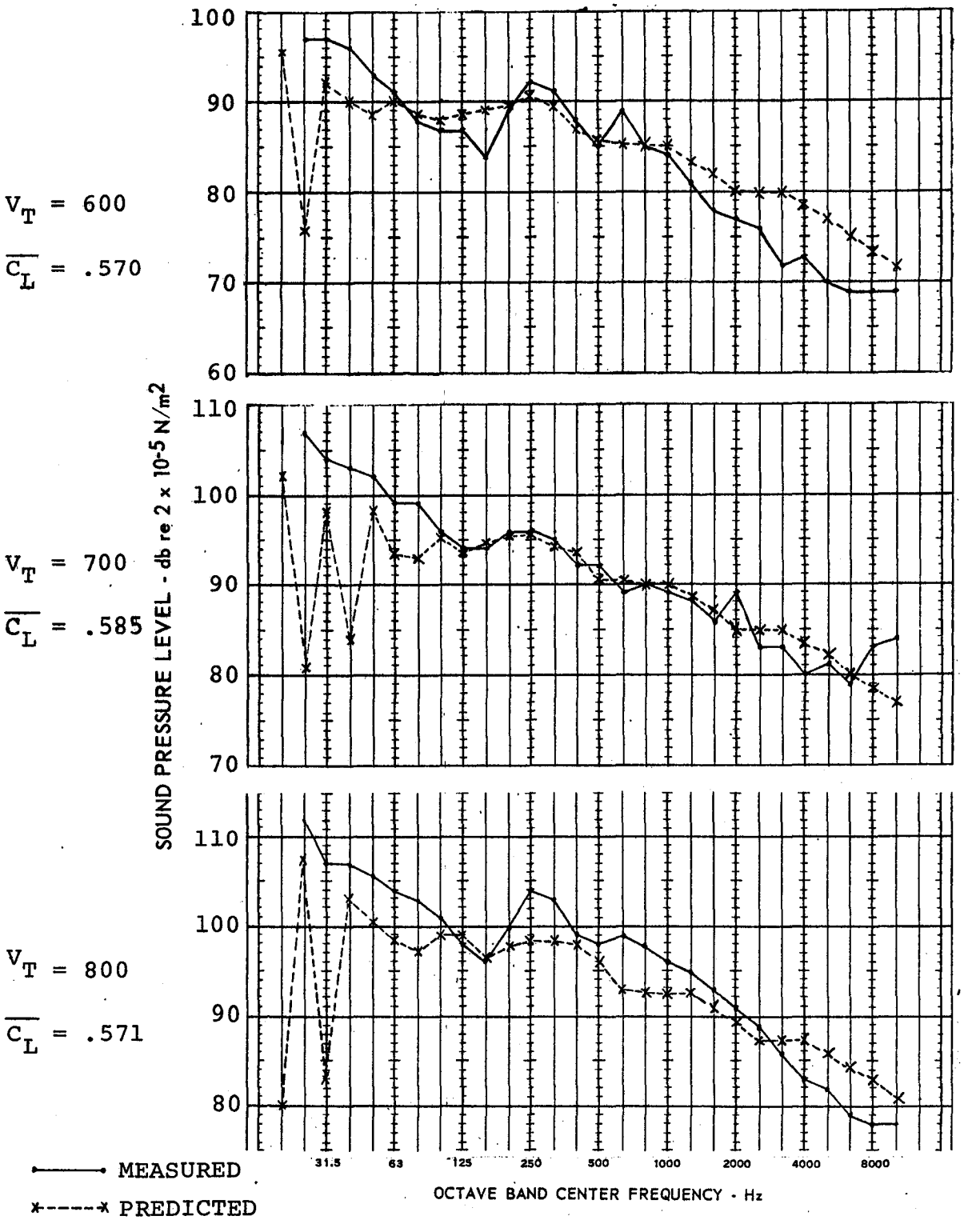

Figure 13. Comparison of Predicted and Measured Spectra - CH-47 Rotor on Test Tower - High $\overline{C_L}$

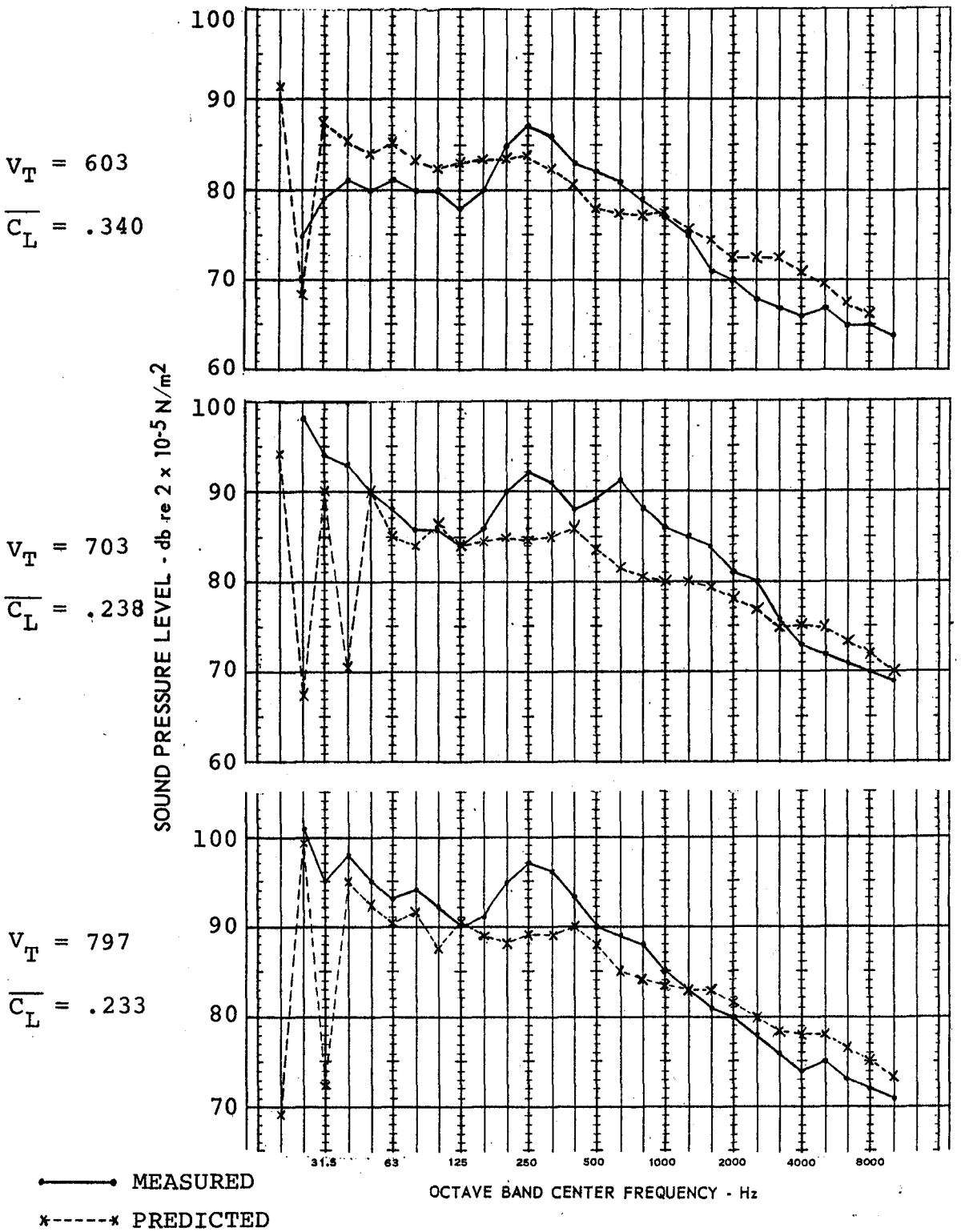

Figure 14. Comparison of Predicted and Measured Spectra - CH-47 Rotor on Test Tower - Low $\overline{C_L}$

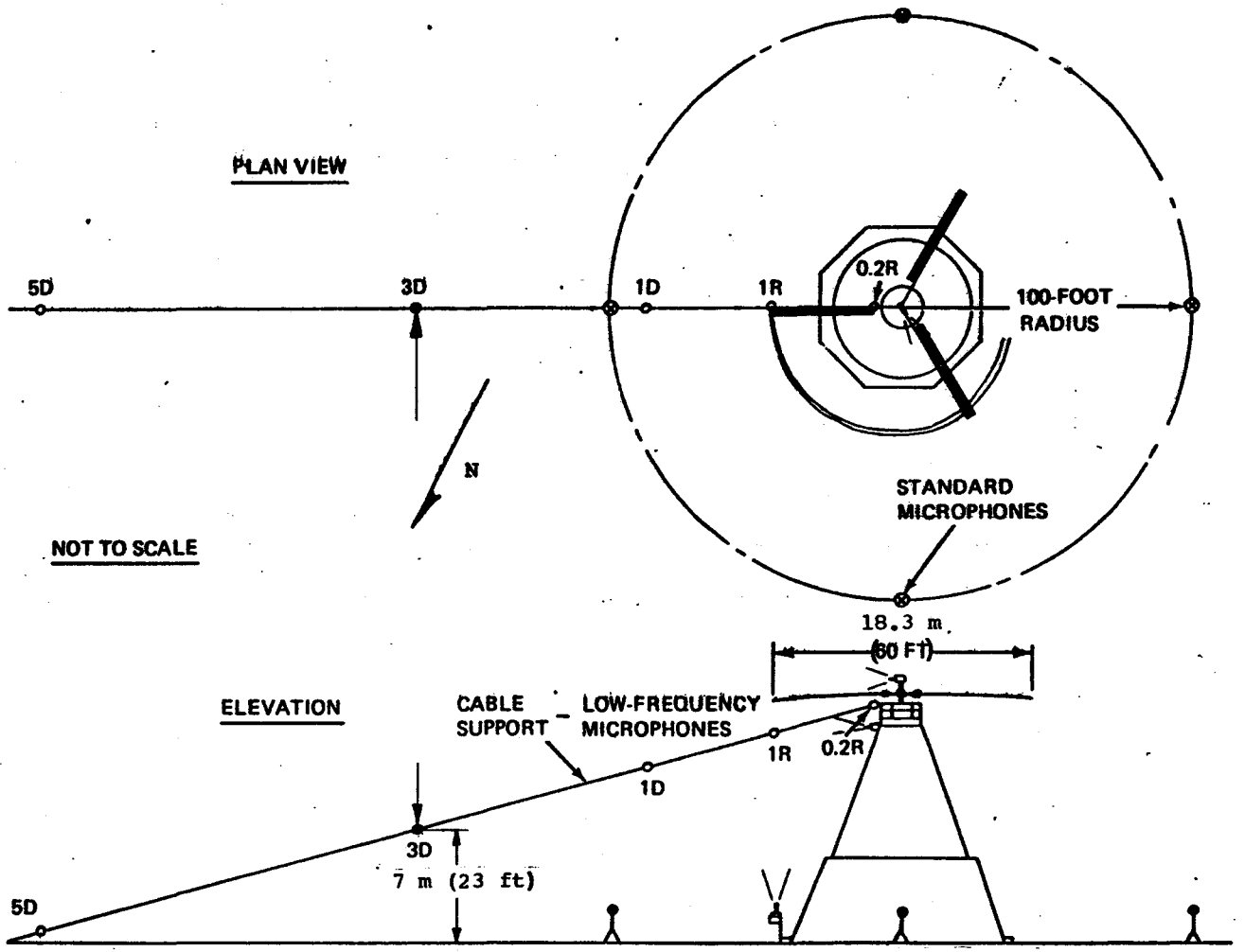

Figure 15. Microphone Array for Data Acquisition

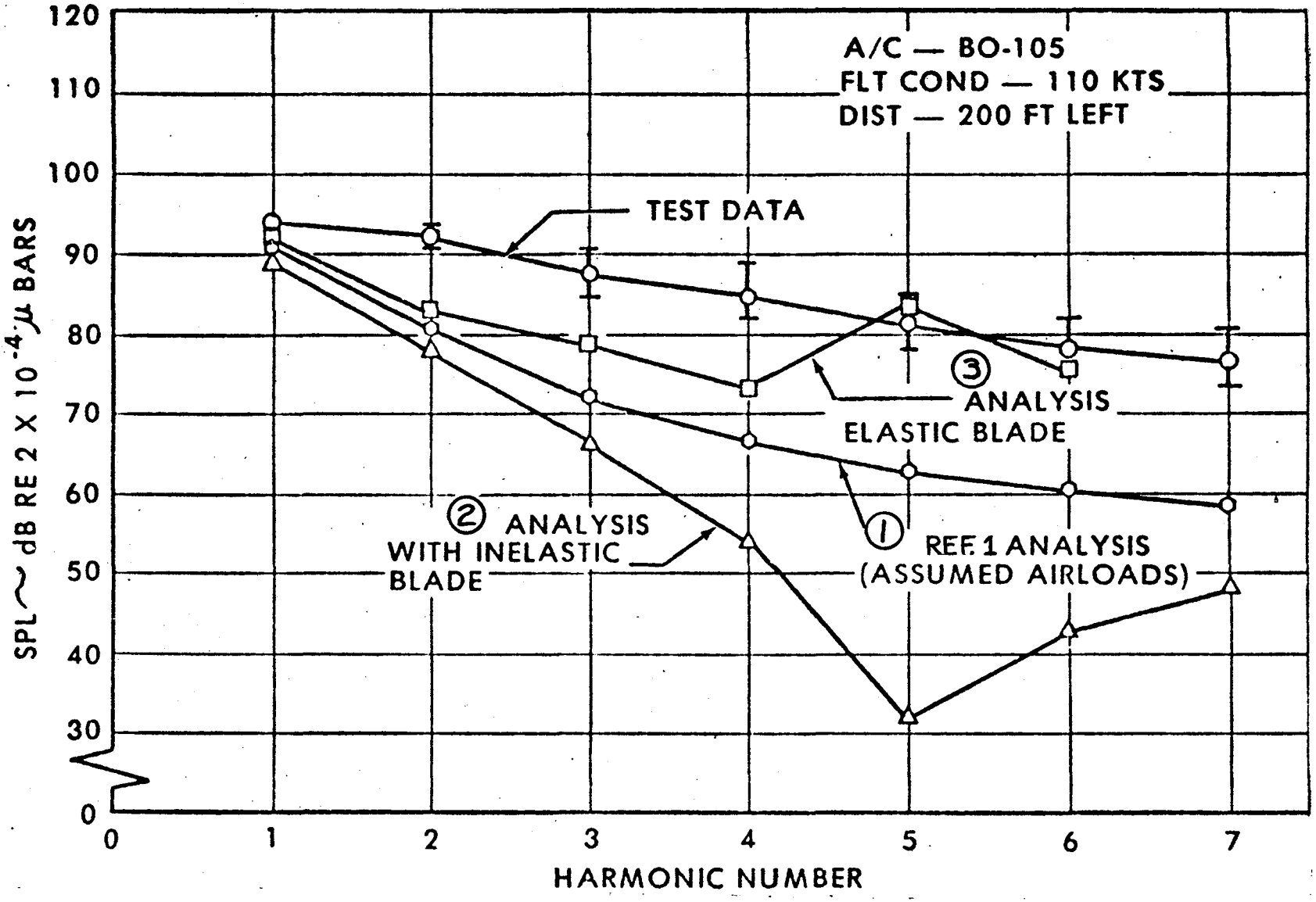

Figure 16. Effect of Torsional Elasticity on Rotational Noise

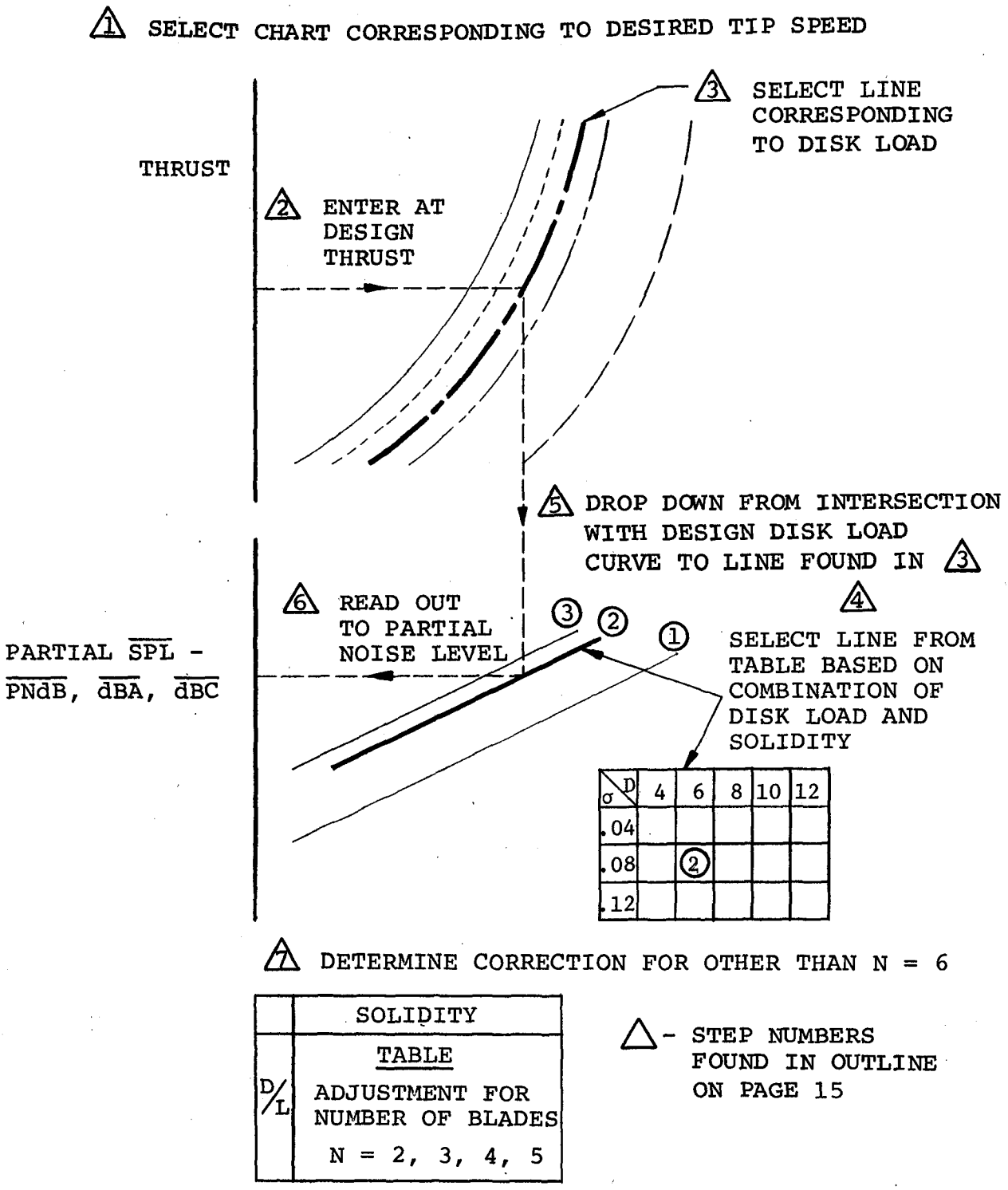

Figure 17. Use of Design Charts

(1) PERFORM THIS OPERATION FOR V_T = 500, 600, 700, 800 FT/SEC

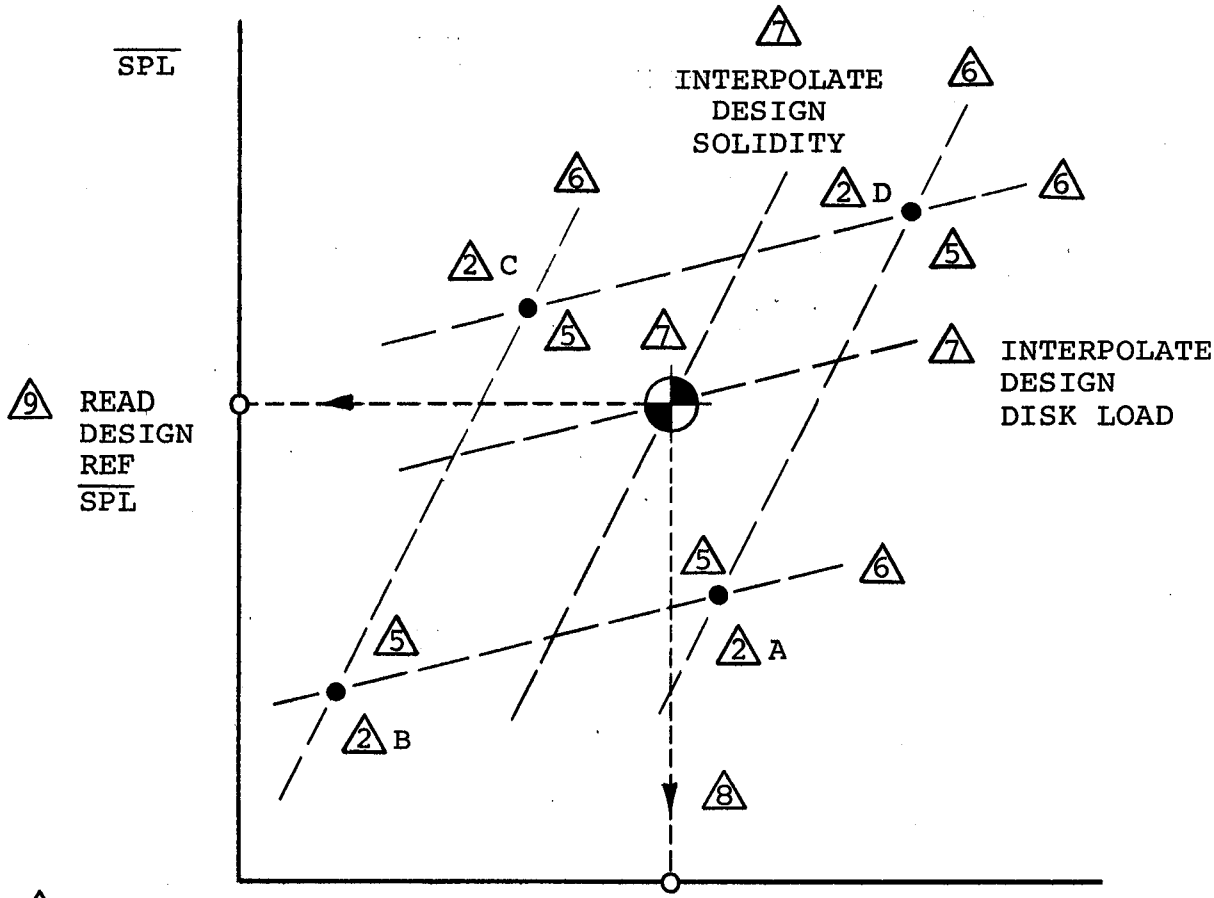

△ - STEP NUMBERS FOUND IN OUTLINE ON PAGE 16

(8) CHECK - DESIGN REF $\overline{C_L}$ SHOULD = $\frac{6 \times D/L}{(\rho)\ (\sigma)\ (V_T^2)}$ AS GIVEN ON PAGE 11

WHERE: D/L AND σ ARE THE DESIGN VALUES AND V_T IS THE TIP SPEED FOR THE CHART FROM WHICH THE BRACKETING VALUES OF D/L AND σ (A,B,C,D) WERE READ

Figure 18. Method of Interpolating Disk Load and Solidity

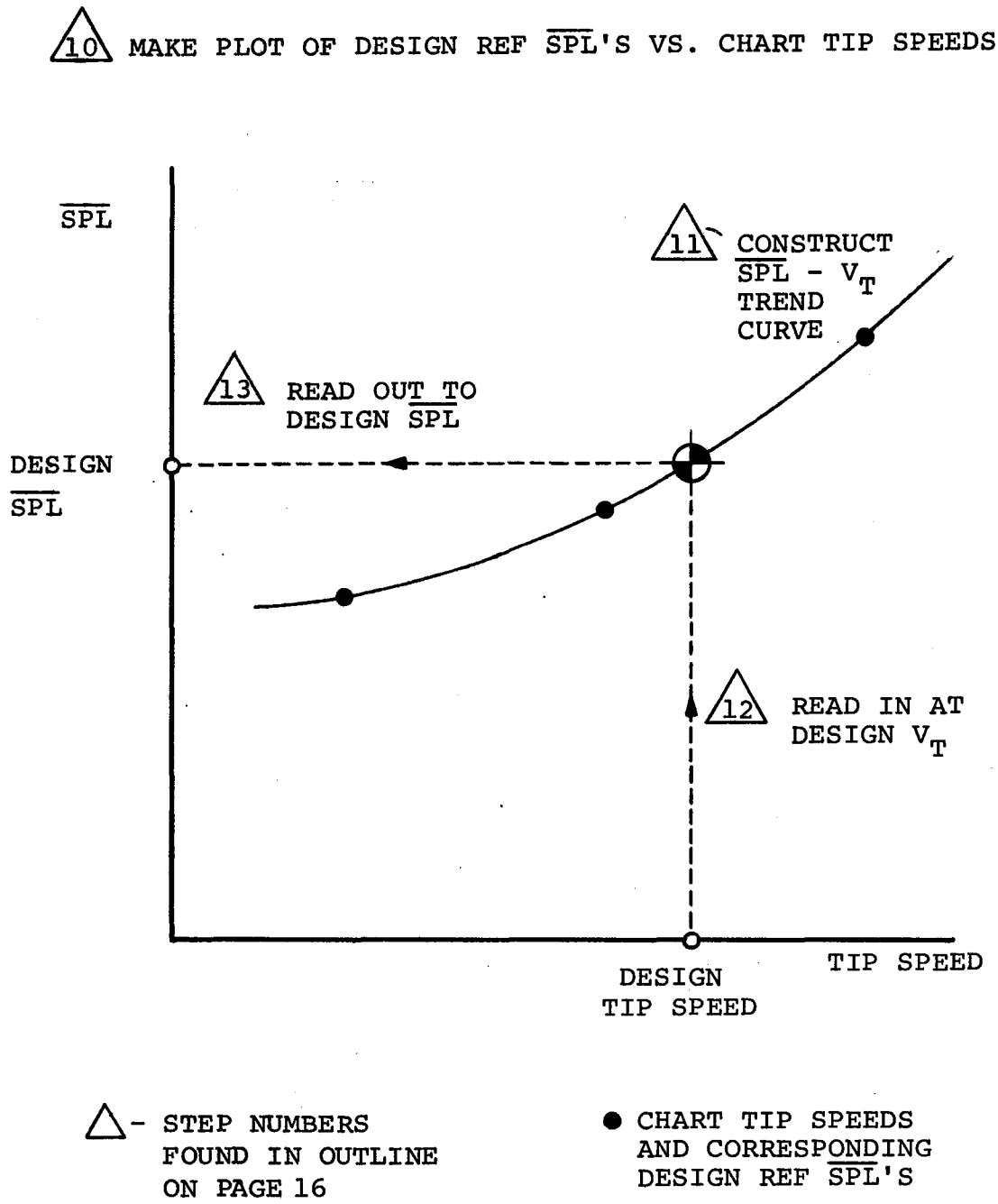

Figure 19. Method of Interpolating Tip Speed

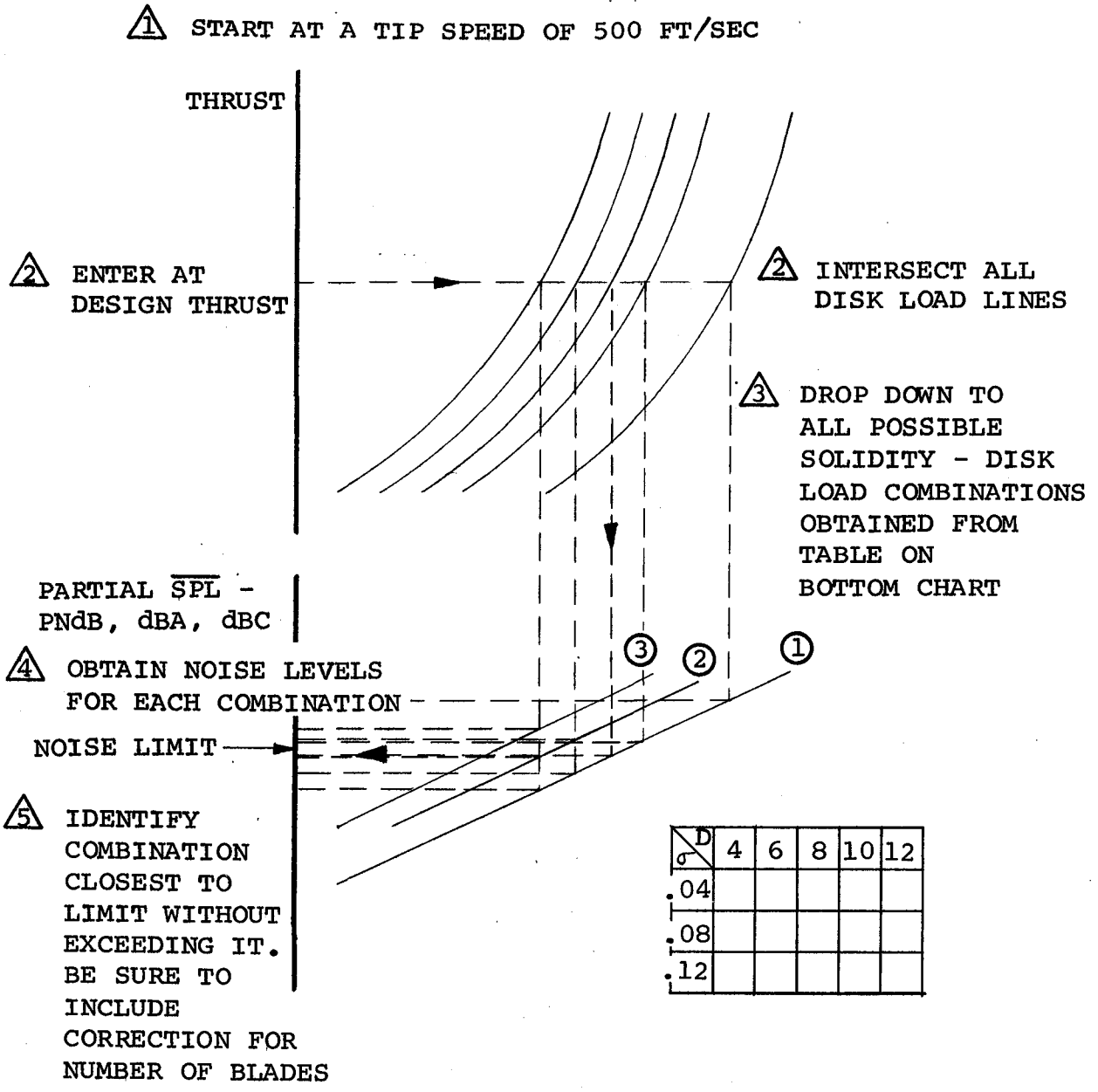

Figure 20. Finding a Rotor Configuration to Meet a Noise Specification

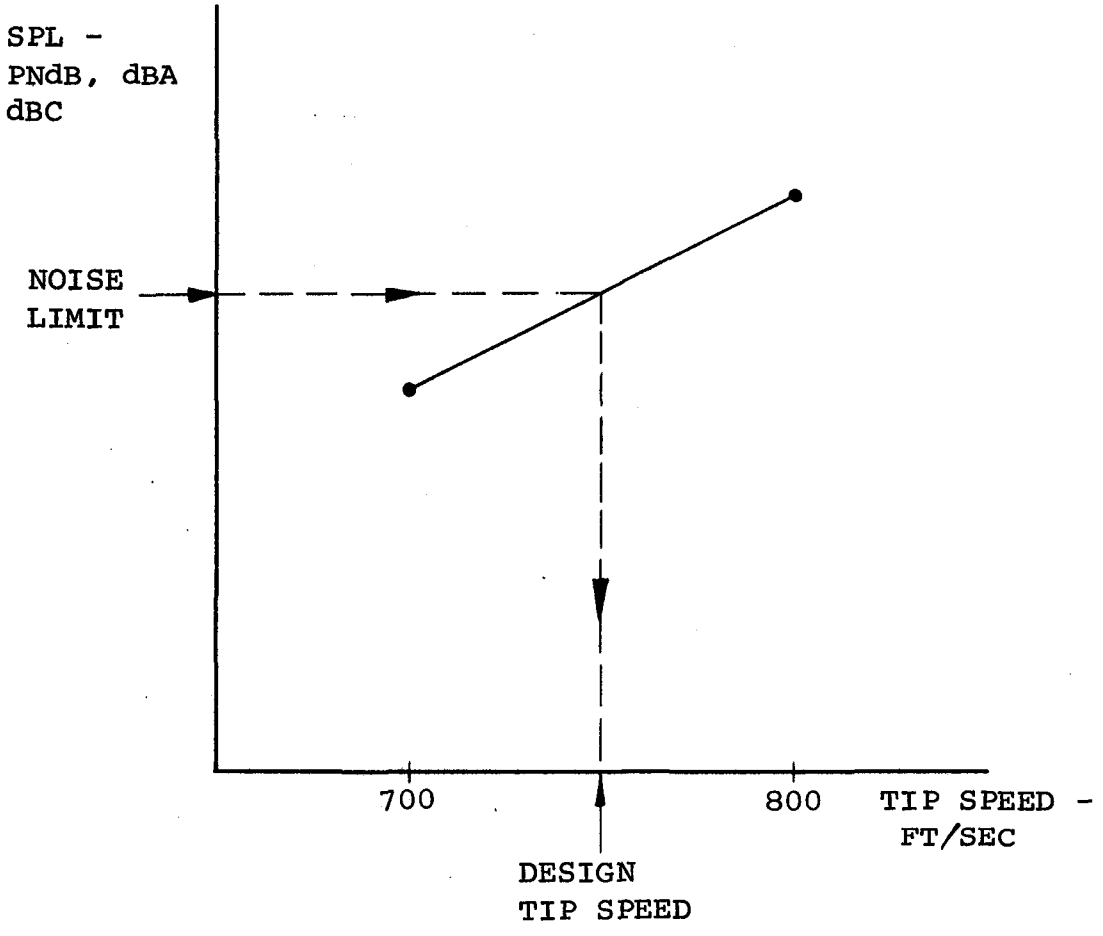

Figure 21. Example of Finding a Tip Speed to Meet a Noise Specification

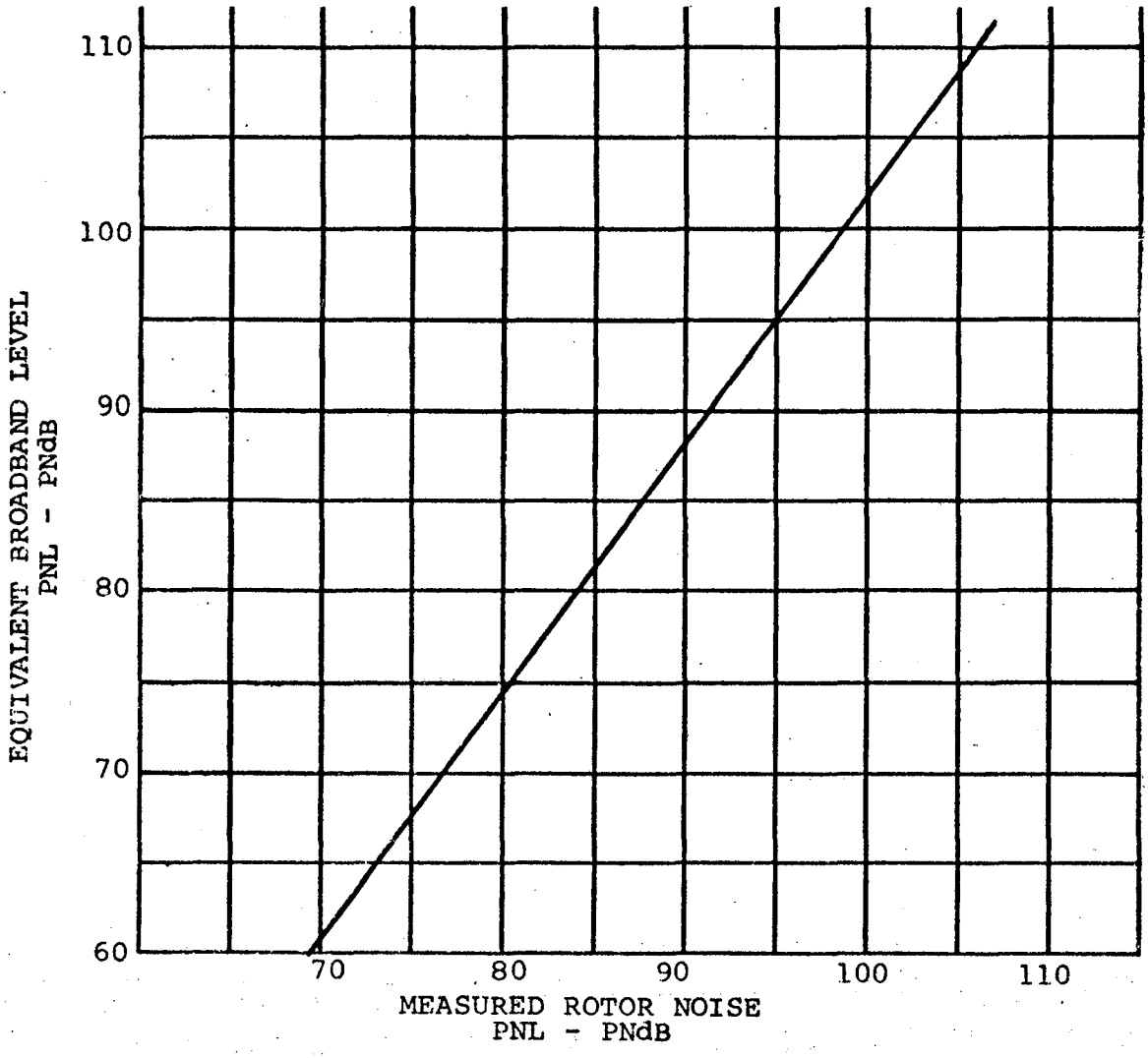

Figure 22. Correlation Between PNL of Rotor Noise and PNL of Equivalent Broadband Noise (Ref 14)

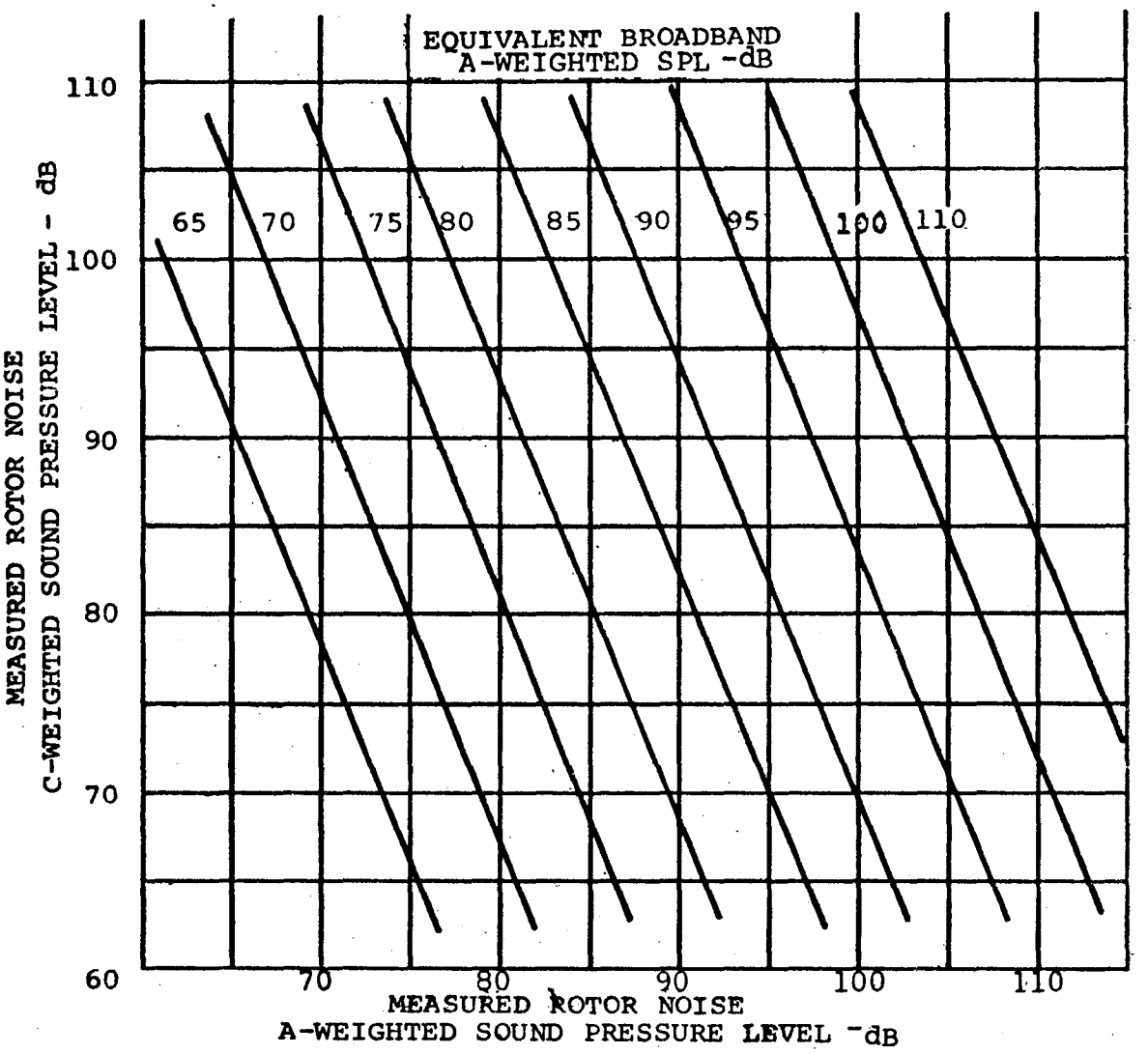

Figure 23. Determination of Equivalent Broadband A-Weighted SPL Using C-Weighted SPL (Ref 14)

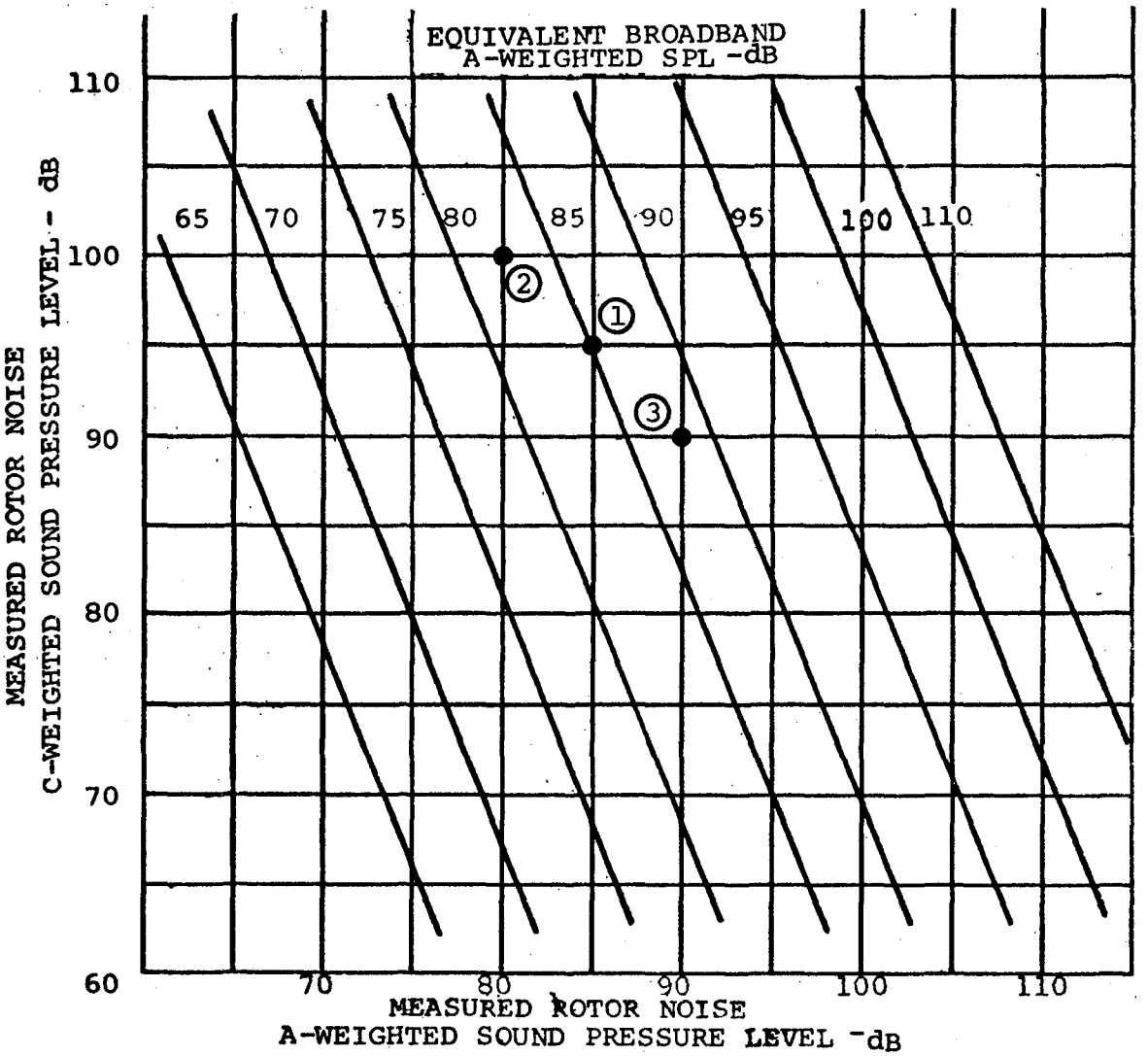

Figure 24. Examples of the Determination of Equivalent Broadband A-Weighted SPL Using C-Weighted SPL (Ref 14)